Cooperative Effects in the Multiple Scattering of Photons by Atomic Gases

Research Thesis

In Partial Fulfillment of the Requirements for the Degree of

Doctor of Philosophy

Aharon P. Gero

Submitted to the Senate of

the Technion - Israel Institute of Technology

Tevet 5768 Haifa December 2007

.

To my parents, Judith and Tomi

.

The research thesis was done under the supervision of
Prof. Eric Akkermans in the department of physics.

I am greatly indebted to Prof. Eric Akkermans for his most fruitful guidance, his true interest and involvement in my work and his support along all stages of this research.

I am grateful to my colleague Ohad Assaf for his help through discussions, criticisms and suggestions.

I am also grateful to my friend and colleague Netanel Lindner for his encouragement, for endless hours of triathlon training and for the establishment of the Order.

The generous financial help of the Technion is gratefully acknowledged.

.

Contents

List of Figures

List of Symbols

a	system size
$a_{\mathbf{k}\hat{\varepsilon}}, a^{\dagger}_{\mathbf{k}\hat{\varepsilon}}$	annihilation & creation operators
$\mathtt{b}$	optical depth
$b, b^{\dagger}$	lowering & raising operators
c	speed of light in vacuum
$\mathbf{D}, \mathbf{d}$	electric dipole moment operator
$\mathcal{D}$	diffusion coefficient
$\mathtt{d}$	system dimension
$\mathbf{E}$	electric field operator
E	energy
$\|e\rangle$	atomic excited state
$\|f\rangle$	final state
G	resolvent operator
$\mathcal{G}$	graph
g	scaling function
$\|g\rangle$	atomic ground state
H	Hamiltonian
$\hbar$	Planck's constant
I	unit matrix
$\|i\rangle$	initial state
J	angular momentum quantum number
$\mathbf{k}$	wave vector
k_B	Boltzmann's constant
L	cooperation number
$\mathtt{L}$	system size
l	average path length
l_0, l_e	elastic mean free path
M	measure of atomic inversion
m	Zeeman quantum number
n	atomic density
P	spectral density
$\mathbf{R}, \mathbf{r} = (r, \theta, \varphi)$	position vector
T	collision operator

t	time
$\mathtt{t}$	scattering amplitude
U	coupling matrix
$\mathtt{u}$	scattering potential
V	interaction potential
v	speed
$\mathtt{v}$	scattering potential
v_0, v_g	group velocity
W	disorder strength
α	atomic polarizability
Γ	spontaneous emission rate
Δ^+, Δ^-	collective raising & lowering operators
δ	detuning from resonance
$\hat{\varepsilon}$	polarization vector
ϵ_0	vacuum dielectric constant
η	refractive index
λ	wavelength
μ	atomic mass
ν	spectral density
ρ	density operator
Σ	self-energy
σ	scattering cross section
τ	time
ϕ	probability
Ω	volume
ω	angular frequency

Abstract

We study multiple scattering of photons in disordered atomic media while taking into account cooperative effects, which originate from the interaction between atoms through the radiation field. We show that in atomic gases cooperative effects, like superradiance and subradiance, lead to a potential between two atoms that decay as the inverse inter-atomic distance, where in the case of superradiance, this potential is attractive for close enough atoms. The contribution of superradiant pairs to multiple scattering properties of a dilute gas, such as photon elastic mean free path and group velocity, is significantly different from that of independent atoms. Near resonance, it leads to a finite and positive group velocity, unlike the one obtained for light interaction with independent atoms. We also study the photon propagation in a gas of N atoms, using an effective Hamiltonian that accounts for photon mediated atomic dipolar interactions. The density of photon escape rates is obtained from the spectrum of the $N \times N$ random matrix $U_{ij} = \sin x_{ij}/x_{ij}$, where x_{ij} is the dimensionless random distance between any two atoms. A scaling function is defined to study photon escape rates as a function of disorder and system size. Photon localization is described using statistical properties of random networks whose mean field solution displays a "small world" behavior.

.

CHAPTER 1

Introduction

Wave propagation in disordered media plays an important role in various fields of physics [1, 2]. A few examples are electronic transport in metals, light propagation in random media, scattering of acoustic waves in fluids and propagation of seismic waves. The general aspects are common to these examples, but each type of wave exhibits its own characteristic behavior. When the medium is thin enough, the wave scatters only one time in the random medium before it emerges on its way out. This regime is called *single scattering*. But, when the medium is thick, the wave scatters many times before leaving and we may speak of *multiple scattering*. In this thesis we are interested in the multiple scattering of light by atomic gases.

The problem of a single scattering of light from a dielectric particle of an arbitrary volume has been studied by Mie [3]. His solution is rather formal so let us focus on its limiting cases. When the radius of scatter, a, is much smaller compared to the radiation wavelength, λ, Rayleigh limit is obtained and the scattering cross section varies as λ^{-4}. This dependence is the origin of the blue sky. On the opposite limit, when $a \gg \lambda$, the geometrical optics regime is approached and the scattering cross section does not depend on λ and is of the order of πa^2.

When the scatterer is an atom, rather than a classical object as in Mie scattering, new features appear due to the internal structure of the atom. The existence of energy levels in the atomic spectrum leads to a different expression of the scattering cross section [4]. Moreover, if the energy levels are degenerate, then the additional degrees of freedom reflect in a tensorial structure of the differential cross section [1]. In the low frequency regime, when the radiation frequency, ω, is much smaller than the atomic Bohr's frequency, ω_0, Rayleigh limit is recovered and the cross section varies as λ^{-4}, as in the classical case. But for the case of resonant scattering, namely $\omega \simeq \omega_0$, the cross section is very large of the order of λ^2. This large value is a substantial advantage in the experimental study of scattering from atomic gases.

The issue of multiple scattering of light in disordered media may be treated at several levels of complexity. The first one describes the scattering

of a scalar wave by classical scatterers. This simple approach disregards the polarization of light and its quantum nature, as well as the internal degrees of freedom of the scatterers, [5, 6, 7]. The second takes into account the vectorial nature of light, but the scatterers and the radiation field are still been treated classically [5, 6]. The third one is a semiclassical treatment where the multiple scattering of an electro-magnetic wave by atoms is studied [8]. The last level considers photons (within the formalism of second quantization) and atoms and hence represents a full quantum treatment [1, 9, 10].

However, all these approaches neglect the mutual influence between scatterers. Thus, the aim of this research is to study multiple scattering of photons in disordered media, while taking into account cooperative effects as *superradiance* and *subradiance* [11, 12], which originate from the interaction between atoms through the radiation field. Superradiance is the phenomenon where, under certain circumstances, the spontaneous emission rate from an ensemble of $N \gg 1$ interacting atoms is proportional to N^2 rather than N. The complementary phenomenon is subradiance in which, under other circumstances, the spontaneous emission rate is zero although half of the N atoms occupy the excited states. We will show that these effects modify considerably the transport properties of light in disordered media.

The dissertation is organized as follows: Chapter 2 deals with the multiple scattering of light by a gas of non-interacting atoms. To this purpose a brief description of single scattering is given, then several models of disorder are presented and finally the resolvent operator formalism as well as the self-energy concept are introduced. Chapter 3 reviews cooperative effects by defining Dicke states and calculating the cooperative spontaneous emission rate and the cooperative level shift for different cases. In the rest of the dissertation we combine the two elements presented in the previous chapters, *i.e.,* study multiple scattering of photons in disordered media while taking into account cooperative effects. Chapter 4 deals with the multiple scattering of superradiant pairs [13, 14], while Chapter 5 considers higher order terms that account for cooperative effects between more than two atoms [15].

We will show that in atomic gases cooperative effects lead to a potential between two atoms that decay as the inverse inter-atomic distance, where in the case of superradiance, this potential is attractive for close enough atoms. It will be proven that the contribution of superradiant pairs to multiple scattering properties of a dilute gas, such as photon elastic mean free path and group velocity, is significantly different from that of independent atoms. For instance, near resonance, it leads to a finite and positive group velocity,

unlike the one obtained for light interaction with independent atoms.

We will also show that photon escape rates from a gas of N atoms can be derived from the spectrum of an $N \times N$ random matrix U. For a three-dimensional geometry, $U_{ij} = \sin x_{ij}/x_{ij}$, while for a one-dimensional gas $U_{ij} = \cos x_{ij}$, where x_{ij} is the dimensionless random distance between any two atoms. In order to study photon escape rates as a function of disorder and system size, we will define a scaling function which measures the relative number of states having a vanishing escape rate. With its help we will prove that for a large enough three-dimensional geometry, the photons undergo a crossover from delocalization towards localization, while in a one-dimensional atomic gas, the photons are always localized. We will suggest an explanation to these results in the framework of random networks.

.

CHAPTER 2

Multiple scattering of light

This chapter deals with the multiple scattering of light by a gas of non-interacting atoms. First, a brief description of a single scattering is given and Rayleigh scattering as well as resonant scattering are studied. Then, in order to describe the multiple scattering of light in random media, several model of disorder are presented and the resolvent operator formalism is introduced. Finally, the self-energy concept is studied and the physical parameters that characterize multiple scattering of a photon, *e.g.*, the elastic mean free path and the group velocity, are derived from it.

2.1 Single scattering

We start with a description of a single scattering of a photon by a degenerate two-level atom [1]. The atomic ground state is denoted as $|g\rangle = |J_g m_g\rangle$ and the excited state is $|e\rangle = |J_e m_e\rangle$, where J is the quantum number of the total angular momentum and m is its projection on a quantization axis, taken as the $\hat{z}$ axis. The energy separation between the two levels is $\hbar\omega_0$ and the natural width of the excited level is $\hbar\Gamma_0$. This simple picture of a two-level atom neglects the rather complicated energy structure of a real atom which reflects various internal interactions, *e.g.*, Coulomb interactions, spin-orbit interactions, hyperfine interactions, etc. But, due to selection rules which limit the allowed transitions between states, in some cases a certain state may couple to only one other. Thus, the two-level atom approximation is close to reality and not merely a mathematical convenience. Since the wavelength of the light emitted by the atom is usually much larger than the typical atomic size, the long wavelength approximation is made, so that the electric dipole representation of the interaction can be used. The corresponding Hamiltonian of the system is

$$H = H_0 + V, \tag{1}$$

where the non-ineracting Hamiltonian is the sum of the atomic and the radiation Hamiltonians

$$H_0 = \hbar\omega_0 \sum_{m_e} |J_e m_e\rangle\langle J_e m_e| + \sum_{\mathbf{k}\varepsilon} \hbar\omega_k a^\dagger_{\mathbf{k}\varepsilon} a_{\mathbf{k}\varepsilon}, \tag{2}$$

while the interaction is given by

$$V = -\mathbf{d} \cdot \mathbf{E}(\mathbf{0}), \tag{3}$$

where $\mathbf{d}$ is the dipole moment operator of the atom and $\mathbf{E}(\mathbf{r})$ is the electric field operator at position $\mathbf{r}$

$$\mathbf{E}(\mathbf{r}) = i \sum_{\mathbf{k}\varepsilon} \sqrt{\frac{\hbar\omega_k}{2\epsilon_0 \Omega}} (a_{\mathbf{k}\varepsilon} \hat{\varepsilon}_{\mathbf{k}} e^{i\mathbf{k}\cdot\mathbf{r}} - a^{\dagger}_{\mathbf{k}\varepsilon} \hat{\varepsilon}^{*}_{\mathbf{k}} e^{-i\mathbf{k}\cdot\mathbf{r}}). \tag{4}$$

$a_{\mathbf{k}\varepsilon}$ and $a^{\dagger}_{\mathbf{k}\varepsilon}$ are, respectively, the annihilation and creation operators of a mode of the field of wave vector $\mathbf{k}$, polarization $\hat{\varepsilon}_{\mathbf{k}}$ and angular frequency $\omega_k = ck$. Ω is a quantization volume, ϵ_0 is the vacuum dielectric constant, and c is the light speed in vacuum.

We assume that the typical speed of the atoms,

$$v \simeq \sqrt{\frac{k_B T_0}{\mu}}, \tag{5}$$

is small compared to $v_{max} = \Gamma_0/k$ but large compared to $v_{min} = \hbar k/\mu$ where μ is the mass of the atom and T_0 is the temperature, so that it is possible to neglect the Doppler shift and recoil effects. Indeed, for a temperature of $T_0 = 10^{-3}$ K, the typical speed of the atom is $v \simeq 0.3$ m/s. Since, for a wave number of $k = 10^7$ m^{-1} and a natural width of $\Gamma_0 = 10^7$ s^{-1}, $v_{max} \simeq 1$ m/s and $v_{min} \simeq 0.01$ m/s, both assumptions are fulfilled.

In order to calculate the scattering cross section we introduce the collision operator

$$T(z) = V + VG(z)V, \tag{6}$$

where its Born expansion is given by

$$T(z) = V + VG_0(z)V + VG_0(z)VG_0(z)V + ... \tag{7}$$

$G(z)$ is the resolvent of the total system, while $G_0(z)$ is the resolvent of the non-interacting system and they are defined as

$$G(z) = \frac{1}{z - H} \tag{8}$$

and

$$G_0(z) = \frac{1}{z - H_0}. \tag{9}$$

The transition matrix element, known also as the scattering amplitude, describes the transition from the initial state $|i\rangle = |J_g m_g; \mathbf{k}\hat{\varepsilon}\rangle$, where the atom is in a state $|J_g m_g\rangle$ in the presence of a photon of frequency $\omega = ck$ and polarization $\hat{\varepsilon}$, to a final state $|f\rangle = |J_g m'_g; \mathbf{k}'\hat{\varepsilon}'\rangle$ and it is defined as

$$T_{fi} = \langle f|T(z = \hbar\omega)|i\rangle, \tag{10}$$

with $k = k'$. Using (1)-(9) up to the second order of the Born expansion gives

$$T_{fi} = \frac{\omega}{2\epsilon_0\Omega}\sum_{m_e}\frac{A_R}{\omega - \omega_0} - \frac{A_{AR}}{\omega + \omega_0}, \tag{11}$$

where

$$A_R = \langle J_g m'_g|\mathbf{d}\cdot\hat{\varepsilon}'^*|J_e m_e\rangle\langle J_e m_e|\mathbf{d}\cdot\hat{\varepsilon}|J_g m_g\rangle \tag{12}$$

and

$$A_{AR} = \langle J_g m'_g|\mathbf{d}\cdot\hat{\varepsilon}|J_e m_e\rangle\langle J_e m_e|\mathbf{d}\cdot\hat{\varepsilon}'^*|J_g m_g\rangle. \tag{13}$$

The first term of (11) represents the resonant process in which the atom absorbs the original photon and then emits a new one, while the second term describes the anti-resonant process in which the atom emits a new photon and then absorbs the original one.

Let us distinguish between two cases, Rayleigh scattering and a resonant scattering.

2.1.1 Rayleigh scattering

When the photon energy is much smaller than the energy difference between the atomic levels ($\omega \ll \omega_0$) and for a non-degenerate ground state ($J_g = 0$), (11) can be rewritten as

$$T_{fi} = -\frac{\hbar\omega}{2\Omega}\sum_{ij}\alpha_{ij}(\hat{\varepsilon}'^*\cdot\hat{\mathbf{e}}_i)(\hat{\varepsilon}\cdot\hat{\mathbf{e}}_j), \tag{14}$$

where the static atomic polarizability is

$$\alpha_{ij} = \frac{1}{\epsilon_0}\sum_{m_e}\frac{\langle J_g m_g|d_i|J_e m_e\rangle\langle J_e m_e|d_j|J_g m_g\rangle + \langle J_g m_g|d_j|J_e m_e\rangle\langle J_e m_e|d_i|J_g m_g\rangle}{\hbar\omega_0} \tag{15}$$

and d_i is the component of the electric dipole moment operator along the unit vector $\hat{e}_i$. Assuming the tensor to be isotropic, that is $\alpha_{ij} = \alpha_0 \delta_{ij}$, we obtain

$$T_{fi} = -\frac{\hbar\omega}{2\Omega}\alpha_0(\hat{\varepsilon}'^* \cdot \hat{\varepsilon}). \tag{16}$$

Using the Fermi golden rule and summing over the polarizations of the scattered photon yield the differential cross section for the scattered photon to emerge towards a solid angle $d\Omega_{\mathbf{k}'}$ about $\mathbf{k}'$,

$$\frac{d\sigma}{d\Omega_{\mathbf{k}'}} = \frac{\alpha_0^2\pi^2}{\lambda^4}(1 - |\hat{\varepsilon} \cdot \hat{k}'|^2), \tag{17}$$

where $\lambda = 2\pi/k$ is the photon wavelength and $\hat{k} = \mathbf{k}/k$ is a unit vector. The corresponding total cross section is

$$\sigma = \frac{8\pi^3\alpha_0^2}{3\lambda^4} \tag{18}$$

and the λ^{-4} dependence is well-known as the origin of the blue sky.

2.1.2 Resonant scattering

Now, we are interested in a resonant scattering, in which the photon energy is very close to the energy difference between the atomic levels ($\delta = \omega - \omega_0 \ll \omega_0$). The non-pertubative expression for the transition matrix element (10) reads

$$T_{fi} = \frac{\omega}{2\epsilon_0\Omega}\frac{1}{\delta + i\Gamma_0/2}\sum_{m_e}\langle J_g m_g'|\mathbf{d} \cdot \hat{\varepsilon}'^*|J_e m_e\rangle\langle J_e m_e|\mathbf{d} \cdot \hat{\varepsilon}|J_g m_g\rangle. \tag{19}$$

Applying the Wigner-Eckart theorem yields

$$T_{fi} = \frac{3\pi\hbar c^3}{\Omega\omega^2}\frac{\Gamma_0/2}{\delta + i\Gamma_0/2}\sum_{m_e}(\hat{d}^* \cdot \hat{\varepsilon}'^*)(\hat{d} \cdot \hat{\varepsilon}), \tag{20}$$

where the natural width of the excited state is

$$\hbar\Gamma_0 = \frac{d^2\omega_0^3}{3\pi\epsilon_0 c^3}, \tag{21}$$

the reduced matrix element and the corresponding unit vector are

$$d = \frac{\langle J_e\|\mathbf{d}\|J_g\rangle}{\sqrt{2J_e+1}} \qquad \hat{d} = \frac{1}{d}\langle J_e m_e|\mathbf{d}|J_g m_g\rangle \tag{22}$$

and the small radiative shift of the excited level has been neglected. The total cross section in this case is

$$\sigma = \frac{3\lambda^2}{2\pi} \frac{\Gamma_0^2/4}{\delta^2 + \Gamma_0^2/4} \sum_{m_e} (\hat{d}^* \cdot \hat{\varepsilon}^*)(\hat{d} \cdot \hat{\varepsilon}). \tag{23}$$

The average of (23) with respect to the internal degrees of freedom, *i.e.,* Zeeman sub-levels m, assuming equal probability to find the atom in each of them, is

$$\langle \sigma \rangle_m = C_{J_g J_e} \frac{3\lambda^2}{2\pi} \frac{\Gamma_0^2/4}{\delta^2 + \Gamma_0^2/4}, \tag{24}$$

where

$$C_{J_g J_e} = \frac{2J_e + 1}{3(2J_g + 1)}. \tag{25}$$

We conclude that the resonant scattering cross section varies as the photon wavelength squared. In particular, for $\delta = 0$, $J_g = 0$, and $J_e = 1$ we recover from (24) the known result of the resonant scattering of a classical electromagnetic wave by an elastically bound classical electron [16]

$$\sigma_{cl} = \frac{3\lambda^2}{2\pi}. \tag{26}$$

2.2 Multiple scattering

In order to describe the multiple scattering of light in random media, we start by presenting several models of disorder. Then, the resolvent operator formalism is introduced and the photon self-energy concept is studied. Finally, the physical parameters that characterize multiple scattering of a photon, *e.g.*, the elastic mean free path and the group velocity, are derived from it.

2.2.1 Models of disorder

For light propagating in a disordered medium, the scattering potential may takes different forms [1]. The disorder may be a spatially continuous function as in the case of the refractive index of the atmosphere. On the other hand, light scattering by a colloidal suspension corresponds to a model of discrete scatterers. In the following we will study both cases and show that they are equivalent under a certain limit. If the disorder potential, $V(\mathbf{r})$, is a

continuous and random function of the position, we may define the *Gaussian model* in the following way

$$\langle V(\mathbf{r})\rangle_d = 0 \tag{27}$$

$$\langle V(\mathbf{r})V(\mathbf{r}')\rangle_d = B(\mathbf{r}-\mathbf{r}'), \tag{28}$$

where $\langle\cdots\rangle_d$ denotes a disorder average, meaning an average over the different realizations of the medium. In the particular case where the scattering potential is short range compared to the the radiation wavelength, we may approximate the second-order correlation function as

$$\langle V(\mathbf{r})V(\mathbf{r}')\rangle_d = B\delta(\mathbf{r}-\mathbf{r}'). \tag{29}$$

A random potential with such a property is called *white noise potential*.

A microscopic picture of the disorder is given by *Edwards model* [17]. This model describes the medium as a discrete collection of N identical scatterers in a volume Ω. Each scatterer, located at a random point $\mathbf{r}_j$, is characterized by its scattering potential $\mathtt{v}(\mathbf{r}-\mathbf{r}_j)$. Therefore, the disorder potential is given by

$$V(\mathbf{r}) = \sum_{j=1}^{N} \mathtt{v}(\mathbf{r}-\mathbf{r}_j). \tag{30}$$

We assume that the scattering potential is short range compared to the radiation wavelength, so it can be approximated by a δ function potential, *i.e.,* $\mathtt{v}(\mathbf{r}) = \mathtt{v}_0\delta(\mathbf{r})$. In the limit of a high density, $n = N/\Omega \gg 1$, of weak scatterers, but with a constant value of $n\mathtt{v}_0^2$, it can be shown [1] that the second-order correlation function is

$$\langle V(\mathbf{r})V(\mathbf{r}')\rangle_d = n\mathtt{v}_0^2\delta(\mathbf{r}-\mathbf{r}'). \tag{31}$$

In other words, in this limit the Edwards model reduced to a white noise model discussed above, with $B = n\mathtt{v}_0^2$. This equivalence can be generalized to the case of a Gaussian model whose second-order correlation function has a finite range.

2.2.2 Photon self-energy

In order to describe multiple scattering of light in a disordered medium, we use the resolvent operator formalism [1]. From (8)-(9) we obtain the relation between the resolvent of the scattered photon, G, and the resolvent of the free photon, G_0, *i.e.,* in the absence of the disorder potential V

$$G = G_0 + G_0VG. \tag{32}$$

Formally, the expansion of (32) reads

$$G = G_0 + G_0VG_0 + G_0VG_0VG_0 + ... \tag{33}$$

As V represents a single scattering event and G_0 stands for the free propagation of the photon, (33) describes multiple scattering events. Using the white noise model (29), the disorder average of (33) yields

$$\langle G\rangle_d = G_0 + BG_0G_0G_0 + B^2G_0G_0G_0G_0G_0 + ..., \tag{34}$$

or

$$\langle G\rangle_d = G_0 + G_0\Sigma G_0 + G_0\Sigma G_0\Sigma G_0 + ..., \tag{35}$$

where Σ is the *photon self-energy*. Expression (35) is the iterative solution of the Dyson equation, namely

$$\langle G\rangle_d = G_0 + G_0\Sigma\langle G\rangle_d. \tag{36}$$

The self-energy represents the sum of all irreducible scattering diagrams. The pertubative expansion of the self-energy in a power series, controlled by the parameter B, is represented in Figure 1. The first term Σ_1, proportional to B, accounts for independent scattering events while the second term Σ_2, proportional to B^2, describes interference effects between pairs of scatterers. For small values of B, the main contribution is obtained by keeping only the first term Σ_1 which describes independent scattering events. Therefore, the first contribution to the self-energy is proportional to the density of scatterers and to the average single scattering amplitude. It should be noticed that the results above can be generalized to the case of a Gaussian model whose second-order correlation function has a finite range.

As the solution of the Dyson equation (36) reads

$$\langle G\rangle_d = \frac{1}{G_0^{-1} - \Sigma}, \tag{37}$$

the imaginary part of the self-energy is related to the decrease in the light wave amplitude due to scattering events, while its real part represents an energy correction. Therefore, several physical parameters that characterize multiple scattering of a photon are derived from the self-energy. The first one is the *elastic mean free path*, l_e, obtained from the imaginary part of the self-energy, namely

$$\frac{k}{l_e} = -\mathrm{Im}\Sigma_1, \tag{38}$$

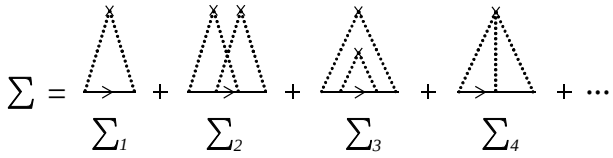

Figure 1: *Pertubative expansion of the self-energy in a power series in the parameter B. Solid lines account for the free photon propagator G_0. Pairs of dotted lines, connected by $\times$, stand for the second-order correlation function B. The first term Σ_1, proportional to B, accounts for independent scattering events while the second term Σ_2, proportional to B^2, describes interference effects between pairs of scatterers. After [1].*

where k is the photon wave number. Expression (38) is equivalent to the known formula

$$l_e = \frac{1}{n\langle\sigma\rangle_m} \tag{39}$$

where $\langle\sigma\rangle_m$ is the average single cross section, given for a resonant scattering by (24). The equivalence between the two expressions can be proven if one uses the optical theorem

$$\langle\sigma\rangle_m = -\frac{2\Omega}{\hbar c}\mathrm{Im}\langle\, T_{fi}(\mathbf{k}=\mathbf{k}', \hat{\varepsilon}=\hat{\varepsilon}')\rangle_m, \tag{40}$$

where T_{fi} is the scattering amplitude discussed in section 2.1. It can be shown [1] that

$$\mathrm{Im}\Sigma_2 = \frac{\pi}{2kl_e}\mathrm{Im}\Sigma_1. \tag{41}$$

Thus, in the *weak disorder* limit, *i.e.,* for $kl_e \gg 1$, we may neglect the interference effects between successive collisions represented by Σ_2. The physical meaning of this limit is that the light wave reaches its far field behavior between successive scattering events and therefore they may be considered as independent ones.

Another important physical quantity that characterizes multiple scattering of a photon is its *group velocity*, v_g, given in terms of the refraction index η by the usual relation

$$\frac{c}{v_g} = \eta + \omega\frac{d\eta}{d\omega}. \tag{42}$$

The refraction index for a dilute medium is

$$\eta = \sqrt{1 + n\mathrm{Re}\,\alpha}, \tag{43}$$

where the dynamic atomic polarizability α is proportional to the self-energy

$$\alpha = -\frac{1}{n}\left(\frac{c}{\omega}\right)^2 \Sigma_1. \tag{44}$$

Thus, we obtain that

$$\eta = \sqrt{1 - \left(\frac{c}{\omega}\right)^2 \mathrm{Re}\Sigma_1}. \tag{45}$$

Substituting (45) into (42) yields

$$\frac{c}{v_g} = \frac{1}{\eta}\left(1 - \frac{c^2}{2\omega}\frac{d}{d\omega}\mathrm{Re}\Sigma_1\right). \tag{46}$$

.

CHAPTER 3

Cooperative effects

This chapter reviews cooperative effects, such as superradiance and subradiance, which originate from collective atomic interactions with the radiation field. First, the classical analogous phenomenon of a system of coupled harmonic oscillators is presented. Then, a simple formalism for describing collective atomic states is introduced by defining the product atomic states and the Dicke states. After obtaining a convenient description of collective atomic states, the interaction with the quantum radiation field is considered. The rate of the collective spontaneous emission is calculated in an atomic product state, as well as in a Dicke state, for the case in which the atoms are confined to a volume much smaller than the radiation wavelength cubed. Next, for two atoms with an arbitrary inter-atomic distance, the cooperative emission rate and the cooperative level shift are obtained. Then, the finite propagation time of light is taken into account and retardation effects are studied. Finally, cooperative effects in a one-dimensional geometry and superradiance associated with a scalar radiation field are analyzed.

3.1 Classical superradiance

We start with a demonstration that superradiance is not a unique quantum effect, but also exists in classical systems such as coupled damped harmonic oscillators [18]. The equation of motion of a single classical harmonic oscillator is given by

$$\frac{d^2x}{dt^2} + 2\beta\frac{dx}{dt} + \omega_0^2 x = 0, \tag{47}$$

where ω_0 is the natural undamped angular frequency, β is the damping constant and x is the displacement. Its well-known solution is

$$x(t) = x(0)e^{-\beta t}\cos(\omega t + \phi), \tag{48}$$

with

$$\omega = \sqrt{\omega_0^2 - \beta^2}. \tag{49}$$

Now consider N similar oscillators, which are placed close together such as each one of them is damped by the other $N-1$ oscillators. The corresponding

equation of motion of the i-th oscillator is

$$\frac{d^2x_i}{dt^2} + 2\beta\frac{dx_i}{dt} + \omega_0^2 x_i = -2\beta\sum_{j\neq i}^{N}\frac{dx_j}{dt}. \tag{50}$$

Denoting $X = \sum_{i=1}^{N} x_i$ and summing over the N equations represented by (50), we obtain that

$$\frac{d^2X}{dt^2} + 2N\beta\frac{dX}{dt} + \omega_0^2 X = 0. \tag{51}$$

The solution of (51) is

$$X(t) = X(0)e^{-N\beta t}\cos(\omega t + \Phi), \tag{52}$$

with

$$\omega = \sqrt{\omega_0^2 - N^2\beta^2}. \tag{53}$$

If $x_i(t)$ are initially equal and in phase, then the solution indicates that the damping constant of each coupled oscillator is N times larger than the one of a single oscillator. This is a *superradiant* effect, and it will be discussed in the next sections.

3.2 Collective atomic states

Consider an ensemble of N identical non-degenerate two-level atoms, where the ground state and the excited state of the j-th atom are denoted, respectively, as $|g_j\rangle$ and $|e_j\rangle$. The single atom raising operator $b_j^\dagger$ and lowering operator b_j are defined [19] as

$$b_j^\dagger = |e_j\rangle\langle g_j| \qquad b_j = |g_j\rangle\langle e_j|, \tag{54}$$

while the collective raising operator Δ^+ and lowering operator Δ^- are

$$\Delta^+ = \sum_{j=1}^{N} b_j^\dagger \qquad \Delta^- = \sum_{j=1}^{N} b_j. \tag{55}$$

We also define the collective atomic spin operators

$$\Delta_1 = \frac{1}{2}\sum_{j=1}^{N}(b_j^\dagger + b_j) \qquad \Delta_2 = \frac{1}{2i}\sum_{j=1}^{N}(b_j^\dagger - b_j) \tag{56}$$

$$\Delta_3 = \frac{1}{2}\sum_{j=1}^{N}(b_j^\dagger b_j - b_j b_j^\dagger) \qquad \Delta^2 = \sum_{i=1}^{3}\Delta_i^2, \tag{57}$$

which obey the commutation relations

$$[\Delta_l, \Delta_m] = i\varepsilon_{lmn}\Delta_n \qquad [\Delta_l, \Delta^2] = 0, \tag{58}$$

where ε_{lmn} is the Levi-Civita tensor.

3.2.1 Atomic product states

An *atomic product state* $|\Phi\rangle$ is defined [19] as a state in which N_g atoms occupy the ground states, while the rest N_e atoms are in the excited states. This state is of the form

$$|\Phi\rangle = |g_1 g_2 e_3 ... g_N\rangle. \tag{59}$$

The total number of atoms is

$$N = N_g + N_e, \tag{60}$$

and a measure of the total atomic inversion is

$$M = \frac{1}{2}(N_e - N_g), \tag{61}$$

where M is either an integer or a half integer. Using the definitions (57) and (61), we may conclude that the atomic product state is an eigenstate of the collective spin operator Δ_3 with an eigenvalue M, namely

$$\Delta_3|\Phi\rangle = M|\Phi\rangle. \tag{62}$$

3.2.2 Dicke states

A *Dicke state* $|LM\rangle$ is defined [11] as a simultaneous eigenstate of the collective atomic spin operators Δ_3 and Δ^2, as they commute according to (58), namely

$$\Delta_3|LM\rangle = M|LM\rangle \qquad \Delta^2|LM\rangle = L(L+1)|LM\rangle, \tag{63}$$

where L is either an integer or a half integer ($|M| \leq L \leq N/2$). It is easy to show that the effects of the collective raising and lowering operators on a Dicke state are

$$\Delta^+|LM\rangle = \sqrt{(L-M)(L+M-1)}|LM+1\rangle, \tag{64}$$

$$\Delta^-|LM\rangle = \sqrt{(L+M)(L+M+1)}|LM-1\rangle. \tag{65}$$

As an example, consider the atomic product states of a two-atom system

$$|g_1g_2\rangle, \qquad |g_1e_2\rangle, \qquad |e_1g_2\rangle, \qquad |e_1e_2\rangle. \tag{66}$$

The corresponding Dicke states are the singlet state

$$|00\rangle = \frac{1}{\sqrt{2}}[|e_1g_2\rangle - |g_1e_2\rangle] \tag{67}$$

and the triplet states

$$\begin{aligned} |11\rangle &= |e_1e_2\rangle \\ |10\rangle &= \frac{1}{\sqrt{2}}[|e_1g_2\rangle + |g_1e_2\rangle] \\ |1-1\rangle &= |g_1g_2\rangle \end{aligned} \tag{68}$$

The states $|11\rangle$ and $|1-1\rangle$ correspond, respectively, to both atoms in their excited states and both atoms in their ground states. The singlet state $|00\rangle$ and the triplet state $|10\rangle$ both correspond to one atom in the excited state and the other in the ground state, but $|00\rangle$ is anti-symmetric where $|10\rangle$ is symmetric under an exchange of the atoms.

3.3 Cooperative spontaneous emission

After obtaining a convenient description of collective atomic states in the previous section, the interaction with the quantum radiation field is considered. The rate of the collective spontaneous emission is calculated in an atomic product state, as well as in a Dicke state, for the case in which the atoms are confined to a volume much smaller than the radiation wavelength cubed.

3.3.1 Dicke states

In the quantum vacuum $|0\rangle$, consider an ensemble of N identical non-degenerate atoms in a Dicke state $|LM\rangle$, placed close enough to each other, so one can use the long wavelength approximation discussed in Section 2.1 [11]. The corresponding interaction Hamiltonian is

$$V = -\mathbf{D}\cdot\mathbf{E}(\mathbf{0}). \tag{69}$$

The total electric dipole moment,

$$\mathbf{D} = \sum_{j=1}^{N} \mathbf{d}_j, \tag{70}$$

by using the closure relation and the Wigner-Eckart theorem, may be written as

$$\mathbf{D} = \langle g|\mathbf{d}|e\rangle \Delta^- + \langle e|\mathbf{d}|g\rangle \Delta^+, \tag{71}$$

where $\langle g|\mathbf{d}|e\rangle$ is the electric dipole matrix element of a single atom. The rate of transitions from the initial state $|LM;0\rangle$ to a final state $|f\rangle$ for energy conserving processes in which a photon is being emitted is

$$\Gamma \propto \sum_f |\langle f|S|LM;0\rangle|^2, \tag{72}$$

where

$$S = \langle g|\mathbf{d}|e\rangle \cdot \mathbf{E}^-(\mathbf{0})\Delta^- \tag{73}$$

and $\mathbf{E}^-(\mathbf{0})$ represents the creation part of the electric field operator at the origin of the coordinate system. Using the closure relation yields

$$\Gamma \propto \langle LM|\Delta^+\Delta^-|LM\rangle \tag{74}$$

and with the help of (64)-(65) we finally get for the cooperative emission rate

$$\Gamma = (L+M)(L-M+1)\Gamma_0, \tag{75}$$

where Γ_0 is the single atom spontaneous emission rate (21).

Let us examine several cases:

1. All the atoms occupy the excited states $|LM\rangle = |\frac{N}{2}\frac{N}{2}\rangle$

   The rate of the photon emission is

   $$\Gamma = N\Gamma_0, \tag{76}$$

   which corresponds to N atoms radiating independently.

2. Half the atoms occupy the excited states $|LM\rangle = |L0\rangle$

   The emission rate is

   $$\Gamma = L(L+1)\Gamma_0, \tag{77}$$

   where $0 \leq L \leq N/2$.

   As the emission rate varies as L, the latter is called the *cooperation number*. When the cooperation number has its highest value $|LM\rangle = |\frac{N}{2}0\rangle$, the emission rate is

   $$\Gamma = \frac{N}{2}\left(\frac{N}{2}+1\right)\Gamma_0, \tag{78}$$

   which for $N \gg 1$ is

   $$\Gamma \simeq \frac{N^2}{4}\Gamma_0. \tag{79}$$

   Thus, the emission rate of each coupled atom is $N/4$ times larger than the rate of a single atom! This is a *superradiant* effect and it has been already discussed classically in Section 3.1.

   But, if the cooperation number has its lowest value $|LM\rangle = |00\rangle$, the emission rate is $\Gamma = 0$, although half of the atoms are excited! Such a phenomenon is called *subradiance*.

3. One atom is excited $|LM\rangle = |L1 - \frac{N}{2}\rangle$

   The emission rate is

   $$\Gamma = \left(L+1-\frac{N}{2}\right)\left(L+\frac{N}{2}\right)\Gamma_0, \tag{80}$$

   where $|1 - N/2| \leq L \leq N/2$.

   Thus, for $L = N/2 - 1$ the emission rate is $\Gamma = 0$ in spite of the fact that one atom is excited, while for $L = N/2$ the emission rate is

   $$\Gamma = N\Gamma_0, \tag{81}$$

   although only one atom is excited.

4. All the atoms occupy the ground states $|LM\rangle = |\frac{N}{2} - \frac{N}{2}\rangle$

   The photon emission rate is $\Gamma = 0$ as expected.

Finally, we calculate the expectation value of the total electric dipole moment operator in a Dicke state. With the help of (71) and (64)-(65) we find that

$$\langle LM|\mathbf{D}|LM\rangle = \langle g|\mathbf{d}|e\rangle\langle LM|\Delta^-|LM\rangle + \langle e|\mathbf{d}|g\rangle\langle LM|\Delta^+|LM\rangle = 0. \quad (82)$$

Thus, the expectation value of the electric dipole moment operator vanishes in all Dicke states, including in the superradiant one!

3.3.2 Atomic product states

In the quantum vacuum $|0\rangle$, consider an ensemble of N identical non-degenerate atoms in the following product state

$$|\Phi\rangle = \prod_{j=1}^{N} \left(C_g|g_j\rangle + C_e|e_j\rangle\right), \quad (83)$$

where

$$|C_g|^2 + |C_e|^2 = 1. \quad (84)$$

The atoms placed at time t_0 close enough to each other, so one can use the long wavelength approximation [20]. The density operator of the coupled system at time t_0 is

$$\rho(t_0) = |\Phi\rangle\langle\Phi| \times |0\rangle\langle 0|, \quad (85)$$

and it obeys the following equation of motion

$$\frac{d\rho}{dt} = \frac{1}{i\hbar}[V(t), \rho(t)], \quad (86)$$

where the interaction Hamiltonian (69) is in the interaction picture. The iterative solution of (86) up to the second order reads

$$\rho(t) = \rho(t_0) + \frac{1}{i\hbar}\int_{t_0}^{t} dt_1[V(t_1), \rho(t_0)] + \frac{1}{(i\hbar)^2}\int_{t_0}^{t} dt_1 \int_{t_0}^{t_1} dt_2[V(t_1), [V(t_2), \rho(t_0)]]. \quad (87)$$

We are interested in transitions within a short time Δt from the initial state described by (85) to a final state in which a photon of wave vector $\mathbf{k}$ and polarization $\hat{\varepsilon}$ is emitted. The probability transition of such a photon is given by

$$\Gamma\Delta t = \sum_f \langle f; \mathbf{k}\hat{\varepsilon}|\rho(t_0 + \Delta t)|f; \mathbf{k}\hat{\varepsilon}\rangle, \quad (88)$$

where f denotes a final atomic state. As the final one-photon state is orthogonal to the initial vacuum state, by substituting (87) in (88), the first two terms of (87) vanish and we have to the lowest order

$$\Gamma \Delta t = \frac{1}{\hbar^2} \sum_f \int_{t_0}^{t+\Delta t} dt_1 \int_{t_0}^{t_1} dt_2 \langle f; \mathbf{k}\hat{\varepsilon}|V(t_1)\rho(t_0)V(t_2)|f; \mathbf{k}\hat{\varepsilon}\rangle + h.c. \quad (89)$$

After inserting the interaction Hamiltonian and the density operator, we obtain for energy conserving processes[1] that

$$\Gamma \propto \sum_f \langle f|\Delta^-|\Phi\rangle\langle\Phi|\Delta^+|f\rangle, \quad (90)$$

or with the help of the closure relation and (55)

$$\Gamma \propto \langle\Phi| \sum_{i=1}^{N} \sum_{j=1}^{N} b_i^\dagger b_j |\Phi\rangle. \quad (91)$$

Substituting (83) yields

$$\Gamma \propto \left(N|C_e|^2 + N(N-1)|C_e|^2|C_g|^2\right). \quad (92)$$

Finally, summing over all possible wave vectors and polarizations of the emitted photon leads to the following rate of the cooperative photon emission

$$\Gamma = \left(N|C_e|^2 + N(N-1)|C_e|^2|C_g|^2\right)\Gamma_0. \quad (93)$$

Let us examine several cases:

1. All the atoms occupy the excited states $C_g = 0$

   The rate of the photon emission is

   $$\Gamma = N\Gamma_0, \quad (94)$$

   which corresponds to N atoms radiating independently.

[1] Taking into account only energy conserving processes is equivalent to disregarding any highly oscillating contributions of the time integrals in (89).

2. Half the atoms occupy the excited states $C_g = C_e = \frac{1}{\sqrt{2}}$

   The emission rate is

$$\Gamma = \frac{N}{4}\left(N+1\right)\Gamma_0, \tag{95}$$

   which for $N \gg 1$ is

$$\Gamma \simeq \frac{N^2}{4}\Gamma_0. \tag{96}$$

   Thus, the emission rate of each coupled atom is $N/4$ times larger than the rate of a single atom. This is a *superfluorescence* effect which is partially analogous to superradiance.

3. All the atoms occupy the ground states $C_e = 0$

   The photon emission rate is $\Gamma = 0$ as expected.

Let us stress that although superradiance and superfluorescence are similar in their enhanced emission rates, they are different phenomena due to the following reasons:

1. Superradiance exists in a Dicke state, while superfluorescence appears in an atomic product state.

2. The expectation value of the electric dipole moment operator in a superradiant state is zero, while it has a non-vanishing value in a superfluorescent state.

3. Superradiance, unlike superfluorescence, has a complementary effect, namely subradiance.

3.4 Interaction potential and lifetime of a pair of atoms

So far, we have assumed that the atoms are confined to a volume much smaller than the radiation wavelength cubed and have used the long wavelength approximation. In this section we remove this assumption and calculate, for the case of two atoms, the lifetime and the interaction potential of the pair.

To this purpose, consider two identical two-level atoms[2], placed at positions $\mathbf{r}_1$ and $\mathbf{r}_2$, in the quantum radiation field [22, 23]. The ground state is a non-degenerate s state, $|g\rangle = |J_g = 0, m_g = 0\rangle$ and the excited state is

[2]The calculation below can be straightforwardly extended to the case of non-identical atoms [21].

a triply degenerate p state, $|e\rangle = |J_e = 1, m_e = 0, \pm 1\rangle$. The corresponding Hamiltonian is

$$H = H_0 + V, \tag{97}$$

where the non-interacting Hamiltonian is given by

$$H_0 = \frac{\hbar\omega_0}{2} \sum_{j=1}^{2} \sum_{m_e=-1}^{1} (|J_e m_e\rangle\langle J_e m_e| - |J_g m_g\rangle\langle J_g m_g|)_j + \sum_{\mathbf{k}\varepsilon} \hbar\omega_k a^\dagger_{\mathbf{k}\varepsilon} a_{\mathbf{k}\varepsilon}, \tag{98}$$

while the interaction Hamiltonian is

$$V = -\sum_{j=1}^{2} \mathbf{d}_j \cdot \mathbf{E}(\mathbf{r}_j). \tag{99}$$

$\mathbf{d}_j$ is the electric dipole moment operator of the j-atom and $\mathbf{E}(\mathbf{r})$ is the electric field operator given in (4). The Schrödinger equation is

$$i\hbar \frac{dc_n}{dt} = E_n c_n(t) + \sum_m c_m(t) \langle \phi_n | V | \phi_m \rangle, \tag{100}$$

where $c_n(t)$ is the probability amplitude of the eigenstate $|\phi_n\rangle$ of the non-interacting Hamiltonian (98), with the corresponding eigenenergy E_n. The states of the uncoupled atomic system and the radiation field are chosen to be

$$\begin{aligned} |\phi^+\rangle = |\phi_{10}\rangle &= \frac{1}{\sqrt{2}}[|e_1 g_2\rangle + |g_1 e_2\rangle]; 0\rangle \\ |\phi^-\rangle = |\phi_{00}\rangle &= \frac{1}{\sqrt{2}}[|e_1 g_2\rangle - |g_1 e_2\rangle]; 0\rangle \\ |\phi_{1-1}\rangle &= |g_1 g_2; \mathbf{k}\hat{\varepsilon}\rangle \\ |\phi_{11}\rangle &= |e_1 e_2; \mathbf{k}\hat{\varepsilon}\rangle. \end{aligned} \tag{101}$$

The first two states are the Dicke states $|10\rangle$ and $|00\rangle$ in vacuum. The third state refers to the Dicke state $|1-1\rangle$ where one photon in mode $(\mathbf{k}\hat{\varepsilon})$ exists, while the last state refers to the Dicke state $|11\rangle$ where one photon is in mode $(\mathbf{k}\hat{\varepsilon})$. For the sake of simplicity, the three transition possibilities $\Delta m = m_e - m_g = 0, \pm 1$ are being treated separately. Thus, in the states

$|\phi^{\pm}\rangle$, the Zeeman sub-level of $|e_1\rangle$ is the same as the one of $|e_2\rangle$, *i.e.*, $m_{e1} = m_{e2} = m_e$.

Substituting (101) in (100) and using the Laplace transform

$$c(s) = \int_0^\infty dt e^{-st} c(t) \tag{102}$$

for the initial condition $c^{\pm}(t=0) = 1$, yield

$$c^{\pm}(s) = \frac{1}{s + P(s) \pm Q(s)}, \tag{103}$$

where

$$P(s) = \sum_{\mathbf{k}\hat{\varepsilon}} |\zeta_1(\mathbf{k}\hat{\varepsilon})|^2 \left[\frac{1}{s + i(\omega_k - \omega_0)} + \frac{1}{s + i(\omega_k + \omega_0)} \right], \tag{104}$$

$$Q(s) = \sum_{\mathbf{k}\hat{\varepsilon}} \zeta_1(\mathbf{k}\hat{\varepsilon}) \zeta_2^*(\mathbf{k}\hat{\varepsilon}) \left[\frac{1}{s + i(\omega_k - \omega_0)} + \frac{1}{s + i(\omega_k + \omega_0)} \right], \tag{105}$$

with

$$\zeta_j(\mathbf{k}\hat{\varepsilon}) = \frac{1}{\hbar} \sqrt{\frac{\hbar\omega_k}{2\epsilon_0 \Omega}} \langle g|\mathbf{d}|e\rangle \cdot \hat{\varepsilon} e^{i\mathbf{k}\cdot\mathbf{r_j}}. \tag{106}$$

Going to the free continuum limit and summing over the wave vectors and the polarizations in (104) give

$$P(s = iz + \epsilon)|_{z=0} = \frac{\Gamma_0}{2}, \tag{107}$$

where the z-dependence has been neglected, as the single atom radiative shift is irrelevant for our purpose, and Γ_0 is given in (21). Using the plane wave expansion of spherical harmonics $Y_l^m(\theta, \varphi)$, namely

$$e^{i\mathbf{k}\cdot\mathbf{r}} = 4\pi \sum_{l=0}^{\infty} \sum_{m=-l}^{l} i^l J_l(kr) Y_l^m(\theta, \varphi)^* Y_l^m(\beta, \gamma), \tag{108}$$

where $\mathbf{r} = \mathbf{r}_1 - \mathbf{r}_2 = (r, \theta, \varphi)$, $\mathbf{k} = (k, \beta, \gamma)$ and $J_l(x)$ is the Bessel function of the first kind, we obtain from (105) that

$$Q(s = iz + \epsilon)|_{z=0} = -\frac{3\Gamma_0}{4} \left[\frac{ip(\theta)}{k_0 r} - \frac{iq(\theta)}{(k_0 r)^3} - \frac{q(\theta)}{(k_0 r)^2} \right] e^{ik_0 r}, \tag{109}$$

where $k_0 = \omega_0/c$. For $m_e = 0$

$$p(\theta) = \sin^2\theta \qquad q(\theta) = 1 - 3\cos^2\theta, \tag{110}$$

while for $m_e = \pm 1$

$$p(\theta) = \frac{1}{2}(1 + \cos^2\theta) \qquad q(\theta) = \frac{1}{2}(3\cos^2\theta - 1). \tag{111}$$

The inverse Laplace transform of (103) with (107)-(109) yields the probability amplitudes of $|\phi^{\pm}\rangle$

$$c^{\pm}(t) = e^{-\frac{\Gamma_0}{2}t[1\pm\xi(\mathbf{r})]}, \tag{112}$$

with

$$\mathrm{Re}\xi(\mathbf{r}) = \frac{3}{2}\left[\frac{p(\theta)\sin(k_0 r)}{k_0 r} - \frac{q(\theta)\sin(k_0 r)}{(k_0 r)^3} + \frac{q(\theta)\cos(k_0 r)}{(k_0 r)^2}\right] \tag{113}$$

and

$$\mathrm{Im}\xi(\mathbf{r}) = -\frac{3}{2}\left[\frac{p(\theta)\cos(k_0 r)}{k_0 r} - \frac{q(\theta)\cos(k_0 r)}{(k_0 r)^3} - \frac{q(\theta)\sin(k_0 r)}{(k_0 r)^2}\right]. \tag{114}$$

Thus, the cooperative spontaneous emission rate or the inverse lifetime, $\Gamma^{\pm}$, is

$$\frac{\Gamma^{\pm}}{\Gamma_0} = 1 \mp \frac{3}{2}\left[-p\frac{\sin k_0 r}{k_0 r} + q\left(\frac{\sin k_0 r}{(k_0 r)^3} - \frac{\cos k_0 r}{(k_0 r)^2}\right)\right] \tag{115}$$

and the cooperative radiative level shift or the interaction potential, $\Delta E^{\pm}$, is

$$\Delta E^{\pm} = \pm\frac{3\hbar\Gamma_0}{4}\left[-p\frac{\cos k_0 r}{k_0 r} + q\left(\frac{\cos k_0 r}{(k_0 r)^3} + \frac{\sin k_0 r}{(k_0 r)^2}\right)\right]. \tag{116}$$

When the atoms are well separated ($k_0 r \gg 1$), then the single atom emission rate is recovered from (115), namely

$$\Gamma^{\pm} = \Gamma_0, \tag{117}$$

but when the atoms are close enough ($k_0 r \ll 1$) we have

$$\Gamma^{\pm} = (1 \pm 1)\Gamma_0, \tag{118}$$

regardless of the value of m_e. The last result demonstrate, for the case of $N = 2$ atoms, Dicke superradiance and subradiance, as discussed in the previous section.

3.5 Retardation effects

In the previous section, we have neglected the propagation time of light due to the approximations employed in solving the equation of motion. Thus, the retardation time, r/c, does not appear in (112), so each atom is allowed to influence the other instantaneously. However, by keeping the leading z-dependence of Q one obtains [24] from (105) that

$$Q(s=iz+\epsilon)|_{|z|\ll\omega_0} = -\frac{3\Gamma_0}{4}\left[\frac{ip(\theta)}{k_0 r} - \frac{iq(\theta)}{(k_0 r)^3} - \frac{q(\theta)}{(k_0 r)^2}\right] e^{\frac{i(\omega_0 - z)r}{c}}. \tag{119}$$

Substituting in (103), for $\epsilon \ll 1$, yields

$$C^{\pm}(z) = -i\left[z - i\frac{\Gamma_0}{2} \pm i\frac{3\Gamma_0}{4}\left(\frac{ip(\theta)}{k_0 r} - \frac{iq(\theta)}{(k_0 r)^3} - \frac{q(\theta)}{(k_0 r)^2}\right) e^{\frac{i(\omega_0 - z)r}{c}}\right]^{-1}, \tag{120}$$

and by expanding the denominator into a power series we obtain

$$C^{\pm}(z) = -i\sum_{n=0}^{\infty}\left[\pm\frac{3\Gamma_0}{4}\left(\frac{p(\theta)}{k_0 r} - \frac{q(\theta)}{(k_0 r)^3} + \frac{iq(\theta)}{(k_0 r)^2}\right) e^{ik_0 r}\right]^n \frac{e^{-\frac{inzr}{c}}}{(z - i\frac{\Gamma_0}{2})^{n+1}}. \tag{121}$$

Finally, the inverse Laplace transform of (121) yields

$$c^{\pm}(t) = \sum_{n=0}^{\infty} R^{\pm}(n) e^{-\frac{\Gamma_0}{2}\left(t - \frac{nr}{c}\right)} 1\left(t - \frac{nr}{c}\right), \tag{122}$$

where

$$R^{\pm}(n) = \frac{1}{n!}\left[\pm\frac{3i}{2}\left(\frac{p(\theta)}{k_0 r} - \frac{q(\theta)}{(k_0 r)^3} + \frac{iq(\theta)}{(k_0 r)^2}\right) e^{ik_0 r}\right]^n \left[\frac{\Gamma_0}{2}\left(t - \frac{nr}{c}\right)\right]^n \tag{123}$$

and $1(t)$ is the unit step function. This solution describes many virtual photon exchanges between the two atoms, taking into account the retardation times nr/c, due to the finite speed of light. When neglecting these times in (122), we have

$$c^{\pm}(t) = e^{-\frac{\Gamma_0}{2}t}\sum_{n=0}^{\infty}\frac{1}{n!}\left[\pm\frac{3i}{2}\left(\frac{p(\theta)}{k_0 r} - \frac{q(\theta)}{(k_0 r)^3} + \frac{iq(\theta)}{(k_0 r)^2}\right) e^{ik_0 r}\right]^n \left(\frac{\Gamma_0}{2}t\right)^n, \tag{124}$$

thus (112) is recovered.

As pointed out in Section 3.1, superradiance also exists in classical systems. Therefore, an analogous discussion can be given for the coupling of two dipole oscillators by a classical electromagnetic field [25].

3.6 One-dimensional geometry

In the previous sections we have studied a three-dimensional system, where the photons could be emitted into any of the free space modes. Now, we consider superradiance in a one-dimensional geometry, a long pencil-shaped system of atoms, where the wave vectors of the radiation are restricted to be along the inter-atomic axis [24]. This situation corresponds to a directional emission along the system axis. We follow the calculation given in Sections 3.4-3.5 and add in (106) the constrain that $\mathbf{k} = k\hat{r}$, where $\hat{r}$ is a unit vector along the inter-atomic axis. Going to the one-dimemsional continuum limit gives

$$P'(s = iz + \epsilon)|_{z=0} = \frac{\Gamma'_0}{2}, \tag{125}$$

where the one-dimensional spontaneous emission rate is

$$\Gamma'_0 = \frac{d^2\omega_0}{\hbar\epsilon_0 c} \tag{126}$$

and the reduced matrix element is given in (22). We also obtain that

$$Q'(s = iz + \epsilon)|_{|z|\ll\omega_0} = \frac{\Gamma'_0}{2} e^{\frac{i(\omega_0 - z)r}{c}}. \tag{127}$$

The corresponding inverse Laplace transform yields the probability amplitudes

$$c'^{\pm}(t) = \sum_{n=0}^{\infty} R'^{\pm}(n) e^{-\frac{\Gamma'_0}{2}\left(t - \frac{nr}{c}\right)} 1\left(t - \frac{nr}{c}\right), \tag{128}$$

where

$$R'^{\pm}(n) = \frac{1}{n!}\left[\mp e^{ik_0 r}\right]^n \left[\frac{\Gamma'_0}{2}\left(t - \frac{nr}{c}\right)\right]^n. \tag{129}$$

When neglecting retardation effects in (128) one obtains that

$$c'^{\pm}(t) = e^{-\frac{\Gamma'_0}{2} t[1 \pm \xi'(r)]}, \tag{130}$$

with

$$\xi'(r) = e^{ik_0 r}. \tag{131}$$

Thus, the one-dimensional cooperative spontaneous emission rate or the inverse lifetime, $\Gamma'^{\pm}$, is

$$\frac{\Gamma'^{\pm}}{\Gamma'_0} = 1 \pm \cos k_0 r \tag{132}$$

and the one-dimensional cooperative radiative level shift or the interaction potential, $\Delta E'^{\pm}$, is

$$\Delta E'^{\pm} = \pm \frac{\hbar \Gamma'_0}{2} \sin k_0 r. \tag{133}$$

When the atoms are close enough ($k_0 r \ll 1$), Dicke limit is obtained

$$\Gamma'^{\pm} = (1 \pm 1)\Gamma'_0, \tag{134}$$

as in the three-dimensional case (118). But, when the atoms are well separated ($k_0 r \gg 1$), the single atom limit (117) is not recovered since the one-dimensional inverse lifetime (132) is a periodic function of the inter-atomic distance, while the three-dimensional one (115) falls off with the inter-atomic separation. Similarly, the range of the one-dimensional interaction potential (133) is infinite, while it is finite in the three-dimensional case (116).

Thus, we may conclude that there is a fundamental difference between the one the the tree dimensional geometries. This difference is going to be reflected in the calculation of photon escape rates from an atomic gas, presented in Chapter 5.

3.7 Scalar radiation field

Finally, we consider the case where non-degenerate atoms interact with a scalar radiation field [26]. The corresponding Hamiltonian is

$$H = \frac{\hbar\omega_0}{2} \sum_{j=1}^{2} (|e\rangle\langle e| - |g\rangle\langle g|)_j + \sum_{\mathbf{k}} \hbar\omega_k a^\dagger_{\mathbf{k}} a_{\mathbf{k}} - \sum_{j=1}^{2} d_j E(\mathbf{r}_j), \tag{135}$$

where the scalar field is

$$E(\mathbf{r}) = i \sum_{\mathbf{k}} \sqrt{\frac{\hbar\omega_k}{2\epsilon_0 \Omega}} (a_{\mathbf{k}}\ e^{i\mathbf{k}\cdot\mathbf{r}} - a^\dagger_{\mathbf{k}} e^{-i\mathbf{k}\cdot\mathbf{r}}). \tag{136}$$

We follow the calculation given in Sections 3.4-3.5, omit the summation over the polarizations in (104)-(105) and replace (106) with

$$\zeta''_j(\mathbf{k}) = \frac{1}{\hbar} \sqrt{\frac{\hbar\omega_k}{2\epsilon_0 \Omega}} \langle g|d|e\rangle e^{i\mathbf{k}\cdot\mathbf{r_j}}. \tag{137}$$

Going to the free continuum limit, we obtain that

$$P''(s = iz + \epsilon)|_{z=0} = \frac{\Gamma_0''}{2} \tag{138}$$

and

$$Q''(s = iz + \epsilon)|_{|z| \ll \omega_0} = -\frac{\Gamma_0''}{2} \frac{i}{k_0 r} e^{\frac{i(\omega_0 - z)r}{c}}, \tag{139}$$

where the scalar spontaneous emission rate is

$$\Gamma_0'' = \frac{3}{2}\Gamma_0. \tag{140}$$

The corresponding inverse Laplace transform yields the probability amplitudes

$$c''^{\pm}(t) = \sum_{n=0}^{\infty} R''^{\pm}(n) e^{-\frac{\Gamma_0''}{2}\left(t - \frac{nr}{c}\right)} 1\left(t - \frac{nr}{c}\right), \tag{141}$$

where

$$R''^{\pm}(n) = \frac{1}{n!}\left[\pm i \frac{e^{ik_0 r}}{k_0 r}\right]^n \left[\frac{\Gamma_0''}{2}\left(t - \frac{nr}{c}\right)\right]^n. \tag{142}$$

When neglecting retardation effects in (141) one obtains that

$$c''^{\pm}(t) = e^{-\frac{\Gamma_0''}{2} t[1 \pm \xi''(r)]}, \tag{143}$$

with

$$\xi''(r) = -i \frac{e^{ik_0 r}}{k_0 r}. \tag{144}$$

Thus, the scalar cooperative spontaneous emission rate or the inverse lifetime, $\Gamma''^{\pm}$, is

$$\frac{\Gamma''^{\pm}}{\Gamma_0''} = 1 \pm \frac{\sin k_0 r}{k_0 r} \tag{145}$$

and the scalar cooperative radiative level shift or the interaction potential, $\Delta E''^{\pm}$, is

$$\Delta E''^{\pm} = \mp \frac{\hbar \Gamma_0''}{2} \frac{\cos k_0 r}{k_0 r}. \tag{146}$$

When the atoms are well separated ($k_0 r \gg 1$), then the single atom emission rate is recovered from (145), namely

$$\Gamma''^{\pm} = \Gamma_0'' \tag{147}$$

and when the atoms are close enough ($k_0 r \ll 1$) Dicke limit is obtained

$$\Gamma''^{\pm} = (1 \pm 1)\Gamma''_0. \tag{148}$$

These results coincide with the ones associated with the vectorial case (117)-(118). We will use the properties of the scalar case in the following chapters.

.

CHAPTER 4

Multiple scattering properties of superradiant pairs

In Chapter 2 we have studied multiple scattering of light by a gas of non-interacting atoms and have defined some physical parameters, like the elastic mean free path and the group velocity, that characterize the photon transport in random media. Let us stress that in this study, the mutual influence between the scatterers has been neglected. In Chapter 3 we have considered cooperative effects, such as superradiance and subradiance, which originate from the interaction between atoms through the radiation field. In the rest of the dissertation we combine these two elements, *i.e.,* study multiple scattering of photons in disordered media while taking into account cooperative effects. Chapter 4 deals with the multiple scattering of superradiant pairs [13, 14], while Chapter 5 considers higher order terms that account for cooperative effects between more than two atoms [15].

We start by describing the model which consists of pairs of two-level atoms placed in an external radiation field where the Doppler shift and recoil effects are negligible. Then, we calculate the average interaction potential of a pair of atoms in a Dicke state by averaging upon the random orientations of pairs of atoms with respect to the wave vector of a photon incident on the atomic cloud. Next, we study the scattering of a photon by such pairs and compare the results to the case where a classical wave is being scattered by a pair of atoms. This comparison allows to find an unexpected connection between superradiance and mesoscopic effects. Finally, we consider the multiple scattering of photons by pairs of atoms and calculate the elastic mean free path and the group velocity of photons in the random medium.

4.1 Model

As in Section 3.4, atoms are taken to be degenerate, two-level systems denoted by $|g\rangle = |J_g = 0, m_g = 0\rangle$ for the ground state and $|e\rangle = |J_e = 1, m_e = 0, \pm 1\rangle$ for the excited state. The energy separation between the two levels is $\hbar\omega_0$ and the natural width of the excited level is $\hbar\Gamma_0$. We consider a pair of such atoms, placed at positions $\mathbf{r}_1$ and $\mathbf{r}_2$, in an external radiation field where the corresponding Hamiltonian is

$$H = H_0 + V, \tag{149}$$

with

$$H_0 = \frac{\hbar\omega_0}{2}\sum_{j=1}^{2}\sum_{m_e=-1}^{1}(|J_e m_e\rangle\langle J_e m_e| - |J_g m_g\rangle\langle J_g m_g|)_j + \sum_{\mathbf{k}\varepsilon}\hbar\omega_k a^\dagger_{\mathbf{k}\varepsilon}a_{\mathbf{k}\varepsilon}. \quad (150)$$

The interaction V between the radiation field and the electric dipole moments of the atoms is

$$V = -\sum_{j=1}^{2}\mathbf{d}_j\cdot\mathbf{E}(\mathbf{r}_j), \quad (151)$$

where $\mathbf{E}(\mathbf{r})$ is the electric field operator given in (4) and $\mathbf{d}_j$ is the electric dipole moment operator of the j-th atom. According to (71), for a given $\Delta m = m_e - m_g$ transition, $\mathbf{d}_j$ may be written as

$$\mathbf{d}_j = \langle g|\mathbf{d}|e\rangle b_j + \langle e|\mathbf{d}|g\rangle b_j^\dagger, \quad (152)$$

where the atomic raising and lowering operators have been defined in (54). As in Section 2.1, we assume that the typical speed of the atoms is small compared to $v_{max} = \Gamma_0/k$ but large compared to $v_{min} = \hbar k/\mu$, where μ is the mass of the atom, so that it is possible to neglect the Doppler shift and recoil effects.

4.2 Dicke states

The absorption of a photon by a pair of atoms in their ground states leads to a configuration where the two atoms, one excited and the second in its ground state, undergo many virtual photon exchanges which give rise to an interaction potential and to a modified lifetime as compared to independent atoms. These two quantities have been obtained in Section 3.4 and are given in (115)-(116).

4.2.1 Average interaction potential and lifetime

For a photon of wave vector $\mathbf{k}$ incident on an atomic cloud, the interaction potential between two atoms is obtained from (116) by averaging upon the random orientations of the pairs of atoms with respect to $\mathbf{k}$. According to (110)-(111), $\langle p\rangle = 2/3$ and $\langle q\rangle = 0$ regardless of m_e, where $\langle\cdots\rangle$ denotes angular averaging. Thus, the average interaction potential is

$$V_e^{\pm}(r) = \langle\Delta E^{\pm}\rangle = \mp\frac{\hbar\Gamma_0}{2}\frac{\cos k_0 r}{k_0 r}. \quad (153)$$

Similarly, the average inverse lifetime is obtained from (115) and is given by

$$\Gamma_e^{\pm}(r) = \langle \Gamma^{\pm} \rangle = \Gamma_0 \left(1 \pm \frac{\sin k_0 r}{k_0 r} \right). \tag{154}$$

We notice that expressions (153)-(154) coincide[3] with the ones obtained by considering the interaction of atoms with a scalar radiation field (145)-(146). This is due to the averaging procedure, in which the longitudinal contribution in (115)-(116) vanishes as $\langle q \rangle = 0$. We also notice that whereas for a single pair of atoms, the potential (116) is anisotropic and decays at short distance like $1/r^3$, on average over angular configurations, the interaction potential (153) becomes isotropic and decays like $1/r$, and for close enough atoms ($k_0 r \ll 1$) in a superradiant state it becomes attractive. A related behavior for the orientation average interaction potential has been obtained for the case of an intense radiation field [27], and it has recently been investigated in order to study effects of a long range and attractive potential between atoms in a Bose-Einstein condensate for a far detuned light [28]. This latter potential corresponds to the interaction energy between two atoms in their ground states in the presence of at least one photon. Let us stress that the average interaction potential (153) is different, as it corresponds to the interaction energy of Dicke states $|L0\rangle$ in vacuum.

4.2.2 Scattering properties

In order to study the scattering properties of Dicke states we use the collision operator

$$T(z) = V + VG(z)V, \tag{155}$$

introduced in Section 2.1, where V is given by (151) and G is the resolvent associated with the Hamiltonian (149). The matrix element that describes the transition amplitude from the initial state $|i\rangle = |1-1; \mathbf{k}\hat{\varepsilon}\rangle$, where the two atoms are in their ground states in the presence of a photon of frequency $\omega = ck$ and polarization $\hat{\varepsilon}$, to the final state $|f\rangle = |1-1; \mathbf{k}'\hat{\varepsilon}'\rangle$ is

$$T_{fi} = \langle f | T(z = \hbar(\omega - \omega_0)) | i \rangle, \tag{156}$$

with $k = k'$. By using the closure relation we may write T_{fi} as a sum of a superradiant and a subradiant contribution

$$T_{fi} = T^{+} + T^{-}, \tag{157}$$

[3]Up to the replacement of Γ_0'' by Γ_0.

with

$$T^{\pm} = \langle f|V|\phi^{\pm}\rangle\langle\phi^{\pm}|G(z=\hbar(\omega-\omega_0))|\phi^{\pm}\rangle\langle\phi^{\pm}|V|i\rangle, \tag{158}$$

where $|\phi^{\pm}\rangle$ are the Dicke states $|L0\rangle$ in vacuum introduced in (101). The two matrix elements in (158) represent the absorption and the emission of a real photon by the pair of atoms. They are easily obtained from (151)-(152) and lead, for resonant scattering, to the following expressions for the scattering amplitudes

$$T^{+} = Ce^{i(\mathbf{k}-\mathbf{k}')\cdot\mathbf{R}}\cos\left(\frac{\mathbf{k}\cdot\mathbf{r}}{2}\right)\cos\left(\frac{\mathbf{k}'\cdot\mathbf{r}}{2}\right)\sum_{m_e=-1}^{1}(\hat{d}^{*}\cdot\hat{\varepsilon}'^{*})(\hat{d}\cdot\hat{\varepsilon})G^{+} \tag{159}$$

and

$$T^{-} = Ce^{i(\mathbf{k}-\mathbf{k}')\cdot\mathbf{R}}\sin\left(\frac{\mathbf{k}\cdot\mathbf{r}}{2}\right)\sin\left(\frac{\mathbf{k}'\cdot\mathbf{r}}{2}\right)\sum_{m_e=-1}^{1}(\hat{d}^{*}\cdot\hat{\varepsilon}'^{*})(\hat{d}\cdot\hat{\varepsilon})G^{-}. \tag{160}$$

We have defined

$$C = \frac{3\pi\hbar^2c^3\Gamma_0}{\Omega\omega^2} \tag{161}$$

$$\mathbf{r} = \mathbf{r}_1 - \mathbf{r}_2 \qquad \mathbf{R} = \frac{\mathbf{r_1}+\mathbf{r_2}}{2} \tag{162}$$

and the natural width, the reduced matrix element and its corresponding unit vector are given in (21)-(22). The propagators $G^{\pm}$ are the expectation values of the resolvent in the Dicke states $|\phi^{\pm}\rangle$, namely

$$G^{\pm} = \langle\phi^{\pm}|G(\hbar\delta)|\phi^{\pm}\rangle, \tag{163}$$

where close to resonance $\delta = \omega - \omega_0 \ll \omega_0$. The propagators result from the sum of an infinite series of virtual photon exchanges between the two atoms in the pair and are given in terms of (115)-(116) by

$$G^{\pm} = \left(\hbar\delta - \Delta E^{\pm} + i\hbar\frac{\Gamma^{\pm}}{2}\right)^{-1}. \tag{164}$$

The average propagator is obtained by averaging (164) over the random orientations of the pairs of atoms with respect to the wave vector $\mathbf{k}$ of the incident photon. However, in a first stage, we replace the average propagator $\langle G^{\pm}\rangle$, by the following effective propagator

$$G_e^{\pm} = \left(\hbar\delta - \langle\Delta E^{\pm}\rangle + i\hbar\frac{\langle\Gamma^{\pm}\rangle}{2}\right)^{-1}. \tag{165}$$

Expression (165), according to Section 4.2.1, is the propagator associated with a scalar radiation field. Using (153)-(154), we obtain that

$$G_e^{\pm} = \left[\hbar\left(\delta + i\frac{\Gamma_0}{2} \pm \frac{\Gamma_0}{2}\frac{e^{ik_0 r}}{k_0 r}\right)\right]^{-1}. \tag{166}$$

This expression constitutes, a priori, a rough approximation of the exact average $\langle G^{\pm}\rangle$. We shall calculate, in Section 4.4, the exact average propagator and show that it is rather complicated, whereas the approximate expression using a scalar wave (166) gives similar qualitative results. Thus, in the following, we will use the scalar wave approximation in order to provide, in a rather simple way, the main features of multiple scattering by superradiant pairs.

With the help of (166), the scattering amplitudes are

$$T_e^{+} = Ce^{i(\mathbf{k}-\mathbf{k}')\cdot\mathbf{R}}\cos\left(\frac{\mathbf{k}\cdot\mathbf{r}}{2}\right)\cos\left(\frac{\mathbf{k}'\cdot\mathbf{r}}{2}\right)G_e^{+}\sum_{m_e=-1}^{1}(\hat{d}^*\cdot\hat{\varepsilon}'^*)(\hat{d}\cdot\hat{\varepsilon}) \tag{167}$$

and

$$T_e^{-} = Ce^{i(\mathbf{k}-\mathbf{k}')\cdot\mathbf{R}}\sin\left(\frac{\mathbf{k}\cdot\mathbf{r}}{2}\right)\sin\left(\frac{\mathbf{k}'\cdot\mathbf{r}}{2}\right)G_e^{-}\sum_{m_e=-1}^{1}(\hat{d}^*\cdot\hat{\varepsilon}'^*)(\hat{d}\cdot\hat{\varepsilon}). \tag{168}$$

We notice that at short distances ($k_0 r \ll 1$), the subradiant amplitude T_e^{-} becomes negligible as compared to the superradiant term T_e^{+}. Therefore, at short distances, only the superradiant term contributes to the scattering amplitude (157). More precisely, at short distances the effective propagator G_e^{-} diverges for $\delta/\Gamma_0 = 1/(2k_0 r)$ and G_e^{+} is purely imaginary for $\delta/\Gamma_0 = -1/(2k_0 r)$. Thus, for $\delta/\Gamma_0 < 1/(2k_0 r)$ the imaginary part of the subradiative term (168) is negligible as compared to the imaginary part of the superradiative term (167) and for $|\delta|/\Gamma_0 < 1/(2k_0 r)$ both the real part and the imaginary part of (168) are negligible as compared to (167).

We can interpret these results by saying that the time evolution of the initial state

$$|e_1 g_2; 0\rangle = \frac{1}{\sqrt{2}}[|\phi^{+}\rangle + |\phi^{-}\rangle] \tag{169}$$

corresponds, for times shorter than $1/\Gamma_0$, to a periodic exchange of a virtual photon between the two atoms at the Rabi frequency

$$\Omega_R = \left|\frac{\langle\Delta E^{-}\rangle - \langle\Delta E^{+}\rangle}{\hbar}\right|. \tag{170}$$

At short distances, with the help of (153), we obtain

$$\Omega_R \simeq \frac{\Gamma_0}{k_0 r}, \tag{171}$$

so that the Rabi frequency is much larger than Γ_0, thus the atoms undergo many virtual photon exchanges before they return to their ground states and a real photon is emitted. At large distances, we have

$$\Omega_R = \frac{\Gamma_0}{k_0 r} |\cos k_0 r|, \tag{172}$$

so that the Rabi frequency becomes much smaller than Γ_0 and the atoms make only a few oscillations before a real photon is emitted. Thus, their interaction potential is negligible.

Finally, we notice that the angular distribution of the light scattered by two atoms in a superradiant state is nearly identical to that of a single atom. This follows from the fact that at short distances the corresponding additional phase shift, $k_0 r \cos\vartheta$, between waves emitted by the two atoms becomes negligible (ϑ is the angle between the direction of the emitted photon and the axis between the two atoms).

4.2.3 Superradiance and mesoscopic effects

It is interesting to derive the results of the previous section in a way that reveals a connection with mesoscopic effects [1]. To this purpose, we consider the resonant interaction of two non-degenerate two-level atoms (each characterized by an energy separation $\hbar\omega_0$ and a natural width $\hbar\Gamma_0$ of the excited state) with the classical scalar radiation field, whose free propagator is given by

$$g_0(r) = -\frac{e^{ikr}}{4\pi r}, \tag{173}$$

where close to resonance $k \simeq k_0$. The scattering amplitude defined in (156) can be rewritten[4] as a sum of two contributions [8], namely

$$T_{fi} = T_1 + T_2. \tag{174}$$

Amplitude T_1 represents two processes, a single scattering by the first atom, placed at $\mathbf{r}_1$, and the process in which the wave is being absorbed by the first

[4]This rewriting of the amplitude T_{fi} is defined up to a proportionality constant, which accounts for the quantum nature of the radiation field and the photon polarization.

atom but emitted by the second one, placed at $\mathbf{r}_2$. It is given by

$$T_1 = \frac{\mathtt{t}}{1-\mathtt{t}^2 g_0^2}\left[e^{i(\mathbf{k}-\mathbf{k}')\cdot\mathbf{r}_1} + \mathtt{t}\, g_0\, e^{i(\mathbf{k}\cdot\mathbf{r}_1 - \mathbf{k}'\cdot\mathbf{r}_2)}\right]. \tag{175}$$

Similarly, amplitude T_2 is

$$T_2 = \frac{\mathtt{t}}{1-t^2 g_0^2}\left[e^{i(\mathbf{k}-\mathbf{k}')\cdot\mathbf{r}_2} + \mathtt{t}\, g_0\, e^{i(\mathbf{k}\cdot\mathbf{r}_2 - \mathbf{k}'\cdot\mathbf{r}_1)}\right]. \tag{176}$$

Here

$$\mathtt{t} = \frac{4\pi}{k_0}\frac{\Gamma_0''/2}{\delta + i\Gamma_0''/2} \tag{177}$$

is the classical, scalar analogous of (20), *i.e.,* is the amplitude of a scalar wave scattered resonantly by a single atom at the origin, and Γ_0'' is given in (140). The prefactor $\mathtt{t}/(1-\mathtt{t}^2 g_0^2)$ accounts for the summation of the infinite series of virtual "scalar photon" exchanges between the two scatterers. Substituting (175)-(176) in (174) yields

$$T_{fi} = 2\mathtt{t}e^{i(\mathbf{k}-\mathbf{k}')\cdot\mathbf{R}}\left[\frac{\cos\left(\frac{\mathbf{k}\cdot\mathbf{r}}{2}\right)\cos\left(\frac{\mathbf{k}'\cdot\mathbf{r}}{2}\right)}{1-\mathtt{t}g_0} + \frac{\sin\left(\frac{\mathbf{k}\cdot\mathbf{r}}{2}\right)\sin\left(\frac{\mathbf{k}'\cdot\mathbf{r}}{2}\right)}{1+\mathtt{t}g_0}\right], \tag{178}$$

where we have used (162). When inserting (173) and (177) in (178) we have

$$T_{fi} = \frac{4\pi}{k_0}e^{i(\mathbf{k}-\mathbf{k}')\cdot\mathbf{R}}\left[\frac{\Gamma_0''\cos\left(\frac{\mathbf{k}\cdot\mathbf{r}}{2}\right)\cos\left(\frac{\mathbf{k}'\cdot\mathbf{r}}{2}\right)}{\delta + i\frac{\Gamma_0''}{2} + \frac{\Gamma_0''}{2}\frac{e^{ik_0 r}}{k_0 r}} + \frac{\Gamma_0''\sin\left(\frac{\mathbf{k}\cdot\mathbf{r}}{2}\right)\sin\left(\frac{\mathbf{k}'\cdot\mathbf{r}}{2}\right)}{\delta + i\frac{\Gamma_0''}{2} - \frac{\Gamma_0''}{2}\frac{e^{ik_0 r}}{k_0 r}}\right]. \tag{179}$$

Thus, the analogous expressions of (167)-(168) have been obtained, and the superradiant and the subradiant terms can be identified.

Now, we single out in the total amplitude T_{fi} the single scattering contribution T_s, where

$$T_s = \frac{\mathtt{t}}{1-\mathtt{t}^2 g_0^2}\left[e^{i(\mathbf{k}-\mathbf{k}')\cdot\mathbf{r}_1} + e^{i(\mathbf{k}-\mathbf{k}')\cdot\mathbf{r}_2}\right], \tag{180}$$

and write the intensity associated with the higher order scattering term shown in Figure 2 as

$$|T_{fi} - T_s|^2 = 2\left|\frac{\mathtt{t}^2 g_0}{1-\mathtt{t}^2 g_0^2}\right|^2 \left[1 + \cos(\mathbf{k}+\mathbf{k}')\cdot(\mathbf{r}_1 - \mathbf{r}_2)\right]. \tag{181}$$

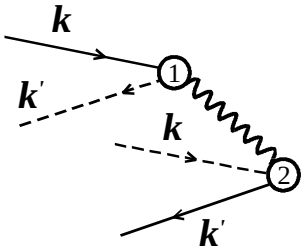

Figure 2: *Schematic representation of the two amplitudes that describe double scattering of a scalar wave. The wavy line accounts for the exchange of a virtual "scalar photon" between the two atoms. This diagram is analogous to the coherent backscattering in mesoscopic physics.*

The structure of relation (181) is very reminiscent to that of the so-called coherent backscattering intensity which occurs in mesoscopic physics in the context of the multiple elastic scattering of light. In the latter case, averaging over the spatial positions $\mathbf{r}_1$ and $\mathbf{r}_2$ makes the interference term $\cos(\mathbf{k}+\mathbf{k}')\cdot(\mathbf{r}_1-\mathbf{r}_2)$ vanish in general, with two exceptions:

1. $\mathbf{k}+\mathbf{k}' \simeq 0$: In the direction exactly opposite to the direction of incidence, the intensity is twice the classical value. This phenomenon is known as coherent backscattering.

2. $\mathbf{r}_1 = \mathbf{r}_2$: Closed multiple scattering trajectories which are at the origin of the phenomenon of weak localization.

In (181) the interference term reaches its maximal value for $\mathbf{r}_1 = \mathbf{r}_2$. When it happens we obtain from (175)-(176), (167) and (178) that $T_1 = T_2 \propto T_e^+/2$, up to a proportionality factor. Thus, for a closed trajectory, the contribution is due to the superradiant term alone.

4.3 Transport properties of superradiant pairs

Now we consider resonant multiple scattering of a photon by superradiant pairs built out of atoms separated by a short distance r and coupled by the attractive interaction potential V_e^+. This situation corresponds to a dilute gas that is assumed to fulfill

$$r \ll \lambda_0 \ll n^{-1/3}, \tag{182}$$

where n is the density of pairs and $\lambda_0 = 2\pi/k_0$ is the atomic transition wavelength. The limiting case (182) corresponds to a situation where the two atoms that form a superradiant pair, through exchange of a virtual photon, constitute an effective scatterer and cooperative interactions between otherwise well-separated pairs are negligible. Let us stress that we study here a simplified model where only pairs of atoms have been taken into account. A more realistic model should include higher order terms that account for cooperative effects between more than two atoms. We do not consider these terms, as the purpose of the current model is to examine the contribution of superradiant pairs to the transport properties of the gas. In Chapter 5 we will study the contribution of the higher order terms to the multiple scattering properties of the photon.

4.3.1 Effective self-energy

We use the Edwards model, introduced in Section 2.2.1, to describe the medium as a discrete collection of N superradiant pairs in a volume Ω. As each pair, located at $\mathbf{R}_j$, is characterized by its scattering potential $\mathtt{u}(\mathbf{R}-\mathbf{R}_j)$, the disorder potential is given by

$$U(\mathbf{R}) = \sum_{j=1}^{N} \mathtt{u}(\mathbf{R} - \mathbf{R}_j). \tag{183}$$

In the limit of a high density of weak scattering pairs the Edwards model reduces to a Gaussian model characterized by the condition (28).

According to Section 2.2.2, the resolvent G of a scattered photon is related to the free photon resolvent G_0, *i.e.*, in the absence of disorder potential, by the equation

$$G = G_0 + G_0 U G. \tag{184}$$

Averaging (184) over disorder and using the properties of the Gaussian model yield the Dyson equation

$$\langle G \rangle_d = G_0 + G_0 \Sigma \langle G \rangle_d, \tag{185}$$

where $\langle \cdots \rangle_d$ denotes averaging over the random potential and Σ is the photon self-energy. As explained above, the first term Σ_1 describes independent scattering events. Therefore, the first contribution to the self-energy is proportional to the density of scatterers and to the average single scattering

amplitude and it is given, for $k_0 r \ll 1$, by

$$\Sigma_1 = \frac{6\pi n}{k_0} C_{J_g J_e} \hbar \Gamma_0 \overline{G}_e^+, \tag{186}$$

where $C_{J_g J_e}$ is obtained by averaging the polarization-dependent part of (167) over Zeeman sublevels m for $\hat{\varepsilon} = \hat{\varepsilon}'$, and it is given in (25).

The additional average, denoted by $\overline{\cdots}$, is taken over distances r up to a maximal value r_m which accounts for all possible mechanisms that may break the pairs. The value of r_m can be estimated by comparing the kinetic energy K of a superradiant pair to its average potential energy V_e^+. We have $K \simeq \hbar^2/(\mu r^2)$ and from (153) we obtain that $V_e^+ \simeq -\hbar\Gamma_0/(2k_0 r)$. Minimizing the average energy

$$E(r) \simeq \frac{\hbar^2}{\mu r^2} - \frac{\hbar\Gamma_0}{2k_0 r} \tag{187}$$

with respect to r yields

$$k_0 r_m = 4\frac{\hbar k_0^2}{\mu\Gamma_0} \tag{188}$$

or

$$k_0 r_m = 4\frac{v_{min}}{v_{max}}, \tag{189}$$

where the speeds v_{min} and v_{max} have been defined in Section 4.1. For typical values, $\Gamma_0 = 10^7$ s^{-1} and $k_0 = 10^7$ m^{-1}, one obtains that $k_0 r_m \simeq 0.05 \ll 1$, as it has been assumed.

For $J_g = 0$ and $J_e = 1$, $C_{01} = 1$ and using (166) we rewrite (186) as

$$\Sigma_1 = \frac{6\pi n}{k_0}\frac{1}{r_m}\int_0^{r_m} \frac{dr}{\frac{\delta}{\Gamma_0} + \frac{1}{2k_0 r} + i}. \tag{190}$$

We stress again that, in our approach, a pair of atoms in a superradiant state is considered as a single scatterer and the medium parameters are derived from Σ_1 as it will be shown in the next sections. In contrast to our treatment, others [29, 30] consider multiple scattering of a real photon by independent atoms and use the second term Σ_2, which describes interference effects between the scatterers, to calculate corrections to the elastic mean free path and to the refractive index of the medium. In the latter approach, no distinction has been made between the external photon that performs multiple scattering on all atoms and virtual photons exchanged between two atoms

in a superradiant state, leading to the average interaction potential V_e^+.

4.3.2 Elastic mean free path

As explained in Section 2.2.2, the elastic mean free path l_e is obtained from the imaginary part of the self-energy, namely

$$\frac{k_0}{l_e} = -\mathrm{Im}\Sigma_1. \tag{191}$$

Therefore, from (190)-(191) we obtain that

$$\frac{1}{l_e(\delta)} = \frac{6\pi n}{k_0^2} f_1\left(k_0 r_m, \frac{\delta}{\Gamma_0}\right), \tag{192}$$

where we have defined the function[5]

$$f_1(u,v) = \frac{1}{2u}\int_0^{2u} \frac{dx}{1+(v+\frac{1}{x})^2}. \tag{193}$$

It is interesting to compare l_e to the elastic mean free path l_0 that corresponds to resonant scattering of a photon by independent atoms. The latter quantity is obtained by replacing Γ_0 by $\Gamma_0/2$ in (192) (since the inverse lifetime of a single atom is half the one related to a superradiant pair) and $1/x$ by 0 in (193) (since the inter-atomic distance is taken to be infinite for a single atom) and it is given by

$$l_0(\delta) = \frac{k_0^2}{6\pi n}\left[1+\left(\frac{2\delta}{\Gamma_0}\right)^2\right]. \tag{194}$$

In Figure 3 the ratio between these two quantities is plotted as a function of the reduced detuning δ/Γ_0 from resonance for several values of $k_0 r_m$. It can be seen that away from resonance, for blue detuning, the elastic mean free path l_e becomes smaller than l_0 in a ratio roughly given by $1/(k_0 r_m)^2$. At resonance, we obtain from (192) that

$$l_e(0) = \frac{k_0^2}{8\pi n}\frac{1}{(k_0 r_m)^2} \tag{195}$$

and hence

$$\frac{l_0(0)}{l_e(0)} = \frac{4}{3}(k_0 r_m)^2 \ll 1. \tag{196}$$

[5]The integral is easily carried out analytically and the explicit expression is given in Appendix A.

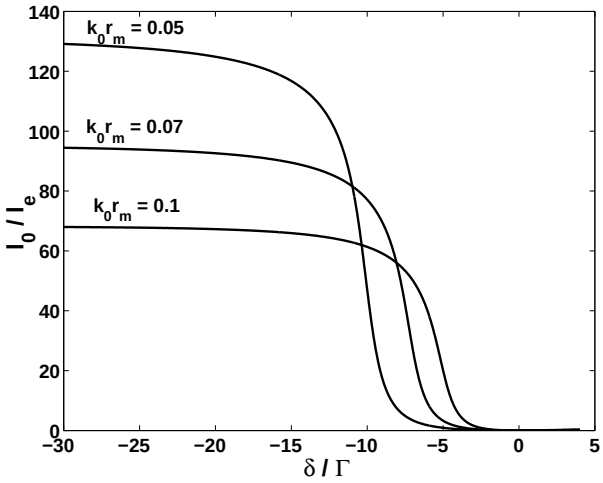

Figure 3: *Ratio between the elastic mean free paths l_0 and l_e as a function of the reduced detuning δ/Γ_0 for $k_0 r_m = 0.05, 0.07,$ and 0.1. Away from resonance, for blue detuning, the elastic mean free path l_e becomes smaller than l_0 in a ratio roughly given by $1/(k_0 r_m)^2$. At resonance, the ratio between the elastic mean free paths is given by (196).*

4.3.3 Group velocity

According to Section 2.2.2, the group velocity of a photon v_g is derived from the real part of the self-energy and is given by

$$\frac{c}{v_g} = \frac{1}{\eta}\left(1 - \frac{c^2}{2\omega}\frac{d}{d\omega}\mathrm{Re}\Sigma_1\right), \tag{197}$$

where the refractive index is

$$\eta = \sqrt{1 - \left(\frac{c}{\omega}\right)^2 \mathrm{Re}\Sigma_1}. \tag{198}$$

For a dilute gas $\eta \simeq 1$, and by substituting (190) in (197) we obtain that

$$\frac{c}{v_g(\delta)} \simeq 1 - \frac{n}{n_c} f_2\left(k_0 r_m, \frac{\delta}{\Gamma_0}\right), \tag{199}$$

where we have defined the characteristic density

$$n_c = \frac{k_0^3}{6\pi}\frac{\Gamma_0}{\omega_0} \tag{200}$$

and the function[6]

$$f_2(u,v) = \frac{1}{2u}\int_0^{2u} dx \frac{1-(v+\frac{1}{x})^2}{\left[1+(v+\frac{1}{x})^2\right]^2}\,. \tag{201}$$

By replacing Γ_0 by $\Gamma_0/2$ in (199) and $1/x$ by 0 in (201), we obtain the group velocity v_0 of light interacting with independent two level-atoms

$$\frac{c}{v_0(\delta)} = 1 - \frac{n}{n_c}\frac{1-(\frac{2\delta}{\Gamma_0})^2}{[1+(\frac{2\delta}{\Gamma_0})^2]^2}\,. \tag{202}$$

For the following typical values, $\Gamma_0 = 10^7$ s^{-1}, $k_0 = 10^7$ m^{-1} and $n = 10^{10}$ cm^{-3}, we obtain that $n/n_c \simeq 10^5$. Figure 4 displays the group velocities v_g and v_0 plotted as a function of the reduced detuning δ/Γ_0 for $n/n_c = 10^5$ and $k_0 r_m = 0.1$. We can see that v_g diverges at quite a large and negative value of the detuning $\delta/\Gamma_0 \simeq -1/(2k_0 r_m)$. But near resonance it is well behaved, meaning that it remains finite and positive. At resonance, according to (199), the group velocity is giving by

$$\frac{c}{v_g(0)} = 1 + 4\pi\frac{n}{k_0^3}\frac{\omega_0}{\Gamma_0}(k_0 r_m)^2. \tag{203}$$

We can also see that this behavior differs substantially from the one obtained for v_0. For densities $n > n_c$, the group velocity v_0 diverges at two symmetric values of order unity of the detuning and it takes negative values in between (*i.e.*, also at resonance). This problem has been recognized a long time ago [31] and an energy velocity, which describes energy transport through a diffusive medium, has been defined [32]. However, the diffusion coefficient, which will be discussed in the next section, is derived from the group velocity and not from the energy velocity [1]. Moreover, a closed expression for the energy velocity has been obtained only for the case of a resonant Mie scattering [8]. Thus, it is interesting to notice that the inclusion of cooperative effects even at the lowest order, *i.e.*, taking into account superradiant pairs, allows to obtain a group velocity which is well behaved at resonance, unlike the case of resonant scattering by independent atoms.

[6]The integral is easily carried out analytically and the explicit expression is given in Appendix A.

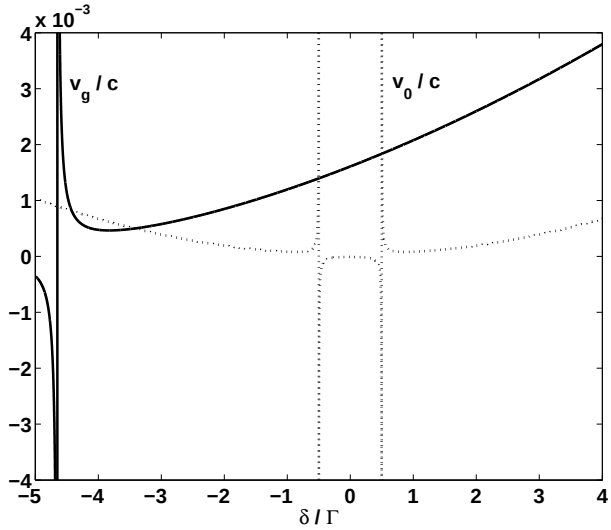

Figure 4: *Group velocities v_g (solid line) and v_0 (dotted line) as a function of the reduced detuning δ/Γ_0 for $n/n_c = 10^5$ and $k_0 r_m = 0.1$. The group velocity v_0 diverges at two symmetric values of order unity of the reduced detuning and it takes negative values in between. The group velocity v_g, near resonance, remains finite and positive.*

4.3.4 Diffusion coefficient and transport time

Diffusive transport of photons through a gas is characterized by the photon diffusion coefficient

$$\mathcal{D}(\delta) = \frac{1}{3} v_g(\delta) l_e(\delta) \tag{204}$$

that combines the elastic mean free path[7] and the group velocity, both derived from the complex valued self-energy (190). The diffusion coefficient is of great importance since it enters into expressions of various measured physical quantities, such as the transmission and the reflection coefficients of a disordered medium [1]. In addition to these average quantities, an incident pulse that probes a nearly static configuration of scatterers may provide

[7]Strictly speaking, the diffusion coefficient is defined by the transport mean free path, $l_{tr} = l_e/(1 - \langle\cos\vartheta\rangle)$, rather than by the elastic mean free path, l_e. Here $\langle\cos\vartheta\rangle = \int d\vartheta \cos\vartheta \; d\sigma/d\Omega$ is the average of the cosine of the scattering angle ϑ with respect to the differential cross section $d\sigma/d\Omega$. However, for a single atom as well as for superradiant pairs the differential cross sections obtained from (20) and (167) yield $\langle\cos\vartheta\rangle = 0$ [9], thus $l_{tr} = l_e$ and definition (204) holds.

an instantaneous picture of the medium that displays a random distribution of bright and dark spots. This snapshot, known as a speckle pattern, can be characterized by the angular-correlation function and the time-correlation function of the light intensity (diffusing wave spectroscopy). In the first case, the correlation function of the transmission coefficient between two distinct directions of the transmitted wave is measured. In the second case, the intensity of the transmitted wave is measured at different times, so that the motion of the scatterers must be taken into account. As pointed before, in both cases the diffusion coefficient plays an important role. Its expression, deduced from (192) and (199), depends on the range r_m and on the detuning δ/Γ_0. Since the group velocity and the elastic mean free path are significantly modified for superradiant states, we thus expect the diffusion coefficient to be different from its value obtained for independent atoms. At resonance and for $n \gg n_c$, the diffusion coefficient, using (195) and (203), is given by

$$\mathcal{D}(0) = \frac{\Gamma_0}{96\pi^2 n^2} r_m^{-4}. \tag{205}$$

We also define the transport time[8] by

$$\tau_{tr}(\delta) = \frac{l_e(\delta)}{v_g(\delta)}. \tag{206}$$

At resonance and for $n \gg n_c$, it can be rewritten with the help of (195) and (203) as

$$\tau_{tr}(0) = \frac{1}{2\Gamma_0}, \tag{207}$$

in accordance with our assumption of superradiant states. Near resonance, the transport time depends weakly on the detuning. But, away from it, τ_{tr} depends on the detuning and thus on frequency, as it can seen from Figure 5, where the inverse of the transport time τ_{tr}^{-1}/Γ_0 is plotted as a function of the reduced detuning δ/Γ_0 for $n = 10^{10}$ cm^{-3}, $\Gamma_0 = 10^7$ s^{-1} and $k_0 = 10^7$ m^{-1} for several values of $k_0 r_m$.

4.4 Average self-energy

So far, we have used the effective approach introduced in Section 4.2.2, where we have considered the case of a scalar wave being scattered by a pair

[8]The transport time is defined as $t_{tr} = l_{tr}/v_g$. But, as explained in the previous footnote, for superradiant pairs $l_{tr} = l_e$, thus definition (206) holds.

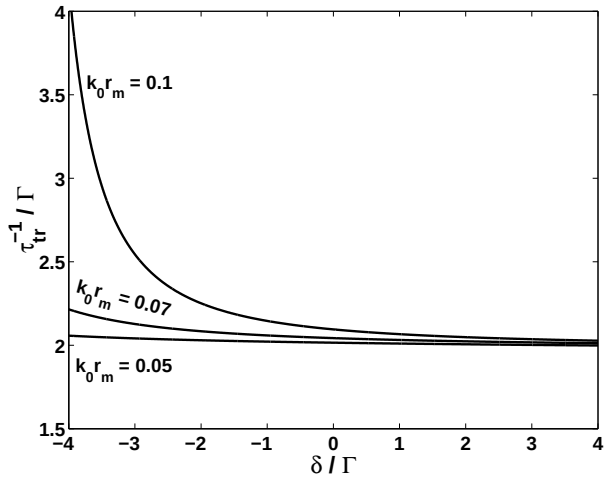

Figure 5: *Inverse of the transport time* τ_{tr}^{-1}/Γ_0 *as a function of the reduced detuning* δ/Γ_0 *for* $n = 10^{10}cm^{-3}$, $\Gamma_0 = 10^7 s^{-1}$ *and* $k_0 = 10^7 m^{-1}$ *for* $k_0 r_m = 0.05, 0.07,$ *and* 0.1. *Near resonance, the transport time depends weakly on the detuning. But, away from it,* τ_{tr} *depends on the detuning and thus on frequency.*

of two-level atoms. In this simple approach, the propagator of a scalar wave (166) has been calculated and the self-energy (186) has been obtained by averaging (166) over the distance between the two atoms in a pair. This effective approach leads to simple expressions for the elastic mean free path (192) and the group velocity (199) of the wave. In this section we calculate these quantities for a given Δm transition and $k_0 r \ll 1$, while taking into account the vectorial nature of the wave. To this purpose, we average the propagator (164) over the random orientations of the pairs of atoms (with respect to the wave vector of the incident photon) as well as over the distance between the two atoms in a pair. Therefore, the average self-energy is now given by

$$\Sigma_1' = \frac{6\pi n}{k_0} \frac{1}{4\pi r_m} \int \hbar \Gamma_0 G^+(\mathbf{r}) d\mathbf{r}, \tag{208}$$

where the averaging is over the inter-atomic axis $\mathbf{r}$ (both over magnitude and orientations). The evaluation of (208) for a $\Delta m = 0$ transition is rather cumbersome and it is presented in Appendix B. By following the procedure described in the previous section, we obtain the corresponding elastic mean free path l_e' and the group velocity v_g'. In Figure 6 the ratio between l_0 given

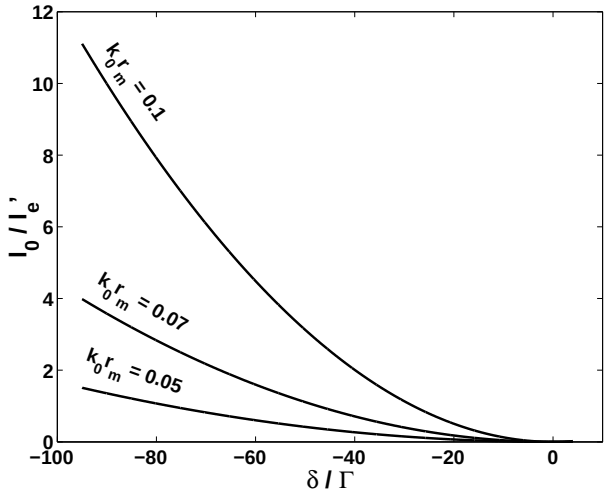

Figure 6: *Ratio between the elastic mean free paths* l_0 *and* l'_e *as a function of the reduced detuning* δ/Γ_0 *for* $k_0 r_m = 0.05, 0.07,$ *and* 0.1*. At resonance* l'_e *is larger than* l_0*, but away from resonance it becomes smaller.*

by (194) and l'_e is plotted as a function of the reduced detuning δ/Γ_0 for several values of $k_0 r_m$. As in the effective approach, at resonance l'_e is found to be larger than l_0, but away from resonance it becomes smaller. In Figure 7 the group velocity v'_g is plotted as a function of the reduced detuning δ/Γ_0 for $n/n_c = 10^5$ and $k_0 r_m = 0.1$. Around resonance, the group velocity v'_g is finite and positive, as in the scalar case, but much larger as compared to (199) and it is close to c. Thus, we may conclude that in both approaches the superradiant effect leads to a finite and positive group velocity, unlike the one obtained for light interaction with independent atoms. However, the group velocity of a scalar wave is much smaller compared to the one of a photon.

4.5 Conclusions

We have considered multiple scattering of a photon by pairs of atoms that are in a superradiant state. On average over disorder configurations, an attractive interaction potential builds up between close enough atoms, and it decays as $1/r$. The contribution of superradiant pairs, resulting from this potential, to scattering properties is significantly different from that of independent atoms. This shows up in the behaviors of the group velocity,

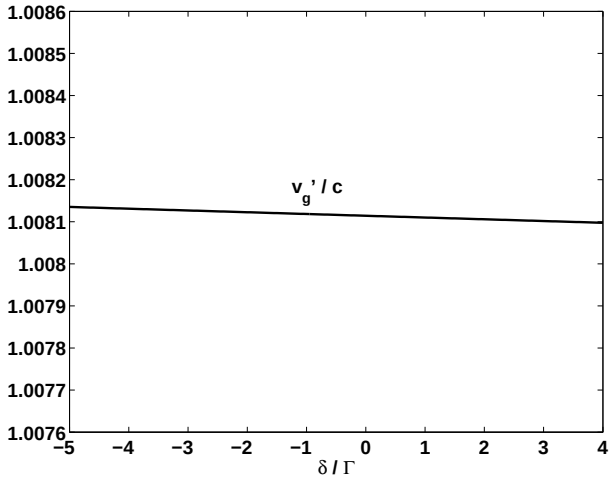

Figure 7: *Group velocity v_g' as a function of the reduced detuning δ/Γ_0 for $n/n_c = 10^5$ and $k_0 r_m = 0.1$. Around resonance, the group velocity v_g' is finite and positive and it is close to c.*

the elastic mean free path and the diffusion coefficient. We have considered a simplified model where only pairs of atoms have been taken into account. The purpose of the current model is to show that already for a dilute gas in the weak disorder limit, cooperative effects modify significantly the transport properties of light. A more realistic model should include higher order terms that account for cooperative effects between more than two atoms and it is presented in the next chapter.

CHAPTER 5

Multiple scattering and cooperative effects

In the previous chapter we have studied the multiple scattering properties of superradiant pairs. We have considered a simplified model of multiple scattering, where only the cooperative effects of pairs of atoms have been taken into account. In the following we consider higher order terms that account for cooperative behavior between more than two atoms [15]. To this purpose we are interested in the cooperative spontaneous emission rate of an arbitrary atomic system, namely the photon escape rate from the atomic gas.

We start by describing the model which consists of N identical atoms placed at random positions in an external radiation field. Then, in order to study the photon escape rate from the atomic gas, the effective Hamiltonian equation is introduced and the average density of photon escape rates is derived from it. Next, numerical results are presented and a scaling function is defined in order to analyze them. Later, the one-dimensional case is considered and compared to the three-dimensional geometry. A possible explanation of the results in the framework of random networks is finally suggested.

5.1 Model

As in Section 3.4, atoms are taken to be degenerate, two-level systems denoted by $|g\rangle = |J_g = 0, m_g = 0\rangle$ for the ground state and $|e\rangle = |J_e = 1, m_e = 0, \pm 1\rangle$ for the excited state. The energy separation between the two levels is $\hbar\omega_0$ and the natural width of the excited level is $\hbar\Gamma_0$. We consider a collection of N identical atoms, placed at random positions $\mathbf{r}_i$, in an external radiation field and the corresponding Hamiltonian is

$$H = H_0 + V, \tag{209}$$

with

$$H_0 = \hbar\omega_0 \sum_{i=1}^{N} \sum_{m_e=-1}^{1} (|J_e m_e\rangle\langle J_e m_e|)_i + \sum_{\mathbf{k}\varepsilon} \hbar\omega_k a^\dagger_{\mathbf{k}\varepsilon} a_{\mathbf{k}\varepsilon}. \tag{210}$$

The interaction V between the radiation field and the electric dipole moments of the atoms is

$$V = -\sum_{i=1}^{N} \mathbf{d}_i \cdot \mathbf{E}(\mathbf{r}_i), \tag{211}$$

where $\mathbf{E}(\mathbf{r})$ is the electric field operator given in (4) and $\mathbf{d}_i$ is the electric dipole moment operator of the i-th atom. As in Section 2.1, we assume that the typical speed of the atoms is small compared to $v_{max} = \Gamma_0/k$ but large compared to $v_{min} = \hbar k/\mu$, where μ is the mass of the atom, so that it is possible to neglect the Doppler shift and recoil effects.

5.2 Photon escape rates from atomic gases

In order to study the cooperative spontaneous emission rates, namely the photon escape rates from the atomic gas, first the effective Hamiltonian equation is introduced, then the photon escape rates are obtained from the effective Hamiltonian equation and finally, the average density of photon escape rates is formally defined.

5.2.1 Effective Hamiltonian equation

For the sake of simplicity, we start by considering a single non-degenerate atom in the quantum radiation field. The corresponding Hamiltonian is obtained from (209) for N =1, $\mathbf{r} = \mathbf{0}$, and $J_e = 0$, namely

$$H = \hbar\omega_0 |e\rangle\langle e| + \sum_{\mathbf{k}\varepsilon} \hbar\omega_k a^\dagger_{\mathbf{k}\varepsilon} a_{\mathbf{k}\varepsilon} \ - \mathbf{d} \cdot \mathbf{E}(\mathbf{0}). \tag{212}$$

When tracing over the radiation degrees of freedom of the density operator associated with (212), the atomic density operator is obtained. Let us denote it by ρ, the corresponding populations by $\rho_{gg} = \langle g|\rho|g\rangle$ and $\rho_{ee} = \langle e|\rho|e\rangle$ and the coherences by $\rho_{ge} = \langle g|\rho|e\rangle$ and $\rho_{eg} = \langle e|\rho|g\rangle$. The evolution equations of these matrix elements are [4]

$$\begin{aligned} \frac{d\rho_{gg}}{dt} &= \Gamma_0 \rho_{ee} \\ \frac{d\rho_{ge}}{dt} &= i\omega_0 \rho_{ge} - \frac{\Gamma_0}{2}\rho_{ge} \\ \frac{d\rho_{eg}}{dt} &= -i\omega_0 \rho_{eg} - \frac{\Gamma_0}{2}\rho_{eg} \\ \frac{d\rho_{ee}}{dt} &= -\Gamma_0 \rho_{ee}. \end{aligned} \tag{213}$$

Set (213) can be rewritten in a form of Lindblad equation [33], namely

$$\frac{d\rho}{dt} = \frac{1}{i\hbar}[H_A, \rho] + \mathcal{L}(\rho), \tag{214}$$

where the atomic Hamiltonian is

$$H_A = \hbar\omega_0 |e\rangle\langle e| \tag{215}$$

and

$$\mathcal{L}(\rho) = -\frac{\Gamma_0}{2}(\rho|e\rangle\langle e| + |e\rangle\langle e|\rho) + \Gamma_0 |g\rangle\langle e|\rho|e\rangle\langle g|. \tag{216}$$

Another way to present (213) is by the effective Hamiltonian equation [4]

$$\frac{d\rho}{dt} = \frac{1}{i\hbar}(H_{eff}\rho - \rho H_{eff}^{\dagger}) + \Gamma_0 b\rho b^{\dagger}, \tag{217}$$

where the raising and lowering operators are defined in (54) and the non-Hermitian effective Hamiltonian describes the atomic Hamiltonian (215), as well as the natural width of the excited state (21), which is due to the coupling to the quantum vacuum, namely

$$H_{eff} = \left(\hbar\omega_0 - i\hbar\frac{\Gamma_0}{2}\right)|e\rangle\langle e|. \tag{218}$$

As in Section 2.1.2, the small radiative level shift of the excited state has been neglected.

Next, we consider N non-degenerate atoms in a scalar radiation field, introduced in Section 3.7. The corresponding Hamiltonian is

$$H = \hbar\omega_0 \sum_{i=1}^{N}(|e\rangle\langle e|)_i + \sum_{\mathbf{k}} \hbar\omega_k a_{\mathbf{k}}^{\dagger} a_{\mathbf{k}} - \sum_{i=1}^{N} d_i E(\mathbf{r}_i), \tag{219}$$

where the scalar field is

$$E(\mathbf{r}) = i\sum_{\mathbf{k}} \sqrt{\frac{\hbar\omega_k}{2\epsilon_0\Omega}}(a_{\mathbf{k}}\ e^{i\mathbf{k}\cdot\mathbf{r}} - a_{\mathbf{k}}^{\dagger} e^{-i\mathbf{k}\cdot\mathbf{r}}). \tag{220}$$

By solving the equations of motion of the creation and annihilation operators, namely

$$\frac{da_{\mathbf{k}}^{\dagger}}{dt} = \frac{1}{i\hbar}[a_{\mathbf{k}}^{\dagger}, H] \tag{221}$$

and

$$\frac{da_{\mathbf{k}}}{dt} = \frac{1}{i\hbar}[a_{\mathbf{k}}, H], \tag{222}$$

the scalar electric field operator in the Heisenberg picture can be written as a sum of two terms[9]

$$E(\mathbf{r}, t) = E_f(\mathbf{r}, t) + E_s(\mathbf{r}, t). \tag{223}$$

$E_f(\mathbf{r}, t)$ represents the contribution of the free field which is independent of the dipole moments (and hence is irrelevant for our purpose), while $E_s(\mathbf{r}, t)$ is the source term which originates from the radiating atoms. The source field is given by

$$E_s(\mathbf{r}, t) = C \sum_{i=1}^{N} \frac{e^{-ik_0|\mathbf{r}-\mathbf{r_i}|}}{k_0|\mathbf{r} - \mathbf{r_i}|} b_i(t) + h.c., \tag{224}$$

where $k_0 = \omega_0/c$ and C depends on the radiation wavelength and on the electric dipole matrix element. Expression (224) represents the contribution of N atomic sources, each one of them is located at $\mathbf{r}_i$ and radiates a scalar wave if it is in its excited state at time t.

The evolution equation of the expectation value of an operator $\mathcal{O}$ in the Schrödinger picture is

$$\frac{d\langle\mathcal{O}\rangle}{dt} = \frac{1}{i\hbar}\langle[\mathcal{O}, H]\rangle. \tag{225}$$

When substituting (223) in (219), from equation (225) applied to an atomic operator, one obtains for the atomic density operator

$$\frac{d\rho}{dt} = \frac{1}{i\hbar}(H_{eff}\rho - \rho H_{eff}^{\dagger}) + \Gamma_0'' \sum_{ij} U_{ij} b_j \rho b_i^{\dagger}. \tag{226}$$

The effective Hamiltonian is

$$H_{eff} = \left(\hbar\omega_0 - i\hbar\frac{\Gamma_0''}{2}\right) \sum_{i=1}^{N} (|e\rangle\langle e|)_i + \hbar\frac{\Gamma_0''}{2} \sum_{i \neq j} V_{ij} b_i^{\dagger} b_j, \tag{227}$$

where

$$U_{ij} = \frac{\sin k_0 r_{ij}}{k_0 r_{ij}} \tag{228}$$

[9]The derivation is given in Appendix C.

and

$$V_{ij} = -\frac{e^{ik_0 r_{ij}}}{k_0 r_{ij}}. \tag{229}$$

Here $r_{ij} = |\mathbf{r}_i - \mathbf{r}_j|$ and Γ_0'' is the scalar spontaneous emission rate of a single atom (140). The effective Hamiltonian has two components. The first is the single atom Hamiltonian including the natural width of the excited state as in (218). The second one is the contribution of the cooperative effects between any two atoms. As discussed in Section 3.7, the real part of (229) is the cooperative level shift of two atoms in a Dicke state $|10\rangle$ interacting with a scalar radiation field, while its imaginary part is the cooperative correction to the single atom emission rate. In particular, for the case of a single atom, $U_{11} = 1$ and (217) is recovered[10].

Finally, we consider N degenerate atoms in the quantum (and vectorial) radiation field, where the corresponding Hamiltonian is given by (209). A similar calculation yields the same effective Hamiltonian equation (226), but now Γ_0'' is replaced by Γ_0, summations over m_e are added,

$$U_{ij} = \frac{3}{2}\left[p_{ij}\frac{\sin k_0 r_{ij}}{k_0 r_{ij}} - q_{ij}\left(\frac{\sin k_0 r_{ij}}{(k_0 r_{ij})^3} - \frac{\cos k_0 r_{ij}}{(k_0 r_{ij})^2}\right)\right] \tag{230}$$

and

$$V_{ij} = \frac{3}{2}\left[-p_{ij}\frac{\cos k_0 r_{ij}}{k_0 r_{ij}} + q_{ij}\left(\frac{\cos k_0 r_{ij}}{(k_0 r_{ij})^3} - \frac{\sin k_0 r_{ij}}{(k_0 r_{ij})^2}\right)\right] - iU_{ij}. \tag{231}$$

For $m_e = 0$

$$p_{ij} = \sin^2\theta_{ij} \qquad q_{ij} = 1 - 3\cos^2\theta_{ij}, \tag{232}$$

while for $m_e = \pm 1$

$$p_{ij} = \frac{1}{2}(1 + \cos^2\theta_{ij}) \qquad q_{ij} = \frac{1}{2}(3\cos^2\theta_{ij} - 1). \tag{233}$$

Here $\theta_{ij} = \cos^{-1}(\hat{z}\cdot\hat{r}_{ij})$, where $\hat{r}_{ij}$ is a unit vector along the direction joining the two atoms. According to Section 3.4, the real part of (231) is the cooperative level shift of two atoms in a Dicke state $|10\rangle$, while its imaginary part is the cooperative correction to the single atom emission rate. As discussed in Section 4.2.1, by averaging (231) upon the random orientation of the pairs

[10] Up to the replacement of Γ_0'' by Γ_0.

of atoms, the scalar case (229) is recovered.

5.2.2 Photon escape rates

After obtaining the effective Hamiltonian equation, in the following we derive from it the cooperative spontaneous emission rates, namely the photon escape rates from the atomic gas. Again, we start with the single atom case, where the effective Hamiltonian equation is given by (217). The evolution of the population of the ground state is

$$\frac{d\rho_{gg}}{dt} = \Gamma_0 \langle g|b\rho b^\dagger|g\rangle, \tag{234}$$

or with the help of (54)

$$\frac{d\rho_{gg}}{dt} = \Gamma_0 \rho_{ee}, \tag{235}$$

as in (213). We may conclude that the evolution rate of the population of the ground state, which is also the photon escape rate, is governed by the last term of the effective Hamiltonian equation. For a single atom the rate is Γ_0.

Now, we generalize to the scalar N-atom problem, where the effective Hamiltonian equation is (226). The evolution of the population of the ground state is given by

$$\frac{d\rho_{g_1...g_N,g_1...g_N}}{dt} = \Gamma_0'' \sum_{ij} U_{ij} \langle g_1...g_N|b_j\rho b_i^\dagger|g_1...g_N\rangle. \tag{236}$$

Following [34, 35], the eigenvalue equation of U_{ij} is

$$\sum_{j=1}^{N} U_{ij} u_j^n = \Gamma^n u_i^n, \tag{237}$$

where Γ^n is the n-th eigenvalue associated with u^n, the n-th eigenfunction. Assuming orthonormality, namely

$$\sum_{n=1}^{N} u_i^n u_j^n = \delta_{ij}, \tag{238}$$

from (236)-(238) we obtain that

$$\frac{d\rho_{g_1...g_N,g_1...g_N}}{dt} = \Gamma_0'' \sum_{n=1}^{N} \Gamma^n \langle g_1...g_N|\hat{\Delta}^{n-}\rho\hat{\Delta}^{n+}|g_1...g_N\rangle, \tag{239}$$

where the generalized collective raising and lowering operators are

$$\hat{\Delta}^{n+} = \sum_{j=1}^{N} u_j^n b_j^\dagger \qquad \hat{\Delta}^{n-} = \sum_{j=1}^{N} u_j^n b_j. \tag{240}$$

By inspecting (239), we conclude that the photon escape rates from the atomic gas (in units of Γ_0'') are the eigenvalues of the coupling matrix U given by (228). In particular, for the single atom case, since $U_{11} = 1$, we have $\Gamma^1 = 1$ and $u^1 = 1$, thus (234) is recovered[11]. For $N = 2$, we obtain from (239) that

$$\frac{d\rho_{g_1g_2,g_1g_2}}{dt} = \Gamma_0'' \sum_{n=1}^{2} \Gamma^n \rho_{DS}^n, \tag{241}$$

where

$$\rho_{DS}^n = (\langle e_1g_2|u_1^n + \langle g_1e_2|u_2^n)\rho(u_1^n|e_1g_2\rangle + u_2^n|g_1e_2\rangle). \tag{242}$$

In the special case where the atoms are confined to a volume much smaller than the radiation wavelength cubed, *i.e.,* in Dicke limit ($k_0 r_{ij} \ll 1$), then

$$U = \begin{pmatrix} 1 & 1 \\ 1 & 1 \end{pmatrix}. \tag{243}$$

Thus, $\Gamma^1 = 2$ with

$$u^1 = \frac{1}{\sqrt{2}} \begin{pmatrix} 1 \\ 1 \end{pmatrix} \tag{244}$$

and $\Gamma^2 = 0$ with

$$u^2 = \frac{1}{\sqrt{2}} \begin{pmatrix} 1 \\ -1 \end{pmatrix}. \tag{245}$$

Therefore, $\rho_{DS}^1 = \langle 10|\rho|10\rangle$ is the expectation value of the atomic density operator in the superradiant Dicke state (68), while $\rho_{DS}^2 = \langle 00|\rho|00\rangle$ is the expectation value of the atomic density operator in the subradiant Dicke state (67). The photon escape rate is $2\Gamma_0''$ in the first case, while it is zero in the second one, as in (148).

The result that the spectrum of the coupling matrix U is the photon escape rate can be straightforwardly generalized to the vectorial case, where U is given by (230). It may also be obtained by either a generalized Wigner-Weisskopf model [36, 37] or a photo-detection theory [4] sketched below for the scalar case.

[11] Up to the replacement of Γ_0'' by Γ_0.

The probability to detect the outgoing photon $\mathbf{k}$ at time t at a detector placed outside the gas at $\mathbf{R} = R\hat{R}$, where $\hat{R} = \hat{k}$, is proportional to

$$S(\mathbf{R}, t) \propto \langle E_s^+(\mathbf{R}, t) E_s^-(\mathbf{R}, t) \rangle, \tag{246}$$

where $E_s^+(\mathbf{R}, t)$ is the annihilation part of the source field (224), $E_s^-(\mathbf{R}, t)$ is its creation part[12] and $\langle \cdots \rangle$ denotes the expectation value with respect to the eigenstates of the effective Hamiltonian (227). Explicitly, (246) reads

$$S(\mathbf{R}, t) \propto \left\langle \sum_{ij} \frac{e^{ik_0(|\mathbf{R}-\mathbf{r_i}|-|\mathbf{R}-\mathbf{r_j}|)}}{k_0^2 |\mathbf{R}-\mathbf{r_i}||\mathbf{R}-\mathbf{r_j}|} b_i^\dagger(t) b_j(t) \right\rangle. \tag{247}$$

When the detector is placed in the far field, one can use the Fraunhoffer approximation,

$$k_0|\mathbf{R} - \mathbf{r}_i| \simeq k_0 R - k_0 \hat{R} \cdot \mathbf{r}_i, \tag{248}$$

and obtain

$$S(t) \propto \left\langle \sum_{ij} e^{ik_0 \hat{R} \cdot \mathbf{r_{ji}}} b_i^\dagger(t) b_j(t) \right\rangle. \tag{249}$$

The probability to detect the outgoing photon at all angles at time t is obtained by integrating (249) over the corresponding solid angle and is given by

$$\Pi(t) \propto \left\langle \sum_{ij} \frac{\sin k_0 r_{ij}}{k_0 r_{ij}} b_i^\dagger(t) b_j(t) \right\rangle. \tag{250}$$

We notice that expression (250) is proportional to the expectation value of the imaginary part of the effective Hamiltonian (227). Thus, the eigenvalues of the coupling matrix (228) determine the photon escape rates from the atomic gas.

5.2.3 Average density of photon escape rates

In the previous section, we have seen that the spectrum of the coupling matrix U, given by (228) in the scalar case and by (230) in the vectorial case, is the photon escape rate (in units of Γ_0[13]) from the atomic gas. Formally, U

[12] The free field, E_f, does not contribute to the detection probability.

[13] In the following, we will ignore the difference between the scalar spontaneous emission rate of a single atom, Γ_0'', and the one corresponds to a vectorial field, Γ_0. We shall denote both quantities by Γ_0.

is an Euclidean random matrix [38], *i.e.,* an $N \times N$ matrix, whose elements are a function of the position of N random points in an Euclidean space. The average density of the photon escape rates (in units of Γ_0) is defined as

$$P(\Gamma) = \frac{1}{N}\overline{\sum_{n=1}^{N} \delta(\Gamma - \Gamma^n)}, \tag{251}$$

where the average, denoted by $\overline{\cdots}$, is taken over the spacial configurations of the atoms. Using the relation

$$\frac{1}{x + i\epsilon} = PP\left(\frac{1}{x}\right) - i\pi\delta(x), \tag{252}$$

where $PP(x)$ is the principal part of x, we have that

$$P(\Gamma) = -\frac{1}{\pi}\mathrm{Im}R(z = \Gamma + i\epsilon), \tag{253}$$

with

$$R(z) = \frac{1}{N}\overline{\mathrm{Tr}(zI - U)^{-1}}, \tag{254}$$

where I is an $N \times N$ unit matrix.

Let us consider some limits:

1. Dilute gas ($k_0 r_{ij} \gg 1$)

   In this case, $U = I$ and $R(z) = (z-1)^{-1}$, thus

   $$P(\Gamma) = \delta(\Gamma - 1). \tag{255}$$

   In this limit the single atom spontaneous emission rate has been recovered.

2. Dicke limit ($k_0 r_{ij} \ll 1$ for $N > 1$)

   Now,

   $$U = \begin{pmatrix} 1 & 1 & \cdots & 1 \\ 1 & 1 & \cdots & 1 \\ \vdots & \vdots & & \vdots \\ 1 & 1 & \cdots & 1 \end{pmatrix} \tag{256}$$

and

$$R(z) = \frac{1}{N}\left(\frac{1}{z-N} + \frac{N-1}{z}\right), \tag{257}$$

thus

$$P(\Gamma) = \frac{1}{N}[\delta(\Gamma - N) + (N-1)\delta(\Gamma)]. \tag{258}$$

In this case the eigenvalue $\Gamma = 0$ is the $(N-1)$-degenerate subradiant mode and $\Gamma = N$ is the non-degenerate superradiant mode, so that (80) has been recovered and in particular for $N = 2$, expressions (118) and (148) are obtained.

In both limits discussed above, U is either given by (228) or (230).

5.3 Numerical results

In order to study the average density of photon escape rates (253) we consider N atoms enclosed in a cubic volume $\mathtt{L}^3 = (a\lambda_0)^3$, where for resonant scattering, $\lambda_0 = 2\pi/k_0$ is the radiation wavelength. The atoms are distributed with a uniform density $n = N/\mathtt{L}^3$. We define the disorder strength by $W = 1/(k_0 l_e)$, where l_e is the photon elastic mean free path (39). According to (24), for resonant scattering, the average single scattering cross section varies as the radiation wavelength squared, so that the disorder strength may be written as

$$W = \frac{N}{2\pi a^3}. \tag{259}$$

Let us discuss the limits of (259):

1. Weak disorder ($W \ll 1$)

   In this limit, as discussed in Section 2.2.2., $l_e \gg \lambda_0$, so that the light reaches its far field behavior between successive scattering events. Thus, the scattering events may be considered as independent ones.

2. Strong disorder ($W \geq 1$)

   Now, $l_e \leq \lambda_0$, thus the scattering events are dependent ones.

By a numerical calculation we have obtained $P(\Gamma)$ for different values of disorder strength W and size a, both for the scalar case, where the coupling matrix U is given by (228), and the vectorial case defined by (230). The behavior of the average density of photon escape rates is presented in Figures 8-10 for the different cases.

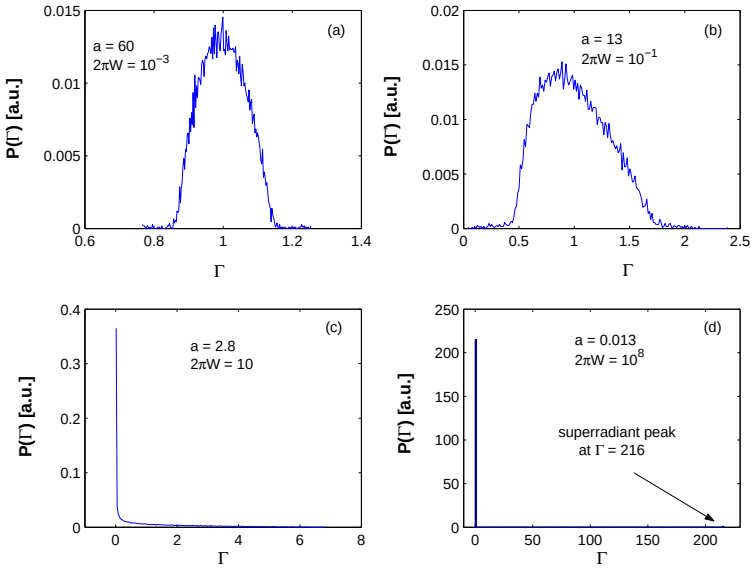

Figure 8: *Behavior of $P(\Gamma)$ for different values of the disorder strength W, of the size a and for $N = 216$ in the scalar case. (a) At low disorder, $P(\Gamma)$ is peaked around $\Gamma = 1$ (b) for larger disorder, $P(\Gamma)$ becomes broader and shifted towards the origin and eventually (c) it accumulates near $\Gamma = 0$ (d) Dicke limit.*

First, we observe that $P(\Gamma)$ obtained for the scalar case (Figure 8) is qualitatively the same as the ones obtained for the vectorial cases (Figures 9-10)[14]. Moreover, the dilute gas limit and Dicke limit are exactly the same, as discussed in Section 5.2.3. Thus, as the scalar model has the advantage of being easier to handle, the reminder of the chapter is devoted to its study.

As presented in Figure 8, for a very dilute gas, we recover the single atom limit namely $U = I$, so that $P(\Gamma)$ is narrowly peaked around $\Gamma = 1$ (in units of Γ_0) as expected from resonant scattering of a photon by a single atom (Figure 8.a). For stronger disorders, $P(\Gamma)$ becomes broader and it is shifted towards lower values of Γ (Figure 8.b). Eventually for large enough disorders, most of the eigenvalues are close to $\Gamma = 0$ (Figure 8.c). Such a vanishing escape rate corresponds to photons localized in the atomic gas. By increasing further the disorder W, at fixed number N of atoms, we reach

[14] Although their similarity, Figures 8-10 are not identical. This is due to the angular dependence of U which exists in the vectorial cases but lacks in the scalar case.

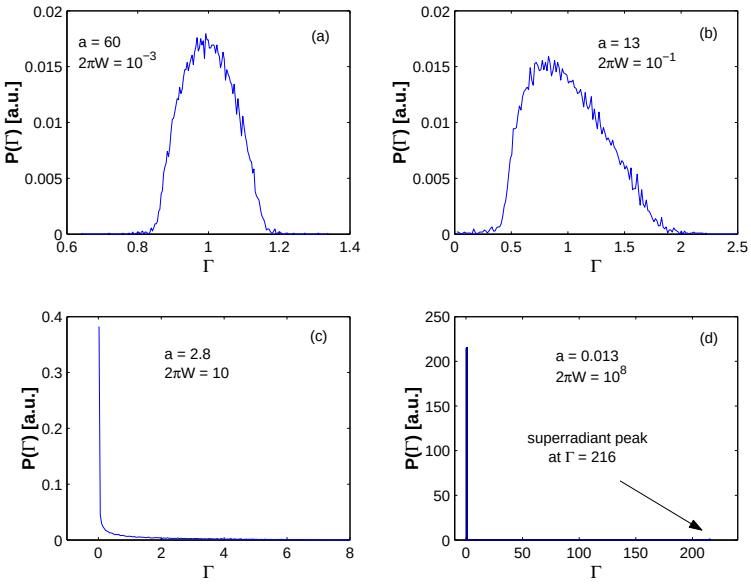

Figure 9: *Behavior of $P(\Gamma)$ for different values of the disorder strength W, of the size a and for $N = 216$ in the vectorial case where $m_e = 0$. (a) At low disorder, $P(\Gamma)$ is peaked around $\Gamma = 1$ (b) for larger disorder, $P(\Gamma)$ becomes broader and shifted towards the origin and eventually (c) it accumulates near $\Gamma = 0$ (d) Dicke limit.*

another regime (Figure 8.d) where $P(\Gamma)$ has two peaks, one at $\Gamma = 0$ and a second one at $\Gamma = N$. This is the Dicke limit which occurs when the atoms are contained in a volume much smaller than λ_0^3. The eigenvalue $\Gamma = 0$ is the $(N-1)$-degenerate subradiant mode and $\Gamma = N$ is the non-degenerate superradiant mode, as discussed in Section 5.2.3.

5.4 Scaling function

In order to characterize $P(\Gamma)$, we look for a suitable parameter. It seems that the mean value of Γ is an appropriate choice. However, since $\Gamma_{mean} = [\mathrm{Tr}(U)]/N$ and, according to (228), $U_{ii} = 1$, we obtain that $\Gamma_{mean} = 1$ regardless of disorder strength and system size. For instance, in the Dicke limit (258), $\Gamma_{mean} = [(N-1) \times 0 + 1 \times N]/N = 1$ and in the dilute gas case (255), $\Gamma_{mean} = 1$ as well. Therefore, we seek for a better parameter that can characterize $P(\Gamma)$.

A possible choice when inspecting the shape of $P(\Gamma)$ displayed in Figure

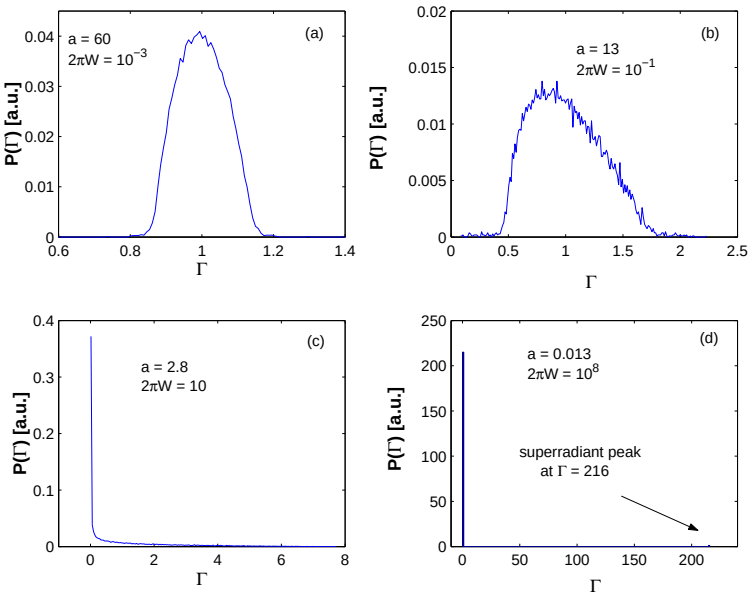

Figure 10: *Behavior of* $P(\Gamma)$ *for different values of the disorder strength* W*, of the size* a *and for* $N = 216$ *in the vectorial case where* $m_e = \pm 1$*. (a) At low disorder,* $P(\Gamma)$ *is peaked around* $\Gamma = 1$ *(b) for larger disorder,* $P(\Gamma)$ *becomes broader and shifted towards the origin and eventually (c) it accumulates near* $\Gamma = 0$ *(d) Dicke limit.*

8 is to consider the relative number of states defined by

$$\Gamma_e(a, W) = \int_1^\infty d\Gamma \;\; P(\Gamma) \;\; , \tag{260}$$

which have an escape rate larger than 1 (in units of Γ_0). To obtain its dependence upon the system size a and the disorder W, we introduce the conveniently normalized function $g(a, W)$ defined between 0 and 1 by

$$g(a, W) = 1 - 2\Gamma_e(a, W) \;\; . \tag{261}$$

When $g(a, W) \to 0$, as in Figure 8.a, the photons are delocalized, while when $g(a, W) \to 1$, as in Figure 8.c, the photons are localized. Thus, g is a measure of the relative number of states having vanishing escape rates.

When the size of the system is increased a bit ($\epsilon \ll 1$), g is given by

$$g[a(1+\epsilon)] \simeq g(a) + \epsilon g \frac{d \ln g}{d \ln a}. \tag{262}$$

If

$$\frac{d\ln g(a,W)}{d\ln a} = \beta(g), \tag{263}$$

where $\beta(g)$ is a function of g alone, then $g(a,W)$ has a *scaling form*, and (262) can be written as

$$g[a(1+\epsilon)] = f[g(a),\epsilon]. \tag{264}$$

Physically, (266) states that the value of g, as the size of the system is increased a bit, is determined solely by its value at the previous length scale. The solution of (263) can be written as

$$g(a,W) = f[a^{\nu}/h(W)], \tag{265}$$

where ν is an exponent and $h(W)$ is some function of W. The validity of the solution can be verified by defining the inverse function $f^{-1}(g) = a^{\nu}/h(W)$. In terms of this function expression (263) reads

$$\beta(g) = \nu\frac{f'[f^{-1}(g)]f^{-1}(g)}{f[f^{-1}(g)]}, \tag{266}$$

which is indeed a function of g alone. A famous example of scaling is the theory of electron localization in disordered media developed by the "gang of four" [39]. In the following we will show that $g(a,W)$ defined by (261) has a scaling form, *i.e.,* it obeys (263) or equivalently (265)[15]. To that purpose, let us distinguish between two regimes, the large sample regime, where $a \geq 1$ and the Dicke regime where $a \ll 1$.

5.4.1 Large sample regime

The behavior of $g(a,W)$ as a function of the system size $a \geq 1$ for different disorder strength W is presented in Figure 11. The results collapse on a single curve (Figure 12) when plotted as a function of $2\pi aW$. Thus, the scaling hypothesis (263) has been verified over a broad range of size and disorder. By using (39) and (259), we recognize that the scaling variable is the optical depth $\mathtt{b}$, namely

$$\mathtt{b} = \frac{\mathtt{L}}{l_e} = 2\pi aW. \tag{267}$$

[15]We have checked that the scaling behavior of g does not depend on the choice of the cutoff parameter in (260), provided it fulfills $0 < c \leq 1$. If it is chosen to be $0 < c < 1$ instead of $c = 1$, then the scaling function obeys $|g| \leq 1$ instead of $0 \leq g \leq 1$, but the scaling behavior is the same, as shown in Appendix D.

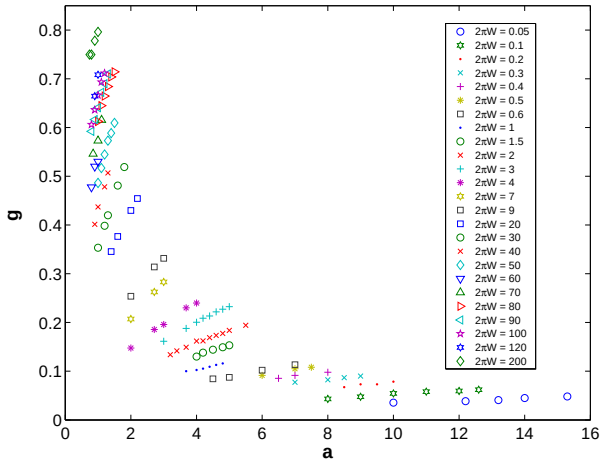

Figure 11: *Behavior of the scaling function g as a function of the system size $a \geq 1$ for different disorder strengths W.*

The observation obtained from Figure 12 that the scaling function increases with the optical depth can be explained as follows. As the number of scattering events is increased, it takes more time for the photon to leave the gas, thus the relative number of states having a vanishing escape rate is increased. Since $\beta(g)$, defined in (263), is always positive, we conclude that the photons undergo a crossover (rather than a phase transition) from delocalization towards localization, and in the thermodynamic limit a localized phase exists. These results differ substantially from those obtained in the context of Anderson localization of photons where weak and strong disordered phases are separated by a phase transition in dimension $\mathtt{d} > 2$. Nevertheless, it must be noticed that in our model, we study the spectral properties of the Euclidian random matrices U and not of the Laplacian in the presence of disorder.

5.4.2 Dicke regime

In the Dicke regime, $P(\Gamma)$ is given by (258). Using (261), we obtain the scaling behavior

$$g(a, W) = 1 - \frac{2}{N} = 1 - \frac{1}{\pi a^3 W}, \tag{268}$$

displayed in Figure 13. We conclude that the scaling variable is the number of the atoms.

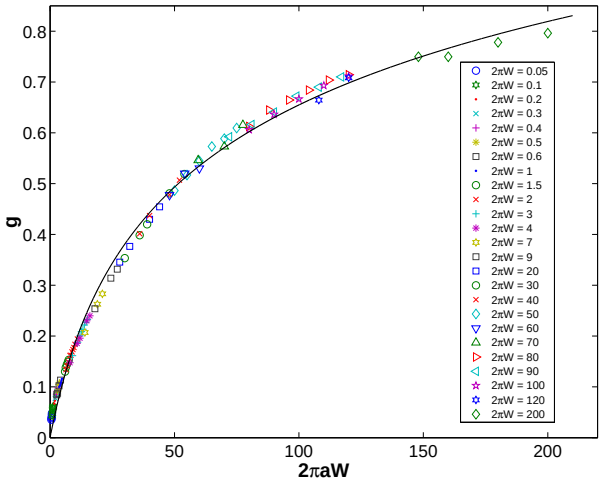

Figure 12: *Behavior of the scaling function g as a function of the optical depth $\mathfrak{b} = 2\pi aW$ in the large sample regime. All the points represented in Figure 11 collapse on the same curve, thus confirming the scaling assumption. The solid line is a fitting function, given by (280).*

5.5 One-dimensional geometry

Now we consider a one-dimensional atomic system, where the coupling matrix, according to Section 3.6, is given by

$$U_{ij} = \cos k_0 r_{ij} \tag{269}$$

The average density of photon escape rates is presented in Figure 14. A remarkable difference between the one-dimensional case and the three-dimensional cases (Figures 8-10) is observed. Unlike in the three-dimensional geometry, the single atom limit is never reached and the photons are always localized in the atomic gas. However, Dicke limit is the same in both geometries. The behavior of $g(a, W)$ as a function of the system size $a \geq 1$ for different disorder strength W is presented in Figure 15. The results collapse on a single curve (Figure 16) when plotted as a function of $1/(2\pi aW)$, so that the scaling hypothesis (263) is verified, namely

$$g(a, W) = 1 - \frac{4}{N} = 1 - \frac{2}{\pi aW}. \tag{270}$$

For system size $a \ll 1$, U is given by (256) and with the help of (258), we

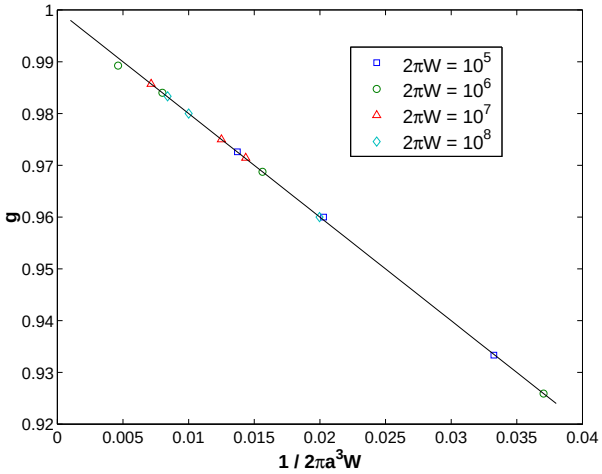

Figure 13: *Behavior of the scaling function g as a function of the inverse number of the atoms $1/N = 1/(2\pi a^3 W)$ in Dicke regime. The solid line is a fitting function, given by (268).*

obtain that

$$g(a, W) = 1 - \frac{2}{N} = 1 - \frac{1}{\pi a W}, \tag{271}$$

as in the three-dimensional case. Thus, in both cases the scaling variable is the number of the atoms.

Since $g(a, W) \to 1$, the photon are always localized and as $\beta(g)$, according to (266), is giving by

$$\beta(g) = \frac{1-g}{g} > 0, \tag{272}$$

a localized phase exists in the thermodynamic limit. The fundamental difference between the one and three-dimensional geometries, *i.e.,* the existence or the absence of a crossover between delocalized and localized photons, is due to the different nature of the coupling matrices. While U falls off with the inter-atomic separation in the three-dimensional case, it is a periodic function of the inter-atomic distance in the one-dimensional geometry. Thus, the single atom limit is never reached.

5.6 Small world networks

In this section we provide a possible explanation to the results obtained above in the framework of random networks. To this purpose, we start with

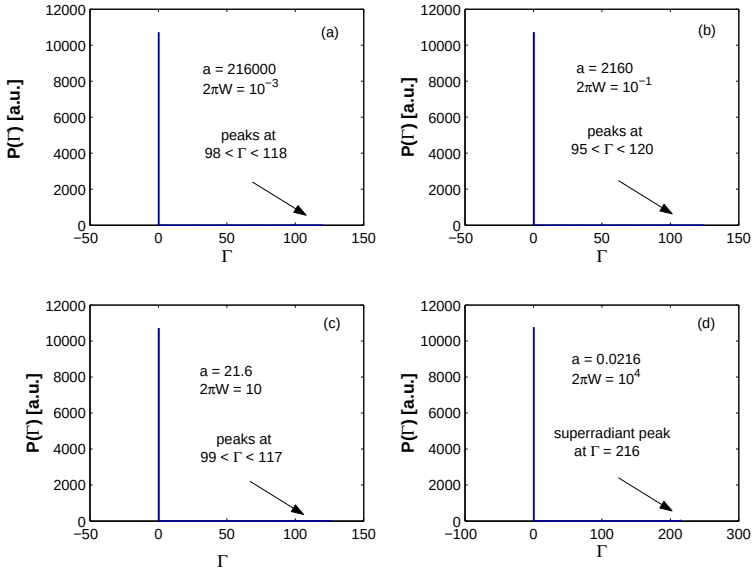

Figure 14: *Behavior of* $P(\Gamma)$ *for different values of the disorder strength* W*, of the size* a *and for* $N = 216$ *in a one-dimensional geometry. The single atom limit is never reached and the photons are always localized in the atomic gas.*

a brief description of random graph theory including small world networks [40], and apply it to our random atomic system.

Mathematically, a network is represented by a graph. A graph is a pair of sets $\mathcal{G} = \{\mathcal{P}, \mathcal{E}\}$, where $\mathcal{P}$ is a set of N vertices $\mathcal{P}_1, \mathcal{P}_2, ..., \mathcal{P}_N$ and $\mathcal{E}$ is a set of links that connect two elements of $\mathcal{P}$. Graphs are usually represented by a set of dots, each corresponding to a vertex, two of these dots being joined by a line if the corresponding vertices are connected.

Any graph $\mathcal{G}$ with N vertices can be represented by its adjacency matrix $A(\mathcal{G})$ with $N \times N$ elements A_{ij}, whose value is $A_{ij} = A_{ji} = 1$ if vertices i and j are connected and 0 otherwise. The spectrum of $\mathcal{G}$ is the set of eigenvalues of the adjacency matrix $A(\mathcal{G})$. A graph with N vertices has N eigenvalues λ_n, and the corresponding spectral density is

$$\nu(\lambda) = \frac{1}{N} \sum_{n=1}^{N} \delta(\lambda - \lambda_n). \tag{273}$$

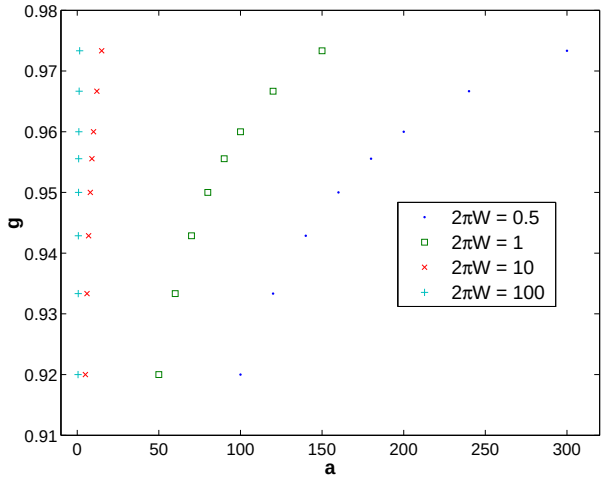

Figure 15: *Behavior of the scaling function g as a function of the system size $a \geq 1$ for different disorder strengths W in a one-dimensional geometry.*

A special case is the fully connected graph, where

$$A = \begin{pmatrix} 1 & 1 & \cdots & 1 \\ 1 & 1 & \cdots & 1 \\ \vdots & \vdots & & \vdots \\ 1 & 1 & \cdots & 1 \end{pmatrix}, \tag{274}$$

and its corresponding spectral density is [41]

$$\nu(\lambda) = \frac{1}{N}[\delta(\lambda - N) + (N-1)\delta(\lambda)]. \tag{275}$$

A more general graph represents a *regular* (or *ordered*) *lattice* in which each vertex is connected to the K vertices closest to it.

Another class of graphs represents *random networks* in which the links are distributed randomly. For example, a random graph can be defined [42] as N labeled vertices connected by s links which are chosen randomly from the $N(N-1)/2$ possible ones.

A model that interpolates between an ordered lattice and a random network and combines their properties has been proposed [43]. The algorithm behind the model is the following (Figure 17):

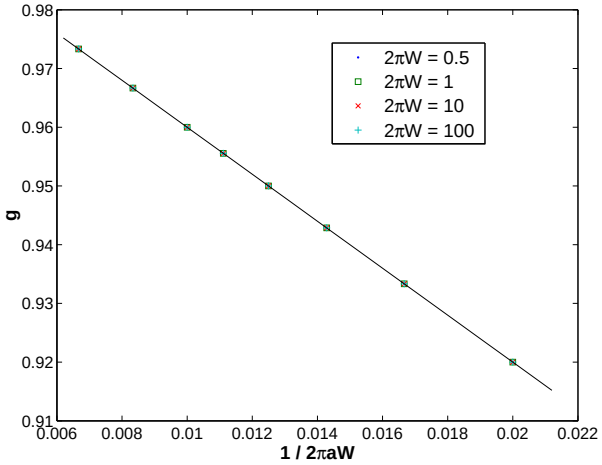

Figure 16: *Behavior of the scaling function g as a function of the inverse number of the atoms $1/N = 1/(2\pi aW)$ in the large sample regime in one-dimensional geometry. All the points represented in Figure 15 collapse on the same curve, thus confirming the scaling assumption. The solid line is a fitting function, given by (270).*

1. Start with order

   Start with a one-dimensional lattice with periodic boundary conditions, *i.e.,* a ring lattice, in which every vertex is connected to its first K neighbors ($K/2$ on either side).

2. Randomize

   Randomly rewire each link of the lattice with probability ϕ, such that self-connections and duplicate links are excluded. This process introduces long-range links which connect vertices that otherwise would be part of different neighborhoods.

By varying ϕ one can monitor the transition between order ($\phi = 0$) and randomness ($\phi = 1$). For small values of ϕ the network behaves as a *small world*, namely that any two vertices can be connected through a short chain of intermediate vertices.

The model has its roots in social systems, which appear to display simultaneously properties typical both of regular lattices and of random graphs. Most people are friends with their immediate neighbors: colleagues, neighbors, etc. In this respect social networks are similar to regular lattices. On

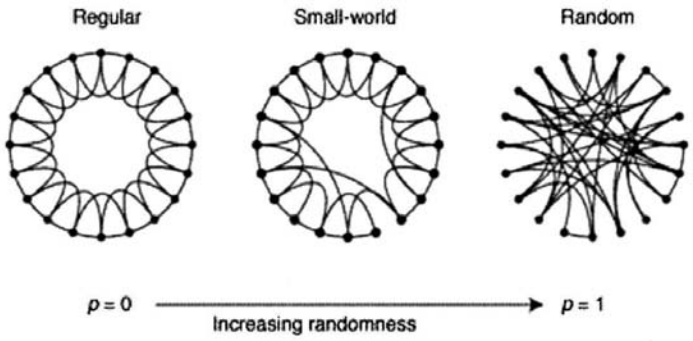

Figure 17: *Small world model, which interpolates between a regular ring lattice and a random network. We start with $N = 20$ vertices, each connected to its $K = 4$ nearest neighbors. For $\phi = 0$ the original ring is unchanged. As ϕ increases, the network becomes increasingly disordered until for $\phi = 1$ all links are rewired randomly. After [43].*

the other hand, it is widely believed that one can get from almost any member of a social network to any other via only a small number of intermediate acquaintances. Within the population of the world, for instance, it has been suggested that there are only about "six degrees of separation" between any human being and any other [44]. This behavior is represented by long range links of the model and it is a property of random graphs.

This small world network, which combines the properties of ordered lattices and random networks, provides a model for the topology of a wide variety of systems, such as the internet, neural networks, and coupled oscillators. The properties of small world networks may have significant consequences for many real-world applications, including biological evolution and information propagation.

In order to understand the coexistence of the properties related to regular lattices and random networks we introduce the *average path length*, $l(\phi)$, which is the average shortest path between any randomly chosen vertices. Formally,

$$l(\phi) = \frac{1}{N(N-1)} \overline{\sum_{i \neq j} y_{ij}}, \tag{276}$$

where y_{ij} is the shortest path between vertices i and j and $\overline{\cdots}$ denotes config-

uration averaging. For a ring lattice $l(0) \propto N$ [45], while $l(1) \propto \ln N$ [46][16]. Thus, for small ϕ, l scales linearly with the system size, while for large ϕ the scaling is logarithmic. The origin of the rapid drop in l as ϕ increases, is the appearances of shortcuts between vertices. Every shortcut, created at random, is likely to connect widely separated parts of the graph, and thus has a significant impact on the characteristic path length of the entire graph. Even a relatively low fraction of shortcuts is sufficient to drastically decrease the average path length, yet locally the network remains highly ordered. This is the small world behavior, mentioned above.

For an arbitrary value of the the fraction ϕ of rewired links, the average path length of a ring lattice is given by

$$l = \frac{N}{2K} f(\phi K N), \tag{277}$$

where $f(x)$ is a scaling function, obtained by a mean field method [47]

$$f(x) = \frac{4}{\sqrt{x^2+4x}} \tanh^{-1}\left(\frac{x}{\sqrt{x^2+4x}}\right). \tag{278}$$

Expression (277) has been confirmed by numerical simulations [48] and renormalization group techniques [49][17]. The scaling function $f(x)$ and the scaling variable $x = \phi K N$ have simple physical interpretations. The variable x is two times the average number of random links on the graph for a given ϕ and $f(x)$ is the average of the fraction by which the distance between two vertices is reduced for a given x. As the asymptotic forms of (278) are

$$f(x \ll 1) = 1 \qquad f(x \gg 1) = \frac{\ln x}{x}, \tag{279}$$

the limits of l discussed above are recovered. According to (277), the onset of small world behavior depends on the system size, N, thus there is a crossover (rather than a phase transition) between a regular lattice to a small world network.

[16] The derivation is given in Appendix E.

[17] While in our treatment each vertex is connected to its first K neighbors ($K/2$ on either side), in [47] each vertex is connected to its first $2K'$ neighbors (K' on either side). Thus, the equivalent expressions of (277)-(278) are $l = \frac{N}{K'} f(\phi K' N)$ and $f(x) = \frac{1}{2\sqrt{x^2+2x}} \tanh^{-1}\left(\frac{x}{\sqrt{x^2+2x}}\right)$.

Now, we return to our random atomic network and explain the results obtained in the previous sections in the framework of random graphs. First, we notice that Dicke regime, whose spectral density is (258), can be exactly mapped onto a fully connected graph, whose spectral density is (275). In the large sample regime, displayed in Figure 12, for $aW \gg 1$ the system may be described as a random graph of atoms sitting at vertices and randomly (but not fully) connected to other atoms by exchange of photons. At small values $aW \ll 1$, we recover a gas of independent atoms, which is the limiting case of a graph of vanishing connectivity. By applying the mean field solution (277) to the data presented in Figure 12, we find that a very good agreement ($R^2 = 0.99$) is obtained when the following fitting function is introduced

$$g(x) = Cxf(x). \tag{280}$$

Here the scaling variable is $x = \mathtt{b}/4$, where $\mathtt{b}$ is the optical depth (267), $C \simeq 0.1$ and $f(x)$ is given in (278). For a dilute gas ($x \ll 1$), using (279), we have that $g(x) = Cx$, so with the help of (261) we obtain

$$2\Gamma_e = 1 - C\frac{\pi aW}{2}. \tag{281}$$

This is the first correction to the value $2\Gamma_e = 1$, associated with the single atom limit. This limit corresponds to a regular graph with vanishing connectivity.

For $x \gg 1$, using (279), we have that $g(x) = C \ln x$, so that

$$2\Gamma_e = 1 - C \ln \frac{\pi aW}{2}. \tag{282}$$

This result corresponds to the random graph limit where cooperative effects, by a photon exchange, connect atoms that otherwise would be part of different neighborhoods. Let us stress that for a fixed number of atoms, by increasing x constantly, (282) eventually breaks down. This is due to the replacement of the large sample regime (280), which exhibits a small world behavior, by Dicke limit (268), which corresponds to a fully connected graph.

To conclude, by using a mapping onto a random network problem, we have described the crossover between a weakly connected network of atoms emitting photons almost independently at small disorder to a small world network where atoms are related through small chains of intermediate atoms exchanging photons.

5.7 Conclusions

We have studied the photon emission rates from an atomic gas while taking into account the cooperative effects between the scatterers. The average density of photon escape rates from a gas of N atoms has been obtained from the spectrum of the $N \times N$ Euclidean random matrix U for a broad range of sample size and disorder strength. A scaling function, which measures the relative number of states having vanishing escape rates has been introduced. For a three-dimensional gas two regimes have been identified: In the large sample regime, the photons undergo a crossover from delocalization towards localization as the optical depth is increased, while in the Dicke regime the photons are always localized. For a one-dimensional geometry, due to the periodic nature of the coupling matrix, the single atom limit is never reached and the photons are always localized.

We have suggested a possible explanation to the three-dimensional results in the framework of random networks. The photons undergo a crossover between a weakly connected network of atoms emitting photons almost independently at small disorder to a small world network where atoms are related through small chains of intermediate atoms exchanging photons.

These results differ substantially from those obtained in the context of Anderson localization of photons where weak and strong disordered phases are separated by a phase transition in dimension $\mathtt{d} > 2$. Nevertheless, it must be noticed that in our model, we study the spectral properties of the Euclidean random matrices U and not of the Laplacian in the presence of disorder.

CHAPTER 6

Conclusions and outlook

In this dissertation we have studied multiple scattering of photons in disordered atomic media while taking into account cooperative effects, which originates from the interaction between atoms through the radiation field.

At first stage we have considered a simplified model where only pairs of atoms have been taken into account. On average over disorder configurations, an attractive interaction potential builds up between close enough atoms in a superradiant state, and it decays as the inverse of the inter-atomic separation. The contribution of superradiant pairs, resulting from this potential, to scattering properties is significantly different from that of independent atoms. This shows up in the behaviors of the group velocity, the elastic mean free path and the diffusion coefficient. For instance, the group velocity corresponds to light scattering by superradiant pairs is finite and positive near resonance (as well as at resonance), unlike the one associated with independent atoms. Thus, already for a dilute gas, cooperative effects modify significantly the transport properties of light.

Next, we have studied a more realistic model that includes higher order terms that account for cooperative effects between more than two atoms. To this purpose we have considered N identical atoms, placed at random positions in an external radiation field. The photon escape rates from the atomic gas have been derived from the effective Hamiltonian equation by diagonalizing the $N \times N$ Euclidean random matrix U for a broad range of sample size and disorder strength. For a three-dimensional geometry $U_{ij} = \sin x_{ij}/x_{ij}$, while for a one-dimensional gas $U_{ij} = \cos x_{ij}$, where x_{ij} is the dimensionless random distance between any two atoms.

A scaling function, which measures the relative number of states having vanishing escape rates has been introduced. For a three-dimensional gas two regimes have been identified: In the large sample regime, the photons undergo a crossover from delocalization towards localization as the optical depth is increased, while in the Dicke regime the photons are always localized. For a one-dimensional geometry, due to the periodic nature of the coupling matrix, the single atom limit is never reached and the photons are always localized.

We have suggested an explanation of the three-dimensional results in the framework of random networks. The photons undergo a crossover between a

weakly connected network of atoms emitting photons almost independently at small disorder to a small world network where atoms are related through small chains of intermediate atoms exchanging photons.

These results differ substantially from those obtained in the context of Anderson localization of photons where weak and strong disordered phases are separated by a phase transition in dimension $\mathtt{d} > 2$. Nevertheless, it must be noticed that in our model, we study the spectral properties of the Euclidean random matrices U and not of the Laplacian in the presence of disorder.

The problem we have considered involves a new class of random operators whose behavior is very different from either the disordered Laplacian or Gaussian random matrices. The mapping of the problem of cooperative effects in atomic gases onto a small world network may be interesting in the study of the statistical properties of random networks. Finally, the analysis we present in this dissertation may suggest a different approach and new protocoles for experiments on photon localization in cold atomic gases.

APPENDIX A

Elastic mean free path and group velocity of superradiant pairs

In this Appendix, we calculate explicitly expressions (192) and (199) for the elastic mean free path and the group velocity. At resonance, simple expressions for the elastic mean free path (195) and the group velocity (203) are obtained by a pertubative expansion with respect to the small parameter $k_0 r_m$.

1. Elastic mean free path

The elastic mean free path is given by (192) in terms of the function f_1 defined in (193). The integral in (193) is easily carried out analytically and it leads to

$$\frac{1}{l_e(\delta)} = \frac{6\pi n}{k_0^2}\frac{1}{aC}\left(\frac{b}{2a}A + \frac{a-2}{2a}B + C\right) \tag{A1}$$

where

$$a = 1 + (\delta/\Gamma_0)^2 \quad b = \delta/\Gamma_0 \tag{A2}$$

$$A = \ln\left(\frac{\frac{1}{4}x_m^2}{a + bx_m + \frac{1}{4}x_m^2}\right) \tag{A3}$$

$$B = \frac{\pi}{2} - \tan^{-1}(b + \frac{1}{2}x_m) \tag{A4}$$

and

$$C = \frac{1}{x_m} = k_0 r_m \ll 1. \tag{A5}$$

At resonance ($\delta = 0$) we have $a = 1$, $b = 0$ and by expanding (A4) with respect to $k_0 r_m$ we obtain

$$B \simeq \frac{2}{x_m}\left(1 - \frac{4}{3x_m^2}\right). \tag{A6}$$

Thus,

$$l_e(0) = \frac{k_0^2}{8\pi n}\frac{1}{(k_0 r_m)^2}, \tag{A7}$$

as given in (195).

2. Group velocity

The group velocity is given by (199) in terms of the function f_2 defined in (201). The integral in (201) is easily carried out analytically and it yields

$$\frac{c}{v_g(\delta)} = 1 - \frac{n}{n_c}\frac{F}{a^2 C} \tag{A8}$$

where

$$F = b(\frac{1}{a} - \frac{1}{4})A + \frac{a-2}{4}A' + (\frac{3}{2} - \frac{2}{a})B - bB' + (1 - \frac{a}{2})C \tag{A9}$$

$$A' = -\frac{b + \frac{1}{2}x_m}{a + bx_m + \frac{1}{4}x_m^2} \tag{A10}$$

and

$$B' = -\frac{\frac{1}{2}}{1 + (b + \frac{1}{2}x_m)^2}. \tag{A11}$$

At resonance ($\delta = 0$) we have $a = 1$, $b = 0$ and by expanding (A10) and (A4) with respect to $k_0 r_m$ we obtain

$$A' \simeq \frac{2}{x_m}\left(\frac{4}{x_m^2} - 1\right) \tag{A12}$$

and

$$B \simeq \frac{2}{x_m}\left(1 - \frac{4}{3x_m^2}\right). \tag{A13}$$

Thus,

$$\frac{c}{v_g(0)} = 1 + \frac{2}{3}\frac{n}{n_c}(k_0 r_m)^2, \tag{A14}$$

as given in (203).

APPENDIX B

Average self-energy of superradiant pairs

The aim of this Appendix is to calculate the average self-energy (208) for a $\Delta m = 0$ transition in the case where $k_0 r \ll 1$. First, we average the superradiative propagator (164) over the orientation of the inter-atomic axis and obtain analytical expressions for its real and imaginary parts. Then, by averaging over the inter-atomic distance up to r_m, we obtain the average self-energy (208).

For a $\Delta m = 0$ transition and $k_0 r \ll 1$, the superradiative propagator (164) may be written with the help of (115) and (116) as

$$\hbar\Gamma_0 G^+ = \left[\frac{\delta}{\Gamma_0} + \frac{3}{4}\left(\frac{3\cos^2\theta - 1}{(k_0 r)^3} + \frac{\frac{1}{2}(1+\cos^2\theta)}{k_0 r}\right) + i\right]^{-1}, \tag{B1}$$

where the inter-atomic axis is $\mathbf{r} = (r, \theta, \varphi)$. Averaging over the orientations

$$\hbar\Gamma_0\langle G^+\rangle = \frac{1}{4\pi}\int \hbar\Gamma_0 G^+ d\cos\theta d\varphi \tag{B2}$$

yields for the imaginary part,

$$\hbar\Gamma_0 \mathrm{Im}\langle G^+\rangle = -\frac{P+Q}{\beta^2} \tag{B3}$$

and for the real part,

$$\hbar\Gamma_0 \mathrm{Re}\langle G^+\rangle = W_- P + W_+ Q, \tag{B4}$$

where we have defined

$$P = \frac{1}{8A\beta\cos(\frac{\gamma}{2})}\ln\left(\frac{1+2\beta\cos(\frac{\gamma}{2})+\beta^2}{1-2\beta\cos(\frac{\gamma}{2})+\beta^2}\right) \tag{B5}$$

$$Q = \frac{1}{4A\beta\sin(\frac{\gamma}{2})}\left(\frac{\pi}{2} + \tan^{-1}\frac{1-\beta^2}{2\beta\sin(\frac{\gamma}{2})}\right) \tag{B6}$$

and

$$W\pm = -\sqrt{A}(\cos\gamma \mp 1). \tag{B7}$$

The auxiliary parameters are given by

$$\beta = (\tfrac{C}{A})^{\frac{1}{4}} \quad \gamma = \cos^{-1}(-\tfrac{B}{2\sqrt{AC}}) \ , \tag{B8}$$

where

$$A = \frac{9}{16(k_0 r)^2}\left(\frac{3}{(k_0 r)^2} + \frac{1}{2}\right)^2 \tag{B9}$$

$$B = \frac{3}{4k_0 r}\left(\frac{3}{(k_0 r)^2} + \frac{1}{2}\right)\left[\frac{2\delta}{\Gamma_0} + \frac{3}{2k_0 r}\left(\frac{1}{2} - \frac{1}{(k_0 r)^2}\right)\right] \tag{B10}$$

and

$$C = 1 + \frac{1}{4}\left[\frac{2\delta}{\Gamma_0} + \frac{3}{2k_0 r}\left(\frac{1}{2} - \frac{1}{(k_0 r)^2}\right)\right]^2 . \tag{B11}$$

Finally, we average (B3) and (B4) over the inter-atomic distance up to r_m, namely

$$\hbar\Gamma_0 \mathrm{Im}\langle\overline{G^+}\rangle = -\frac{1}{r_m}\int_0^{r_m} dr \frac{P+Q}{\beta^2} \tag{B12}$$

and

$$\hbar\Gamma_0 \mathrm{Re}\langle\overline{G^+}\rangle = \frac{1}{r_m}\int_0^{r_m} dr \left(W_- P + W_+ Q\right). \tag{B13}$$

The integrals can be evaluated numerically and give the average self-energy (208) since

$$\frac{1}{4\pi r_m}\int \hbar\Gamma_0 G^+(\mathbf{r}) d\mathbf{r} = \hbar\Gamma_0\langle\overline{G^+}\rangle. \tag{B14}$$

APPENDIX C

Scalar electric field operator in Heisenberg picture

In this Appendix we establish expression (223) for the scalar electric field operator in the Heisenberg picture. The scalar electric field operator (220) can be written as

$$E(\mathbf{r}) = E^{+}(\mathbf{r}) + E^{-}(\mathbf{r}), \tag{C1}$$

where its annihilation part is

$$E^{+}(\mathbf{r}) = \sum_{\mathbf{k}} \mathcal{E}_k e^{i\mathbf{k}\cdot\mathbf{r}} a_{\mathbf{k}}, \tag{C2}$$

with

$$\mathcal{E}_k = i\sqrt{\frac{\hbar\omega_k}{2\epsilon_0\Omega}} \tag{C3}$$

and its creation part is

$$E^{-}(\mathbf{r}) = [E^{+}(\mathbf{r})]^{\dagger}. \tag{C4}$$

The equation of motion of the annihilation operator is

$$\frac{da_{\mathbf{k}}}{dt} = \frac{1}{i\hbar}[a_{\mathbf{k}}, H], \tag{C5}$$

where the Hamiltonian is given in (219). Explicitly,

$$\frac{da_{\mathbf{k}}}{dt} = -i\omega_k a_{\mathbf{k}} + \frac{i}{\hbar}\sum_{i=1}^{N} d_i \mathcal{E}_k^{*} e^{-i\mathbf{k}\cdot\mathbf{r_i}}. \tag{C6}$$

The solution of (C6) reads

$$a_{\mathbf{k}}(t) = e^{-i\omega_k t}\left(a_{\mathbf{k}}(0) + \frac{i}{\hbar}\int_0^t d\tau \sum_{i=1}^{N} d_i(\tau)\mathcal{E}_k^{*} e^{-i\mathbf{k}\cdot\mathbf{r_i}} e^{i\omega_k \tau}\right). \tag{C7}$$

Thus, (C2) can be rewritten as

$$E^{+}(\mathbf{r},t) = E_f^{+}(\mathbf{r},t) + E_s^{+}(\mathbf{r},t), \tag{C8}$$

where the free field contribution is

$$E_f^+(\mathbf{r},t) = \sum_{\mathbf{k}} \mathcal{E}_k e^{i\mathbf{k}\cdot\mathbf{r}} e^{-i\omega_k t} a_{\mathbf{k}}(0), \tag{C9}$$

while the source term, originates from the radiating atoms, is

$$E_s^+(\mathbf{r},t) = \frac{i}{\hbar}\int_0^t d\tau \sum_{i=1}^{N} d_i(\tau) \sum_{\mathbf{k}} |\mathcal{E}_k|^2 e^{i[\omega_k(t-\tau)-\mathbf{k}\cdot(\mathbf{r}-\mathbf{r_i})]}. \tag{C10}$$

According to (152), the electric dipole moment operator can be written as

$$d_i(\tau) = d_i^+(\tau) + d_i^-(\tau), \tag{C11}$$

where

$$d_i^+(\tau) = \langle g|d|e\rangle b_i(\tau) \tag{C12}$$

and

$$d_i^-(\tau) = [d_i^+(\tau)]^\dagger. \tag{C13}$$

Thus, (C10) reads

$$E_s^+(\mathbf{r},t) = \frac{i}{\hbar}\sum_{i=1}^{N}\left[\int_0^t d\tau d_i^+(\tau) f(\mathbf{r}-\mathbf{r}_i, t-\tau) + \int_0^t d\tau d_i^-(\tau) f(\mathbf{r}-\mathbf{r}_i, t-\tau)\right], \tag{C14}$$

with

$$f(\mathbf{r},t) = \sum_{\mathbf{k}} |\mathcal{E}_k|^2 e^{i(\omega_k t - \mathbf{k}\cdot\mathbf{r})}. \tag{C15}$$

By setting

$$d_i^\pm(\tau) = e^{\pm i\omega_0\tau}\hat{d}_i^\pm(\tau) \tag{C16}$$

and defining $\tau' = t - \tau$, we may rewrite (C14) as

$$E_s^+(\mathbf{r},t) = \frac{i}{\hbar}\sum_{i=1}^{N}\left[e^{i\omega_0 t}\int_0^t d\tau' \hat{d}_i^+(t-\tau') g(\mathbf{r}-\mathbf{r}_i,\tau') + e^{-i\omega_0 t}\int_0^t d\tau' \hat{d}_i^-(t-\tau') h(\mathbf{r}-\mathbf{r}_i,\tau')\right], \tag{C17}$$

where

$$g(\mathbf{r}-\mathbf{r}_i,\tau') = e^{-i\omega_0\tau'} f(\mathbf{r}-\mathbf{r}_i,\tau') \tag{C18}$$

and

$$h(\mathbf{r}-\mathbf{r}_i,\tau') = e^{i\omega_0\tau'} f(\mathbf{r}-\mathbf{r}_i,\tau'). \tag{C19}$$

Since (C15) is centered around $t = r/c$, expression (C17) can be approximated as

$$E_s^+(\mathbf{r},t) \simeq A(\mathbf{r},t) + B(\mathbf{r},t), \tag{C20}$$

where

$$A(\mathbf{r},t) = \frac{i}{\hbar}\sum_{i=1}^{N} e^{i\omega_0 t}\hat{d}_i^+ \left(t - \frac{|\mathbf{r}-\mathbf{r}_i|}{c}\right)\int_0^\infty d\tau' g(\mathbf{r}-\mathbf{r}_i,\tau') \tag{C21}$$

and

$$B(\mathbf{r},t) = \frac{i}{\hbar}\sum_{i=1}^{N} e^{-i\omega_0 t}\hat{d}_i^- \left(t - \frac{|\mathbf{r}-\mathbf{r}_i|}{c}\right)\int_0^\infty d\tau' h(\mathbf{r}-\mathbf{r}_i,\tau'). \tag{C22}$$

Similarly, solving the equation of motion of the creation operator, namely

$$\frac{da_{\mathbf{k}}^\dagger}{dt} = \frac{1}{i\hbar}[a_{\mathbf{k}}^\dagger, H] \tag{C23}$$

yields for the creation part of the scalar electric field operator (C4)

$$E^-(\mathbf{r},t) = E_f^-(\mathbf{r},t) + E_s^-(\mathbf{r},t), \tag{C24}$$

where

$$E_f^-(\mathbf{r},t) = [E_f^+(\mathbf{r},t)]^\dagger \tag{C25}$$

and

$$E_s^-(\mathbf{r},t) = [E_s^+(\mathbf{r},t)]^\dagger. \tag{C26}$$

Therefore, the scalar electric field operator in the Heisenberg picture can be written as

$$E(\mathbf{r},t) = E_f(\mathbf{r},t) + E_s(\mathbf{r},t), \tag{C27}$$

with, according to (C9) and (C25),

$$E_f(\mathbf{r},t) = \sum_{\mathbf{k}} \mathcal{E}_k e^{i\mathbf{k}\cdot\mathbf{r}} e^{-i\omega_k t} a_{\mathbf{k}}(0) + h.c. \tag{C28}$$

and, according to (C20) and (C26),

$$E_s(\mathbf{r},t) = \sum_{i=1}^{N} e^{i\omega_0 t}\hat{d}_i^+ \left(t - \frac{|\mathbf{r}-\mathbf{r}_i|}{c}\right)\mathcal{F}(\mathbf{r}-\mathbf{r}_i) + h.c., \tag{C29}$$

where

$$\mathcal{F}(\mathbf{r}) = \frac{i}{\hbar}\int_0^\infty d\tau e^{-i\omega_0\tau}[f(\mathbf{r},\tau) - f^*(\mathbf{r},\tau)]. \tag{C30}$$

A standard calculation [16] leads to

$$\mathcal{F}(\mathbf{r}) = \frac{1}{\epsilon_0}\left[\delta(\mathbf{r}) + \frac{k_0^3}{4\pi}\frac{e^{ik_0 r}}{k_0 r}\right], \tag{C31}$$

where $k_0 = \omega_0/c$.

Finally, for $\mathbf{r} \neq \mathbf{r}_i$ and by neglecting retardation effects, substituting (C31) in (C29), yields

$$E_s(\mathbf{r},t) = C\sum_{i=1}^{N}\frac{e^{-ik_0|\mathbf{r}-\mathbf{r_i}|}}{k_0|\mathbf{r}-\mathbf{r_i}|}b_i(t) + h.c., \tag{C32}$$

where C depends on the radiation wavelength and on the electric dipole matrix element. Thus, expression (223) has been established.

APPENDIX D

Generalized scaling function

In this Appendix we show that the scaling behavior of g defined by (261) does not depend on the choice of the cutoff parameter in (260), provided it fulfills $0 < c \leq 1$. To this purpose we define a generalized version of the function g, namely

$$g_c(a, W) = 1 - 2 \int_c^\infty d\Gamma \;\; P(\Gamma). \tag{D1}$$

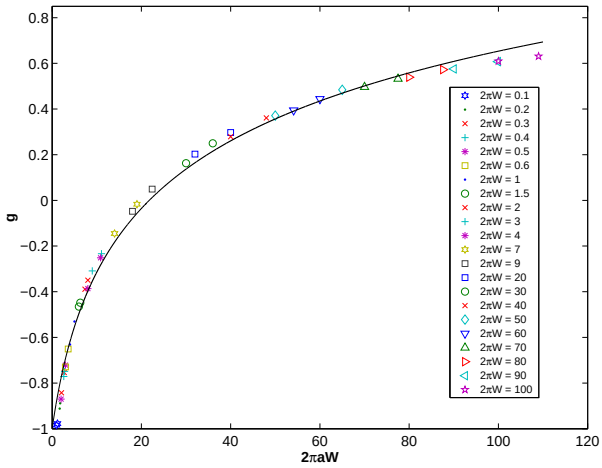

Behavior of the scaling function g with $c = 1/2$ as a function of the optical depth $\mathtt{b} = 2\pi aW$ in the large sample regime. The solid line is a fitting function, given by (D4).

We start with the three-dimensional geometry discussed in Section 5.4. In Dicke regime ($a \ll 1$), the average density of photon escape rates is given for $N > 1$ by (258), *i.e.*,

$$P(\Gamma) = \frac{1}{N}[\delta(\Gamma - N) + (N - 1)\delta(\Gamma)]. \tag{D2}$$

Thus, in order to characterize $P(\Gamma)$, the cutoff parameter must fulfill $0 < c < N$ and the generalized function (D1), under this constrain, is

$$g_c(a, W) = 1 - \frac{2}{N} = 1 - \frac{1}{\pi a^3 W}, \tag{D3}$$

regardless of c.

In the large sample regime ($a \geq 1$), according to Figure 8, in order to characterize $P(\Gamma)$ the cutoff parameter must fulfill $0 < c \leq 1$. We have checked that the scaling behavior of g_c does not depend on the choice of the cutoff parameter, provided it fulfills the previous condition. However, if it is chosen to be $0 < c < 1$ instead of $c = 1$, then the generalized function (D1) obeys $|g_c| \leq 1$ instead of $0 \leq g_1 \leq 1$, but the scaling behavior is the same, as shown in the enclosed figure for $c = 1/2$ and in Figure 12 for $c = 1$.

The fitting function of the data presented in the enclosed figure is the shifted small world function (280), namely

$$g_{1/2}(x) = -1 + Cxf(x). \tag{D4}$$

Here the scaling variable is $x = 2\mathtt{b}/3$, where $\mathtt{b}$ is the optical depth (267), $C \simeq 0.2$ and $f(x)$ is given in (278).

Therefore, by combining the constrains on c, we obtain that for $0 < c \leq 1$ the scaling behavior of g does not depend on the choice of the cutoff parameter.

This result can be applied directly to the one-dimensional case discussed in Section 5.5.

APPENDIX E

Average path length of ring lattices

The average path length (276), which is the average shortest path between any randomly chosen vertices, is defined for a network of N vertices with a rewiring probability ϕ as

$$l(\phi) = \frac{1}{N(N-1)} \overline{\sum_{i \neq j} y_{ij}}, \tag{E1}$$

where y_{ij} is the shortest path between vertices i and j and $\overline{\cdots}$ denotes configuration averaging. In this Appendix we calculate (E1) for a ring lattice in the limiting cases where $\phi = 0$ and $\phi = 1$.

1. Regular lattice

For a regular ring lattice, where each vertex is connected to its K first neighbors ($K/2$ on either side), expression (E1) can be written as

$$l(0) = \frac{1}{N-1} \sum_{i=1}^{N-1} y_i, \tag{E2}$$

where y_i is the shortest distance between vertex 0 and vertex i. This shortest distance is given for $1 \leq i \leq \text{floor}(N/2)$ by

$$y_i = \begin{cases} \frac{2i}{K} & \text{mod}(\frac{2i}{K}) = 0 \\ \text{floor}(\frac{2i}{K}) + 1 & \text{mod}(\frac{2i}{K}) \neq 0 \end{cases}, \tag{E3}$$

where due to boundary conditions $y_{N-i} = y_i$. Substituting (E3) in (E2) reads

$$l(0) = \frac{KF(1+F)}{2(N-1)} + \frac{(N-1-KF)(1+F)}{N-1}, \tag{E4}$$

or

$$l(0) = \left(1 - \frac{KF}{2(N-1)}\right)(1+F), \tag{E5}$$

where we have defined

$$F = \text{floor}\left(\frac{N-1}{K}\right). \tag{E6}$$

For $N \gg 1$, (E5) gives $l(0) \propto N$. Thus, in a regular lattice the average path length scales linearly with the system size.

For example, for $N = 11$ and $K = 4$, we have

$$y_1 = y_2 = y_9 = y_{10} = 1, \tag{E7}$$

$$y_3 = y_4 = y_7 = y_8 = 2 \tag{E8}$$

and

$$y_5 = y_6 = 3. \tag{E9}$$

Thus, (E2) or (E4) yield

$$l(0) = \frac{4 \times (1+2)}{10} + \frac{2 \times 3}{10} = \frac{18}{10}, \tag{E10}$$

which coincides with a direct substitution in (E5).

2. Random network

The simplest case of a random network defines the probability p that any two randomly chosen vertices are connected. In the limit of small p and large N, but with a finite value of $\Lambda = pN$, the Poisson distribution is obtained. Therefore, the average number of first neighbors of a specific vertex is Λ. Since a given vertex has on average Λ first neighbors, Λ^2 second neighbors, etc., $l(1)$ obeys the following relation

$$\Lambda^{l(1)} \simeq N. \tag{E11}$$

Thus, $l(1) \propto \ln(N)$, and we conclude that in a random network the average path length scales logarithmically with the system size.

APPENDIX F

Publications

This Appendix includes the papers written during the research. The first one "Effect of superradiance on transport of diffusing photons in cold atomic gases", published in the Physical Review Letters journal, deals with the scalar model of superradiant pairs presented in Sections 4.1-4.3. The second paper "Superradiance and multiple scattering of photons in atomic gases", published in the Physical Review A journal, studies the vectorial model of superradiant pairs developed in Section 4.4 and compares the latter approach to the scalar one introduced in the previous article. The last paper, "Photon localization and Dicke superradiance in atomic gases: crossover to a small-world network", submitted to the Physical Review Letters journal, summarizes the results of Chapter 5.

.

Effect of Superradiance on Transport of Diffusing Photons in Cold Atomic Gases

A. Gero and E. Akkermans

Department of Physics, Technion—Israel Institute of Technology, Haifa 32000, Israel

(Received 25 August 2005; published 6 March 2006)

We show that in atomic gases cooperative effects like superradiance and subradiance lead to a potential between two atoms that decays like $1/r$. In the case of superradiance, this potential is attractive for close enough atoms and can be interpreted as a coherent mesoscopic effect. The contribution of superradiant pairs to multiple scattering properties of a dilute gas, such as photon elastic mean free path and group velocity, is significantly different from that of independent atoms. We discuss the conditions under which these effects may be observed and compare our results to recent experiments on photon transport in cold atomic gases.

DOI: 10.1103/PhysRevLett.96.093601 PACS numbers: 42.50.Fx, 32.80.Pj, 42.25.Dd

The issue of coherent multiple scattering of photons in cold atomic gases is important since it presents a path towards the onset of Anderson localization transition, a long standing and still open issue. The large resonant scattering cross section of photons reduces the elastic mean free path to values comparable to the photon wavelength for which the weak disorder approximation breaks down, thus signaling the onset of Anderson localization transition [1,2]. Another advantage of cold atomic gases is that sources of decoherence and inelastic scattering such as Doppler broadening can be neglected. Moreover, propagation of photons in atomic gases differs from the case of electrons in disordered metals or of electromagnetic waves in suspensions of classical scatterers for which mesoscopic effects and Anderson localization have been thoroughly investigated [1]. This problem is then of great interest since it may raise new issues in the Anderson problem such as change of universality class and, therefore, new critical behavior. New features displayed by the photon-atom problem are the existence of internal degrees of freedom (Zeeman sublevels) and cooperative effects such as subradiance or superradiance that lead to effective interactions between atoms [3]. These two differences may lead to qualitative changes of both mesoscopic quantities and Anderson localization. Some of the effects of a Zeeman degeneracy have been investigated in the weak disorder limit [4] using a set of finite phase coherence times [5] which reduce mesoscopic effects, such as coherent backscattering [1,6]. The aim of this Letter is to investigate the influence of cooperative effects and more specifically of superradiance on the multiple scattering of photons. We show that two atoms in a Dicke superradiant state [7] interact by means of a potential which, once averaged over disorder configurations, is attractive at short distances and decays like $1/r$. This potential, analogous to the one considered in [8,9], has important consequences on transport properties since the contribution of superradiant pairs of atoms in a dilute gas provides smaller values of both group velocity and diffusion coefficient so that the photons become closer to the edge of Anderson localization.

Atoms are taken as degenerate two-level systems denoted by $|g\rangle = |j_g = 0, m_g = 0\rangle$ for the ground state and $|e\rangle = |j_e = 1, m_e\rangle$ for the excited state, where j is the total angular momentum and m is its projection on the quantization axis, taken as the $\hat{z}$ axis. The energy separation between the two levels including radiative shift is $\hbar\omega_0$ and the natural width of the excited level is $\hbar\Gamma$. We consider a pair of such atoms in an external radiation field and the corresponding Hamiltonian is $H = H_0 + V$, with

$$H_0 = \frac{\hbar\omega_0}{2}\sum_{l=1}^{2}[|e\rangle\langle e| - |g\rangle\langle g|]_l + \sum_{\mathbf{k}\epsilon}\hbar\omega_k a^\dagger_{\mathbf{k}\varepsilon}a_{\mathbf{k}\varepsilon}, \quad (1)$$

$a_{\mathbf{k}\varepsilon}$ ($a^\dagger_{\mathbf{k}\varepsilon}$) is the annihilation (creation) operator of a mode of the field of wave vector $\mathbf{k}$, polarization $\hat{\varepsilon}_{\mathbf{k}}$, and angular frequency $\omega_k = c|\mathbf{k}|$. The interaction V between the radiation field and the dipole moments of the atoms may be written as

$$V = -\mathbf{d_1}\cdot\mathbf{E}(\mathbf{r_1}) - \mathbf{d_2}\cdot\mathbf{E}(\mathbf{r_2}), \quad (2)$$

where $\mathbf{d}_l$ is the electric dipole moment operator of the lth atom and $\mathbf{E}(\mathbf{r})$ is the electric field operator.

The absorption of a photon by a pair of atoms in their ground state leads to a configuration where the two atoms, one excited and the second in its ground state, have multiple exchange of a photon, giving rise to an effective interaction potential and to a modified lifetime as compared to independent atoms. These two quantities are obtained from the matrix elements of the evolution operator $U(t)$ between states such as $|g_1e_2;0\rangle$. There are six unperturbed and degenerate states with no photon, given by $\{|g_1e_{2i};0\rangle, |e_{1j}g_2;0\rangle\}$ in a standard basis where $i, j = -1, 0, 1$. The symmetries of the Hamiltonian, namely, its invariance by rotation around the axis between the two atoms, and by reflection with respect to a plane containing this axis, allows one to find combinations of these states that are given by $|\phi^\epsilon_i\rangle = \frac{1}{\sqrt{2}}[|e_{1i}g_2;0\rangle + \epsilon|g_1e_{2i};0\rangle]$ with $\epsilon = \pm 1$, so that $\langle\phi^{\epsilon'}_j|U(t)|\phi^\epsilon_i\rangle = \delta_{ij}\delta_{\epsilon\epsilon'}S^\epsilon_i(t)$ and

$$S_i^{\epsilon}(t) = \langle e_{1i}g_2;0|U(t)|e_{1i}g_2;0\rangle + \epsilon\langle g_1e_{2i};0|U(t)|e_{1i}g_2;0\rangle. \quad (3)$$

The states $|\phi_i^{\epsilon}\rangle$ are the well-known Dicke states, otherwise defined as $|LM\rangle$, where L is the cooperation number and M is half of the total atomic inversion [7] so that $|\phi_i^+\rangle = |10\rangle$ and $|\phi_i^-\rangle = |00\rangle$. For large times, $t \gg r/c$, where r is the distance between the two atoms, up to second order in the coupling to the radiation, we obtain that

$$S_i^{\epsilon}(t) \simeq 1 - \frac{it}{\hbar}\left[\Delta E_i^{\epsilon} - i\frac{\hbar\Gamma_i^{\epsilon}}{2}\right]. \quad (4)$$

The two real quantities ΔE_i^{ϵ} and Γ_i^{ϵ} are, respectively, the interacting potential and the probability per unit time of emission of a photon by the two atoms in a Dicke state $|\phi_i^{\epsilon}\rangle$. A standard calculation [10] gives

$$\Delta E_i^{\epsilon} = \epsilon\frac{3\hbar\Gamma}{4}\left[-p_i\frac{\cos k_0r}{k_0r} + q_i\left(\frac{\cos k_0r}{(k_0r)^3} + \frac{\sin k_0r}{(k_0r)^2}\right)\right] \quad (5)$$

and

$$\frac{\Gamma_i^{\epsilon}}{\Gamma} = 1 - \frac{3}{2}\epsilon\left[-p_i\frac{\sin k_0r}{k_0r} + q_i\left(\frac{\sin k_0r}{(k_0r)^3} - \frac{\cos k_0r}{(k_0r)^2}\right)\right], \quad (6)$$

where $k_0 = \omega_0/c$. We have defined $p_i = 1 - \hat{\mathbf{r}}_i^2$ and $q_i = 1 - 3\hat{\mathbf{r}}_i^2$, $\hat{\mathbf{r}}$ being a unit vector along the two atoms. At short distance $k_0r \ll 1$, we obtain that $\Gamma_i^+ = 2\Gamma$ for the superradiant state $|\phi_i^+\rangle = |10\rangle$ and $\Gamma_i^- = 0$ for the subradiant state $|\phi_i^-\rangle = |00\rangle$.

For a photon of wave vector $\mathbf{k}$ incident on an atomic cloud, the potential we shall denote by V_e is obtained by averaging upon the random orientations of the pairs of atoms. Since $\langle q_i\rangle = 0$ and $\langle p_i\rangle = 2/3$ regardless of i, we obtain for the average potential V_e

$$\epsilon V_e(r) = \langle\Delta E_i^{\epsilon}\rangle = -\epsilon\frac{\hbar\Gamma}{2}\frac{\cos k_0r}{k_0r} \quad (7)$$

and the average inverse lifetimes of Dicke states are

$$\langle\Gamma_i^{\epsilon}\rangle = \Gamma\left[1 + \epsilon\frac{\sin k_0r}{k_0r}\right], \quad (8)$$

which retains the same features as (6) for $k_0r \ll 1$.

Let us characterize the interaction potential V_e. Whereas for a single pair of atoms, the potential (5) is anisotropic and decays at short distance like $1/r^3$, a behavior that originates from the transverse part of the photon propagator, we obtain that on average over angular configurations, the potential (7) between two atoms in a Dicke state $M = 0$ becomes isotropic and decays like $1/r$. This behavior is also obtained by considering the interaction of two-level atoms with a scalar wave. This could have been anticipated since the transverse contribution q_i to the photon propagator averages to 0. A similar expression for the interacting potential has been obtained for the case of an intense radiation field [8,9]. But this latter potential is fourth order in the coupling to the radiation and it corresponds to the interaction energy between two atoms in their ground state in the presence of at least one photon. The average potential V_e we have obtained is different. It is second order in the coupling to the radiation and it corresponds to the interaction energy of Dicke states $M = 0$ in vacuum.

We turn now to scattering properties of Dicke states. The collision operator is given by $T(z) = V + VG(z)V$, where V is given by (2) and $G(z)$ is the resolvent whose expectation value in a Dicke state $M = 0$ is obtained by a summation of the series of exchange of a virtual photon between the two atoms. The matrix element that describes the transition from the initial state $|i\rangle = |1 - 1;\mathbf{k}\hat{\varepsilon}\rangle$ where the two atoms are in their ground state in the presence of a photon $(\mathbf{k}\hat{\varepsilon})$ to the final state, $|f\rangle = |1 - 1;\mathbf{k}'\hat{\varepsilon}'\rangle$, is the sum of the superradiant and subradiant contributions, $T = T^+ + T^-$, with $T^{\pm} = \langle f|V|\phi^{\pm}\rangle\langle\phi^{\pm}|G(\omega - \omega_0)|\phi^{\pm}\rangle \times \langle\phi^{\pm}|V|i\rangle$ [11]. A standard derivation leads to the following expressions for the average amplitudes $T_e^{\pm}$

$$T_e^+ = Ae^{i(\mathbf{k}-\mathbf{k}')\cdot\mathbf{R}}\cos\left(\frac{\mathbf{k}\cdot\mathbf{r}}{2}\right)\cos\left(\frac{\mathbf{k}'\cdot\mathbf{r}}{2}\right)G_e^+ \quad (9)$$

and

$$T_e^- = Ae^{i(\mathbf{k}-\mathbf{k}')\cdot\mathbf{R}}\sin\left(\frac{\mathbf{k}\cdot\mathbf{r}}{2}\right)\sin\left(\frac{\mathbf{k}'\cdot\mathbf{r}}{2}\right)G_e^-. \quad (10)$$

We have defined $\mathbf{r} = \mathbf{r}_1 - \mathbf{r}_2$, $\mathbf{R} = (\mathbf{r}_1 + \mathbf{r}_2)/2$, and $A = \frac{\hbar\omega}{\epsilon_0\Omega}d^2(\hat{e}_j\cdot\hat{\varepsilon})(\hat{e}_j^*\cdot\hat{\varepsilon}'^*)$ (d is a reduced matrix element and Ω the quantization volume). The average propagators $G_e^{\pm}$ associated, respectively, to the superradiant and subradiant states are,

$$G_e^{\pm} = \langle\phi^{\pm}|G(\delta)|\phi^{\pm}\rangle = \frac{1}{\hbar(\delta + i\frac{\Gamma}{2} \pm \frac{\Gamma}{2}\frac{e^{ik_0r}}{k_0r})}, \quad (11)$$

where close to resonance, $\delta = \omega - \omega_0 \ll \omega_0$ and where we have used (7) and (8) for the average potential and for the average inverse lifetimes. At short distances $k_0r \ll 1$, the subradiant amplitude T_e^- becomes negligible as compared to the superradiant term (9). Therefore, the potential (7) is attractive and decays like $1/r$. We can interpret these results by saying that, at short distances $(k_0r \ll 1)$, the time evolution of the initial state $|\psi(0)\rangle = |e_1, g_2;0\rangle = \frac{1}{\sqrt{2}}[|\phi^+\rangle + |\phi^-\rangle]$ corresponds for times shorter than $1/\Gamma$ to a periodic exchange of a virtual photon between the two atoms at the Rabi frequency $(\langle\Delta E^-\rangle - \langle\Delta E^+\rangle)/\hbar \simeq \Gamma/(k_0r)$ which is much larger than Γ. For larger times, the two atoms return to their ground state and a real photon $(\mathbf{k}'\hat{\varepsilon}')$ is emitted. At large distances $(k_0r \gg 1)$, the Rabi frequency becomes smaller than Γ, so that the excitation energy makes only a few oscillations between the two atoms, thus leading to a negligible interaction potential [12].

It is interesting to derive the previous results in another way that emphasizes the analogy with weak localization corrections [1,2].

To that purpose, we write the scattering amplitude T defined previously as a superposition of two scalar amplitudes T_1 and T_2 [13], each of them being a sum of single scattering and double scattering contributions, that is

$$T_1 = \frac{t}{1 - t^2 G_0^2}[e^{i(\mathbf{k}-\mathbf{k}')\cdot\mathbf{r}_1} + tG_0 e^{i(\mathbf{k}\cdot\mathbf{r}_1 - \mathbf{k}'\cdot\mathbf{r}_2)}] \quad (12)$$

and

$$T_2 = \frac{t}{1 - t^2 G_0^2}[e^{i(\mathbf{k}-\mathbf{k}')\cdot\mathbf{r}_2} + tG_0 e^{i(\mathbf{k}\cdot\mathbf{r}_2 - \mathbf{k}'\cdot\mathbf{r}_1)}]. \quad (13)$$

Here $t = (2\pi\Gamma/k_0)/(\delta + i\Gamma/2)$ is the amplitude of a scalar wave scattered by a single atom at the origin and the prefactor $t/(1 - t^2 G_0^2)$ where $G_0 = -e^{ik_0 r}/4\pi r$ accounts for the summation of the series of virtual photon exchange between the two scatterers. We single out in the total amplitude $T = T_1 + T_2$, the single scattering contribution T_s, and write the intensity associated to the double scattering term shown in Fig. 1 as

$$|T - T_s|^2 = 2\left|\frac{t^2 G_0}{1 - t^2 G_0^2}\right|^2[1 + \cos(\mathbf{k} + \mathbf{k}')\cdot(\mathbf{r}_1 - \mathbf{r}_2)]. \quad (14)$$

We recognize in the bracket the well-known Cooperon interference term which is at the basis of coherent effects in quantum mesoscopic systems such as weak localization and coherent backscattering [1,2,6]. The interference term reaches its maximum value 1 for $\mathbf{r}_1 = \mathbf{r}_2$ so that we obtain from (12) and (13) that $T_1 = T_2 \propto (1/2)T_e^+$, up to a proportionality factor [13]. Thus, the total amplitude is exactly given by the superradiant term with no subradiant contribution.

We consider now multiple scattering of a photon by superradiant pairs built out of atoms separated by a distance r and coupled by the attractive interaction potential V_e. This situation corresponds to a dilute gas that fulfills $r \ll \lambda_0 \ll n_i^{-1/3}$, where n_i is the density of pairs and $\lambda_0 = 2\pi/k_0$ is the atomic transition wavelength. Based on this inequality, we may consider the two atoms that form a superradiant pair through exchange of a virtual photon as an effective scatterer and neglect cooperative interactions between otherwise well-separated pairs. The photon behavior is described by the configuration average of its Green's function, whose expression is obtained from a standard derivation [1]. In the limit of large enough densities of weakly scattering pairs, it reduces to the calculation of a self-energy given in terms of the average propagator (11) by

$$\overline{\Sigma}_e^{(1)} = \frac{6\pi\hbar\Gamma n_i}{k_0}\overline{G}_e^+ = \frac{6\pi n_i}{k_0 r_m}\int_0^{r_m}\frac{dr}{\frac{\delta}{\Gamma} + \frac{1}{2k_0 r} + i}. \quad (15)$$

The average, denoted by $\overline{\ldots}$, is taken over distances r up to a maximal value $r_m \ll k_0^{-1}$ which accounts for all possible mechanisms that may break those pairs. In the considered limit, the density of the gas can be assimilated to that of the pairs. The imaginary part of $\overline{\Sigma}_e^{(1)}$ defines the elastic mean free path l_e by $k_0/l_e = -\mathrm{Im}\overline{\Sigma}_e^{(1)}$, namely,

$$\frac{1}{l_e} = \frac{3\pi n_i}{k_0^2}\frac{1}{k_0 r_m}\int_0^{2k_0 r_m}\frac{dx}{1 + (\frac{\delta}{\Gamma} + \frac{1}{x})^2}. \quad (16)$$

It is interesting to compare l_e to the mean free path $l_0 = \frac{k_0^2}{6\pi n_i}[1 + (2\delta/\Gamma)^2]$ that corresponds to near resonant elastic scattering of a photon by independent atoms. At resonance ($\delta = 0$), we have $l_0/l_e = \frac{4}{3}(k_0 r_m)^2 \ll 1$. Away from resonance, the elastic mean free path l_e becomes smaller than l_0 and for blue detuning it is reduced in a ratio roughly given by $1/(k_0 r_m)^2$.

Another important physical quantity is the group velocity v_g given in terms of the refraction index η by $c/v_g = \eta + \omega\frac{d\eta}{d\omega}$. Since $\overline{\Sigma}_e^{(1)}$ is proportional to the polarizability, the refraction index depends on its real part, namely $\eta = [1 - (c/\omega)^2\,\mathrm{Re}\overline{\Sigma}_e^{(1)}]^{1/2}$. From (15), we notice that $\eta \simeq 1$ for all values of the detuning δ/Γ and in a large range of densities n_i so that

$$\frac{c}{v_g} = 1 - \frac{n_i}{n_c}\frac{1}{2k_0 r_m} f\left(k_0 r_m, \frac{\delta}{\Gamma}\right), \quad (17)$$

where we have defined $n_c = (k_0^3/6\pi)\frac{\Gamma}{\omega_0}$ and the function

$$f(k_0 r_m, \Delta) = \int_0^{2k_0 r_m} dx \frac{1 - (\Delta + \frac{1}{x})^2}{[1 + (\Delta + \frac{1}{x})^2]^2}. \quad (18)$$

This expression of v_g diverges at a large and negative value of the detuning $\frac{\delta}{\Gamma} \simeq -1/(2k_0 r_m)$ and beyond it takes both positive and negative values. Otherwise it is well behaved, meaning that it remains finite and positive for all values of the density n_i. At resonance, the group velocity is

$$\frac{c}{v_g} = 1 + \frac{4\pi n_i}{k_0^3}\frac{\omega_0}{\Gamma}(k_0 r_m)^2. \quad (19)$$

The present expression of v_g differs substantially from the one obtained for light interaction with independent two-level atoms. There, for densities $n_i > n_c$ where n_c defined above is usually overwhelmingly small, the group

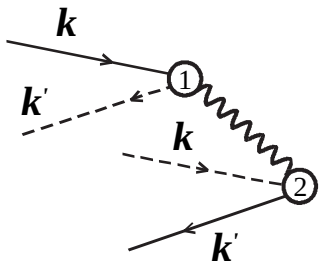

FIG. 1. Diagrammatic representation of the two amplitudes that describe double scattering of a scalar wave. The wavy line accounts for the photon exchange between the two atoms. This diagram is known in quantum mesoscopic physics as a Cooperon.

velocity is known to diverge at two symmetric values of the detuning of order unity and takes negative values in between (i.e., also at resonance). For instance, in a gas of ^{85}Rb atoms, where $n_i = 6 \times 10^{10}$ cm^{-3}, $\lambda_0 = 780$ nm, and $\frac{\Gamma}{2\pi} = 5.9$ MHz, we have $n_i/n_c \simeq 10^5$. The validity of the concept of group velocity in such systems has thus been often questioned [14] and an energy velocity has been defined which describes energy transport through a diffusive medium [15].

Transport of photons through a diffusing gas is characterized by the diffusion coefficient $D = \frac{1}{3} v_g l_e$ that combines the elastic mean free path and the group velocity [1,16], both derived from the complex valued self-energy (15). The diffusion coefficient D is of great importance since it enters in expressions of all measured physical quantities such as reflection and transmission coefficients, angular correlations of speckle patterns, time correlation functions of the intensity (diffusing wave spectroscopy), etc. [1]. Moreover, the critical behavior of transport close to Anderson localization transition at strong disorder is also obtained from the scaling form of D. Its expression, deduced from (16) and (17), depends on the range r_m and on the detuning δ/Γ. Since the group velocity and the elastic mean free path are significantly modified for the case of superradiant pairs, we thus expect the diffusion coefficient to be different from its value obtained for independent atoms. We also define the transport time by $\tau_{\mathrm{tr}}(\delta) = l_e/v_g = 3D/v_g^2$. At resonance, it can be rewritten with the help of (19) as $\tau_{\mathrm{tr}}(0) = \frac{1}{2\Gamma}$ which is consistent with our considering of superradiant pairs. We would like nevertheless to call attention to the fact that, away from resonance, $\tau_{\mathrm{tr}}(\delta)$ depends on frequency.

We now compare our results to recent measurements of the diffusion coefficient D and of the group velocity v_g obtained for multiple scattering of light at resonance, in a cold atomic gas of ^{85}Rb [17]. Since the range r_m cannot be directly determined, we first use Eqs. (16) and (17) to obtain an expression independent of $k_0 r_m$ given by the ratio $\frac{(v_g/c)^2}{3D} = 8\pi n_c/k_0^2 c = 2\Gamma/c^2$. For ^{85}Rb atoms, this ratio equals 8.2×10^{-10} s/m^2, which is in good agreement with the value 4.8×10^{-10} s/m^2 obtained from measurements of D and v_g. Finally, from the previous numerical expression we deduce for the maximal range of interaction r_m the value $k_0 r_m \simeq 0.51$ also consistent with our assumption of superradiant states. Therefore, multiple scattering of photons by superradiant pairs provides a relevant mechanism that needs to be considered, in addition to others, e.g., scattering by independent atoms, for description of multiple scattering properties of dilute cold atomic gases.

We have considered multiple scattering of a photon on pairs of atoms that are in a superradiant state. On average over disorder configurations, an attractive interaction potential builds up between close enough atoms that decays like $1/r$. The contribution of superradiant pairs, resulting from this potential, to scattering properties is significantly different from that of independent atoms. It leads to a well defined but much smaller group velocity as compared to c and correlatively to a smaller diffusion coefficient. For densities considered in recent experiments on cold ^{85}Rb atoms, the quantity $k_0 l_e$ that describes eventually the closeness to a localization transition, is reduced at moderate detunings, by 1 order of magnitude. This effect is expected to be even stronger for larger densities which could then be close to the localization edge.

This research is supported in part by the Israel Academy of Sciences and by the Fund for Promotion of Research at the Technion.

[1] E. Akkermans and G. Montambaux, *Physique Mésoscopique des électrons et des Photons* (EDP Sciences, Paris, 2004) [English translation (Cambridge University Press, Cambridge, England, to be published).]
[2] B. L. Altshuler and B. Simons, in *Mesoscopic Quantum Physics*, Proceedings of the Les Houches Summer School, Session LXI, edited by E. Akkermans *et al.* (Elsevier, Amsterdam, 1995); Y. Imry, *Introduction to Mesoscopic Physics* (Oxford, New York, 2002).
[3] Superradiance in Bose-Einstein condensates has been investigated experimentally in D. Schneble *et al.*, Science **300**, 475 (2003).
[4] G. Labeyrie *et al.*, Phys. Rev. Lett. **83**, 5266 (1999); C. A. Müller and C. Miniatura, J. Phys. A **35**, 10 163 (2002).
[5] E. Akkermans, C. Miniatura, and C. A. Müller, cond-mat/0206298.
[6] E. Akkermans and R. Maynard, J. Phys. (France) Lett. **46**, L-1045 (1985).
[7] R. H. Dicke, Phys. Rev. **93**, 99 (1954).
[8] T. Thirunamachandran, Mol. Phys. **40**, 393 (1980).
[9] D. O'Dell *et al.*, Phys. Rev. Lett. **84**, 5687 (2000); R. Loew *et al.*, quant-ph/0503156.
[10] M. J. Stephen, J. Chem. Phys. **40**, 669 (1964); R. H. Lehmberg, Phys. Rev. A **2**, 883 (1970); P. W. Miloni and P. L. Knight, Phys. Rev. A **10**, 1096 (1974).
[11] It can be shown using (3), that the contribution of mixed terms like $\langle \phi^{\pm} | G | \phi^{\mp} \rangle$ vanishes.
[12] A. Gero and E. Akkermans (to be published).
[13] This rewriting of the amplitude T is defined up to a proportionality constant which accounts for the quantum nature of the problem and the photon polarization.
[14] L. Brillouin, *Wave Propagation and Group Velocity* (Academic, New York, 1960).
[15] M. P. van Albada *et al.*, Phys. Rev. Lett. **66**, 3132 (1991); A. Lagendijk and B. A. van Tiggelen, Phys. Rep. **270**, 143 (1996).
[16] A. Ishimaru, *Wave Propagation and Scattering in Random Media* (Academic, New York, 1978), Chap. 9.
[17] G. Labeyrie *et al.*, Phys. Rev. Lett. **91**, 223904 (2003).

Superradiance and multiple scattering of photons in atomic gases

A. Gero and E. Akkermans
Department of Physics, Technion—Israel Institute of Technology, Haifa 32000, Israel
(Received 30 November 2006; published 25 May 2007)

We study the influence of cooperative effects such as superradiance and subradiance on the scattering properties of dilute atomic gases. We show that cooperative effects lead to an effective potential between two atoms that decays as $1/r$. In the case of superradiance, this potential is attractive for close enough atoms and can be interpreted as a coherent mesoscopic effect. We consider a model of multiple scattering of a photon among superradiant pairs and calculate the elastic mean free path and the group velocity. We study first the case of a scalar wave which allows us to obtain and to understand basic features of cooperative effects and multiple scattering. We then turn to the general problem of a vector wave. In both cases, we obtain qualitatively similar results and derive, for the case of a scalar wave, analytic expressions for the elastic mean free path and for the group velocity for an arbitrary detuning (near resonance).

DOI: 10.1103/PhysRevA.75.053413 PACS number(s): 32.80.Pj, 42.25.Dd, 42.50.Fx

I. INTRODUCTION

Coherent multiple scattering of photons in cold atomic gases is an important problem since it presents a path toward the onset of the Anderson localization transition, a long-standing and still open issue. The large resonant scattering cross section of photons reduces the elastic mean free path to values comparable to the photon wavelength, for which the weak-disorder approximation breaks down, thus signaling the onset of the Anderson localization transition [1,2]. Another advantage of cold atomic gases is that sources of decoherence and inelastic scattering such as Doppler broadening are often negligible. Moreover, propagation of photons in atomic gases differs from the case of electrons in disordered metals or of electromagnetic waves in suspensions of classical scatterers, for which mesoscopic effects and Anderson localization have been thoroughly investigated [1]. This problem is thus of great interest since it may raise new issues in the Anderson problem, such as a change of universality class and therefore new critical behavior. New features displayed by the photon-atom problem are the existence of internal degrees of freedom (Zeeman sublevels) and cooperative effects such as subradiance or superradiance [3], which lead to effective interactions between atoms [4]. These two differences are expected to lead to qualitative changes of both mesoscopic quantities and Anderson localization. Some of the effects of Zeeman degeneracy have been investigated in the weak-disorder limit [5] using a set of finite phase coherence times [6], which reduce mesoscopic effects, such as coherent backscattering [1,7].

The influence of cooperative effects and more specifically of superradiance on the multiple scattering of photons has been recently investigated [8]. It has been shown that in atomic gases superradiance and subradiance lead to a potential between two atoms, analogous to the one considered in [9,10], which decays as the inverse of the distance between them. In the case of superradiance, this potential is attractive for close enough atoms, and can be interpreted as a coherent mesoscopic effect. The contribution of superradiant pairs to multiple-scattering properties of a dilute gas has been calculated by using an effective propagator that describes a scalar wave being scattered by a pair of two-level atoms. Simple expressions for the photon elastic mean free path and group velocity have been derived at resonance and found to be significantly different from those of independent atoms. To be more specific, near resonance, as well as at resonance, the superradiant effect leads to a finite and positive group velocity, unlike the one obtained for light interaction with independent atoms.

In this paper we provide, for the case of a scalar wave, closed expressions for the suprerradiant contribution to the elastic mean free path and the group velocity for an arbitrary (near resonance) detuning, and calculate the dependence of the transport time on it. In addition, we estimate the maximal interatomic separation in a superradiant pair, which accounts for possible mechanisms that may break the pair. We also compare the effective approach presented in [8] to a more realistic one that takes into account the vectorial nature of the wave.

The paper is organized as follows: In Sec. II we describe the model, which consists of pairs of two-level atoms placed in an external radiation field where the Doppler shift and recoil effects are negligible. In order to investigate the influence of the cooperative effects of such pairs on the multiple scattering of photons we briefly review, in Sec. III, Dicke states and some of their properties. Then we calculate the average interaction potential of a pair of atoms in a Dicke state by averaging over the random orientations of pairs of atoms with respect to the wave vector of a photon incident on the atomic cloud. Next, we study the scattering of a photon by such pairs and, in Sec. IV, compare the results to the case where a classical wave is being scattered by a pair of atoms. This comparison allows us to find an unexpected connection between superradiance and mesoscopic effects. In Secs. V and VI, we consider the multiple scattering of photons by pairs of atoms and calculate the elastic mean free path and the group velocity of photons in the random medium. Finally, our analysis is compared to other approaches in Sec. VII and its results are summarized in Sec. VIII.

II. MODEL

Atoms are taken to be degenerate, two-level systems denoted by $|g\rangle=|j_g=0,m_g=0\rangle$ for the ground state and $|e\rangle=|j_e$

$=1, m_e=0,\pm 1\rangle$ for the excited state, where j is the total angular momentum and m is its projection on a quantization axis, taken as the $\hat{z}$ axis. The energy separation between the two levels, including radiative shift, is $\hbar\omega_0$, and the natural width of the excited level is $\hbar\Gamma$. This simple picture of a two-level atom neglects the rather complicated energy structure of a real atom, which reflects various internal interactions, e.g., Coulomb interactions, spin-orbit interactions, hyperfine interactions, etc. But, due to selection rules which limit the allowed transitions between states, in some cases a certain state may couple to only one other. Thus, the two-level atom approximation is close to reality and not merely a mathematical convenience.

We consider a pair of such atoms in an external radiation field and the corresponding Hamiltonian is $H=H_0+V$, with

$$H_0 = \frac{\hbar\omega_0}{2}\sum_{l=1}^{2}(|e\rangle\langle e| - |g\rangle\langle g|)_l + \sum_{\mathbf{k}\varepsilon}\hbar\omega_k a^\dagger_{\mathbf{k}\varepsilon}a_{\mathbf{k}\varepsilon}. \tag{1}$$

$a_{\mathbf{k}\varepsilon}$ ($a^\dagger_{\mathbf{k}\varepsilon}$) is the annihilation (creation) operator of a mode of the field of wave vector $\mathbf{k}$, polarization $\hat{\varepsilon}_{\mathbf{k}}$, and angular frequency $\omega_k=c|\mathbf{k}|$. The interaction V between the radiation field and the dipole moments of the atoms is given by

$$V = -\sum_{l=1}^{2}\mathbf{d}_l\cdot\mathbf{E}(\mathbf{r}_l), \tag{2}$$

where $\mathbf{E}(\mathbf{r})$ is the electric field operator

$$\mathbf{E}(\mathbf{r}) = i\sum_{\mathbf{k}\varepsilon}\sqrt{\frac{\hbar\omega_k}{2\epsilon_0\Omega}}(a_{\mathbf{k}\varepsilon}\hat{\varepsilon}_{\mathbf{k}}e^{i\mathbf{k}\cdot\mathbf{r}} - a^\dagger_{\mathbf{k}\varepsilon}\hat{\varepsilon}^*_{\mathbf{k}}e^{-i\mathbf{k}\cdot\mathbf{r}}). \tag{3}$$

Ω is a quantization volume and $\mathbf{d}_l$ is the electric dipole moment operator of the lth atom. As an odd operator, which changes sign upon inversion, $\mathbf{d}_l$ may be written as

$$\mathbf{d}_l = \langle g|\mathbf{d}|e\rangle\Delta^-_l + \langle e|\mathbf{d}|g\rangle\Delta^+_l \tag{4}$$

where the atomic raising and lowering operators are

$$\Delta^+_l = (|e\rangle\langle g|)_l \quad \Delta^-_l = (|g\rangle\langle e|)_l. \tag{5}$$

We assume that the typical speed of the atoms, $v\simeq\sqrt{k_BT_0/\mu}$, is small compared to $v_{max}=\Gamma/k$ but large compared to $v_{min}=\hbar k/\mu$, where μ is the mass of the atom and T_0 is the temperature, so that it is possible to neglect the Doppler shift and recoil effects. Indeed, for a temperature of $T_0=10^{-3}$ K, the typical speed of the atom is $v\simeq 0.3$ m/s. Since, for a wave number of $k=10^7$ m^{-1} and a natural width of $\Gamma=10^7$ s^{-1}, $v_{max}\simeq 1$ m/s and $v_{min}\simeq 0.01$ m/s, both assumptions are satisfied.

III. DICKE STATES

A. Interaction potential and lifetime

The absorption of a photon by a pair of atoms in their ground state leads to a configuration where the two atoms, one excited and the second in its ground state, have multiple exchange of a photon, giving rise to an effective interaction potential and to a modified lifetime as compared to independent atoms. These two quantities are obtained from the matrix elements of the evolution operator $U(t)$ between states such as $|g_1e_2;0\rangle$. There are six unperturbed and degenerate states with no photon, given by $\{|g_1e_{2i};0\rangle, |e_{1j}g_2;0\rangle\}$ in a standard basis where $i,j=-1,0,1$. The symmetries of the Hamiltonian, namely, its invariance by rotation around the axis between the two atoms, and by reflection with respect to a plane containing this axis, allows us to use combinations of these states that are given by

$$|\phi^\epsilon_i\rangle = \frac{1}{\sqrt{2}}[|e_{1i}g_2;0\rangle + \epsilon|g_1e_{2i};0\rangle] \tag{6}$$

with $\epsilon=\pm 1$, so that

$$\langle\phi^{\epsilon'}_j|U(t)|\phi^\epsilon_i\rangle = \delta_{ij}\delta_{\epsilon\epsilon'}S^\epsilon_i(t) \tag{7}$$

and

$$S^\epsilon_i(t) = \langle e_{1i}g_2;0|U(t)|e_{1i}g_2;0\rangle + \epsilon\langle g_1e_{2i};0|U(t)|e_{1i}g_2;0\rangle. \tag{8}$$

The states $|\phi^\epsilon_i\rangle$ may be rewritten in terms of the well-known Dicke states $|LM\rangle$, where L is the cooperation number and M is half of the total atomic inversion [3]. For two atoms, the singlet Dicke state is

$$|00\rangle = \frac{1}{\sqrt{2}}[|e_1g_2\rangle - |g_1e_2\rangle] \tag{9}$$

and the triplet Dicke states are

$$|11\rangle = |e_1e_2\rangle,$$

$$|10\rangle = \frac{1}{\sqrt{2}}[|e_1g_2\rangle + |g_1e_2\rangle],$$

$$|1-1\rangle = |g_1g_2\rangle. \tag{10}$$

The states $|11\rangle$ and $|1-1\rangle$ correspond, respectively, to both atoms in their excited states and both atoms in their ground states. The singlet state $|00\rangle$ and the triplet state $|10\rangle$ both correspond to one atom in the excited state and the other in the ground state, but $|00\rangle$ is antisymmetric where $|10\rangle$ is symmetric under an exchange of the atoms. Therefore, we may rewrite (6) as $|\phi^+_i\rangle=|10;0\rangle$ and $|\phi^-_i\rangle=|00;0\rangle$.

For times such that $t\gg r/c$, where r is the distance between the two atoms, up to second order in the coupling to the radiation, (8) reads

$$S^\epsilon_i(t) \simeq 1 - \frac{it}{\hbar}\left(\Delta E^\epsilon_i - i\frac{\hbar\Gamma^\epsilon_i}{2}\right). \tag{11}$$

The two real quantities ΔE^ϵ_i and Γ^ϵ_i are, respectively, the interaction potential and the probability per unit time of emission of a photon by the two atoms in the state $|\phi^\epsilon_i\rangle$. The calculation of these two quantities requires second-order perturbation theory with respect to the interaction (2). For this purpose we define an initial state where one atom is excited and the other is in its ground state without any photon, and a final state where the two atoms are exchanged. We also define intermediate states of two types: both atoms in their ground states with one virtual photon present and both atoms

in their excited states with one virtual photon present. Summing the corresponding diagrams [11] gives

$$\Delta E_i^{\epsilon} = \epsilon \frac{3\hbar\Gamma}{4}\left[- p_i \frac{\cos k_0 r}{k_0 r} + q_i \left(\frac{\cos k_0 r}{(k_0 r)^3} + \frac{\sin k_0 r}{(k_0 r)^2} \right) \right] \tag{12}$$

and

$$\frac{\Gamma_i^{\epsilon}}{\Gamma} = 1 - \frac{3}{2}\epsilon\left[- p_i \frac{\sin k_0 r}{k_0 r} + q_i \left(\frac{\sin k_0 r}{(k_0 r)^3} - \frac{\cos k_0 r}{(k_0 r)^2} \right) \right], \tag{13}$$

where we have defined $k_0 = \omega_0 / c$,

$$p_i = 1 - \hat{\mathbf{r}}_i^2, \quad q_i = 1 - 3\hat{\mathbf{r}}_i^2, \tag{14}$$

and $\hat{\mathbf{r}} = (1, \theta, \varphi)$ is a unit vector along the direction joining the two atoms. For a $\Delta m = m_e - m_g = 0$ transition,

$$p_0 = \sin^2\theta, \quad q_0 = 1 - 3\cos^2\theta, \tag{15}$$

while for a $\Delta m = \pm 1$ transition,

$$p_{\pm} = \frac{1}{2}(1 + \cos^2\theta), \quad q_{\pm} = \frac{1}{2}(3\cos^2\theta - 1). \tag{16}$$

At short distance $k_0 r \ll 1$, we obtain that $\Gamma_i^+ \simeq 2\Gamma$ for the superradiant state $|\phi_i^+\rangle = |10;0\rangle$ and $\Gamma_i^- \simeq 0$ for the subradiant state $|\phi_i^-\rangle = |00;0\rangle$.

B. Average interaction potential

For a photon of wave vector $\mathbf{k}$ incident on an atomic cloud, the potential between two atoms that we shall denote by V_e is obtained from (12) by averaging over the random orientations of the pairs of atoms with respect to $\mathbf{k}$. Since, according to (15) and (16), $\langle q_i \rangle = 0$ and $\langle p_i \rangle = 2/3$, we obtain for the average potential V_e

$$\epsilon V_e(r) = \langle \Delta E_i^{\epsilon} \rangle = - \epsilon \frac{\hbar\Gamma}{2} \frac{\cos k_0 r}{k_0 r} \tag{17}$$

and the average inverse lifetimes of Dicke states are

$$\langle \Gamma_i^{\epsilon} \rangle = \Gamma\left(1 + \epsilon \frac{\sin k_0 r}{k_0 r} \right), \tag{18}$$

which retain the same features as (13) for $k_0 r \ll 1$.

Let us now characterize the interaction potential V_e. Whereas for a single pair of atoms the potential (12) is anisotropic and decays at short distance as $1/r^3$, a behavior that originates from the transverse part of the photon propagator, we obtain that, on average over angular configurations, the potential (17) between two atoms in a Dicke state $|L0\rangle$ in vacuum becomes isotropic and decays as $1/r$. This behavior coincides with the one obtained by considering the interaction of two-level atoms with a scalar wave. This could have been anticipated since in that case the transverse contribution q_i to the photon propagator averages to 0. A related behavior for the orientation average interaction potential has been also obtained for the case of an intense radiation field [9], and it has recently been investigated in order to study effects of a long-range and attractive potential between atoms in a Bose-Einstein condensate for far-detuned light [10]. This latter potential, which is fourth order in the coupling to the radiation, corresponds to the interaction energy between two atoms in their ground states in the presence of at least one photon. The average potential V_e we have obtained is different from that case: it is second order in the coupling to the radiation and it corresponds to the interaction energy of Dicke states $|L0\rangle$ in vacuum.

C. Scattering properties

In order to study the scattering properties of Dicke states we introduce the collision operator $T(z) = V + VG(z)V$, where V is given by (2) and $G(z) = (z - H)^{-1}$ is the resolvent where the Hamiltonian H is the sum of (1) and (2). The matrix element that describes the transition amplitude from the initial state $|i\rangle = |1-1;\mathbf{k}\hat{\varepsilon}\rangle$, where the two atoms are in their ground states in the presence of a photon of frequency $\omega = c|\mathbf{k}|$ and polarization $\hat{\varepsilon}$, to the final state $|f\rangle = |1-1;\mathbf{k}'\hat{\varepsilon}'\rangle$ is

$$T = \langle f | T(z = \hbar(\omega - \omega_0)) | i \rangle \tag{19}$$

where $|\mathbf{k}| = |\mathbf{k}'|$. By using the closure relation we may write T as the sum of a superradiant and a subradiant contribution, $T = T^+ + T^-$ [12], with

$$T^{\pm} = \langle f | V | \phi^{\pm} \rangle \langle \phi^{\pm} | G(z = \hbar(\omega - \omega_0)) | \phi^{\pm} \rangle \langle \phi^{\pm} | V | i \rangle, \tag{20}$$

where $|\phi^{\pm}\rangle$ are the Dicke states $|L0\rangle$ in vacuum. The two matrix elements in (20) represent the absorption and the emission of a real photon by the pair of atoms. They are easily obtained from (2)–(5) and lead to the following expressions for the scattering amplitudes:

$$T^+ = A e^{i(\mathbf{k}-\mathbf{k}')\cdot\mathbf{R}} \cos\left(\frac{\mathbf{k}\cdot\mathbf{r}}{2} \right) \cos\left(\frac{\mathbf{k}'\cdot\mathbf{r}}{2} \right) G^+ \tag{21}$$

and

$$T^- = A e^{i(\mathbf{k}-\mathbf{k}')\cdot\mathbf{R}} \sin\left(\frac{\mathbf{k}\cdot\mathbf{r}}{2} \right) \sin\left(\frac{\mathbf{k}'\cdot\mathbf{r}}{2} \right) G^-. \tag{22}$$

We have defined $\mathbf{r} = \mathbf{r}_1 - \mathbf{r}_2$, $\mathbf{R} = (\mathbf{r}_1 + \mathbf{r}_2)/2$, and

$$A = \frac{\hbar\omega}{\epsilon_0 \Omega} d^2 (\hat{d}\cdot\hat{\varepsilon})(\hat{d}^*\cdot\hat{\varepsilon}'^*), \tag{23}$$

where the reduced matrix element and the corresponding unit vector are

$$d = \frac{\langle j_e \| \mathbf{d} \| j_g \rangle}{\sqrt{2j_e + 1}}, \quad \hat{d} = \frac{1}{d}\langle j_e m_e | \mathbf{d} | j_g m_g \rangle. \tag{24}$$

The propagators $G^{\pm}$ are the expectation values of the resolvent in the Dicke states $|\phi^{\pm}\rangle$, namely, $G^{\pm} = \langle \phi^{\pm} | G(\hbar\delta) | \phi^{\pm} \rangle$, where close to resonance $\delta = \omega - \omega_0 \ll \omega_0$. The propagators result from the sum of an infinite series of virtual photon exchanges between the two atoms in the pair and are given in terms of (12) and (13) by

$$G^{\pm} = \left(\hbar\delta - \Delta E^{\pm} + i\hbar\frac{\Gamma^{\pm}}{2} \right)^{-1}. \tag{25}$$

The average propagator is then obtained by averaging $G^{\pm}$ over the random orientations of the pairs of atoms with respect to the wave vector $\mathbf{k}$ of the incident photon. However, we shall consider in a first stage the effective propagator obtained for the case of a scalar wave. This amounts to writing for the effective propagator the expression

$$G_e^{\pm} = \left[\hbar\left(\delta + i\frac{\Gamma}{2} \pm \frac{\Gamma}{2}\frac{e^{ik_0 r}}{k_0 r}\right)\right]^{-1}, \tag{26}$$

where we have used (17) and (18) for the average potential and for the average inverse lifetimes. This expression constitutes *a priori* a rough approximation of the exact average. We shall calculate later, in Sec. VI, the exact expression of the average propagator and show that it is rather complicated, whereas the approximate expression using a scalar wave gives similar qualitative results. Therefore, it allows for a better understanding of relevant physical quantities such as the elastic mean free path and group velocity. From now on, we thus use the scalar wave approximation in order to provide, in a rather simple way, the main features of multiple scattering by superradiant pairs.

With the help of (26), the scattering amplitudes are

$$T_e^{+} = Ae^{i(\mathbf{k}-\mathbf{k}')\cdot\mathbf{R}}\cos\left(\frac{\mathbf{k}\cdot\mathbf{r}}{2}\right)\cos\left(\frac{\mathbf{k}'\cdot\mathbf{r}}{2}\right)G_e^{+} \tag{27}$$

and

$$T_e^{-} = Ae^{i(\mathbf{k}-\mathbf{k}')\cdot\mathbf{R}}\sin\left(\frac{\mathbf{k}\cdot\mathbf{r}}{2}\right)\sin\left(\frac{\mathbf{k}'\cdot\mathbf{r}}{2}\right)G_e^{-}. \tag{28}$$

At short distances $k_0 r \ll 1$, the subradiant amplitude T_e^{-} becomes negligible as compared to the superradiant term T_e^{+}. Therefore, the potential (17) is attractive and decays as $1/r$. More precisely, at short distances the effective propagator G_e^{-} diverges for $\delta/\Gamma = 1/(2k_0 r)$ and G_e^{+} is purely imaginary for $\delta/\Gamma = -1/(2k_0 r)$. Thus, for $\delta/\Gamma < 1/(2k_0 r)$ the imaginary part of the subradiative term (28) is negligible as compared to the imaginary part of the superradiative term (27) and for $|\delta|/\Gamma < 1/(2k_0 r)$ both the real part and the imaginary parts of (28) are negligible as compared to (27).

We can interpret these results by saying that, at short distances ($k_0 r \ll 1$), the time evolution of the initial state

$$|\psi(0)\rangle = |e_1 g_2; 0\rangle = \frac{1}{\sqrt{2}}[|\phi^{+}\rangle + |\phi^{-}\rangle], \tag{29}$$

corresponds, for times shorter than $1/\Gamma$, to a periodic exchange of a virtual photon between the two atoms at the Rabi frequency

$$\Omega_R = \frac{\langle \Delta E^{-}\rangle - \langle \Delta E^{+}\rangle}{\hbar}, \tag{30}$$

which is much larger than Γ since, with the help of (17),

$$\Omega_R \simeq \frac{\Gamma}{k_0 r}. \tag{31}$$

For larger times, the two atoms return to their ground states and a real photon ($\mathbf{k}'\hat{\varepsilon}'$) is emitted. At large distances ($k_0 r \gg 1$), the Rabi frequency becomes smaller than Γ, so that the excitation energy makes only a few oscillations between the two atoms, thus leading to a negligible interaction potential.

We finally notice that the angular distribution of the light scattered by two atoms in a superradiant state is nearly identical to that of a single atom. This follows from the fact that at short distance $k_0 r \ll 1$, we can neglect higher-order multipolar corrections so that the corresponding additional phase shift $k_0 r \cos\vartheta$ between waves emitted by the two atoms becomes negligible (ϑ is the angle between the direction of the emitted photon and the axis between the two atoms).

IV. COOPERATIVE EFFECTS AND COHERENT BACKSCATTERING

It is interesting to derive the previous results in another way that emphasizes the analogy with coherent backscattering [1,2]. To that purpose, we write the scattering amplitude T defined previously in (19) as a superposition of two "classical," scalar amplitudes T_1 and T_2 [13], each of them being a sum of single-scattering and double-scattering contributions, that is,

$$T_1 = \frac{t}{1 - t^2 G_0^2}(e^{i(\mathbf{k}-\mathbf{k}')\cdot\mathbf{r}_1} + tG_0 e^{i(\mathbf{k}\cdot\mathbf{r}_1 - \mathbf{k}'\cdot\mathbf{r}_2)}) \tag{32}$$

and

$$T_2 = \frac{t}{1 - t^2 G_0^2}(e^{i(\mathbf{k}-\mathbf{k}')\cdot\mathbf{r}_2} + tG_0 e^{i(\mathbf{k}\cdot\mathbf{r}_2 - \mathbf{k}'\cdot\mathbf{r}_1)}). \tag{33}$$

Here

$$t = \frac{4\pi}{k_0}\frac{\Gamma/2}{\delta + i\Gamma/2} \tag{34}$$

is the amplitude of a scalar wave scattered by a single atom at the origin, and the prefactor $t/(1-t^2G_0^2)$, where

$$G_0 = -\frac{e^{ik_0 r}}{4\pi r} \tag{35}$$

accounts for the summation of the series of virtual photon exchange between the two scatterers. We can single out in the total amplitude $T = T_1 + T_2$ the single-scattering contribution T_s and write the intensity associated with the higher-order scattering term shown in Fig. 1 as

$$|T - T_s|^2 = 2\left|\frac{t^2 G_0}{1 - t^2 G_0^2}\right|^2 [1 + \cos(\mathbf{k} + \mathbf{k}')\cdot(\mathbf{r}_1 - \mathbf{r}_2)]. \tag{36}$$

The structure of relation (36) is very reminiscent of that of the so-called coherent backscattering intensity, which occurs in the multiple elastic scattering of light. But although they are analogous, (36) differs from coherent backscattering. In the latter case, averaging over the spatial positions $\mathbf{r}_1$ and $\mathbf{r}_2$ makes the interference term $\cos(\mathbf{k}+\mathbf{k}')\cdot(\mathbf{r}_1-\mathbf{r}_2)$ vanish in general, with two exceptions:

(1) $\mathbf{k}+\mathbf{k}' \simeq \mathbf{0}$. In the direction exactly opposite to the direction of incidence, the intensity is twice the classical value.

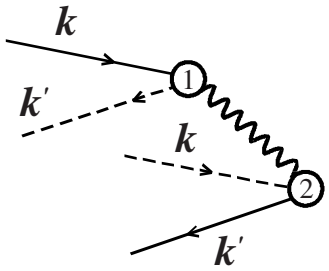

FIG. 1. Schematic representation of the two amplitudes that describe double scattering of a scalar wave. The wavy line accounts for the exchange of a virtual photon between the two atoms. This diagram is analogous to the coherent backscattering in quantum mesoscopic physics.

This phenomenon is known as coherent backscattering.

(2) $\mathbf{r}_1=\mathbf{r}_2$. These are closed multiple-scattering trajectories which are at the origin of the phenomenon of weak localization.

In (36) the interference term, i.e., the second term in the square brackets, reaches its maximum value 1 for $\mathbf{r}_1=\mathbf{r}_2$ so that we obtain from (32), (33), and (27) that $T_1=T_2 \propto (1/2)T_e^+$, up to a proportionality factor [13]. Thus, the total amplitude is given by the superradiant term with no subradiant contribution.

V. MULTIPLE SCATTERING AND COOPERATIVE EFFECTS

A. Effective self-energy

We consider now multiple scattering of a photon by superradiant pairs built out of atoms separated by a distance r and coupled by the attractive interaction potential V_e. This situation corresponds to a dilute gas that is assumed to satisfy

$$r \ll \lambda_0 \ll n_i^{-1/3}, \tag{37}$$

where n_i is the density of pairs and $\lambda_0=2\pi/k_0$ is the atomic transition wavelength. The limiting case (37) corresponds to a situation where the two atoms that form a superradiant pair, through exchange of a virtual photon, constitute an effective scatterer, and cooperative interactions between otherwise well-separated pairs are negligible. Let us stress that we study here a simplified model where only pairs of atoms have been taken into account. A more realistic model should include higher-order terms that account for cooperative effects between more than two atoms, but we do not consider such higher-order terms, i.e., including superradiant clusters of three or more atoms. The purpose of the current model is to examine the contribution of superradiant pairs to the transport properties of the gas. We use the Edwards model [1,14] to describe the medium as a discrete collection of N_i superradiant pairs in a volume Ω. Each pair, located at $\mathbf{R}_l$, is characterized by its scattering potential $u(\mathbf{R}-\mathbf{R}_l)$. Therefore, the disorder potential is given by

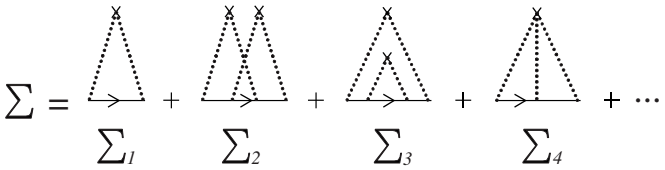

FIG. 2. Pertubative expansion of the self-energy in a power series in the parameter $n_i u_0^2$. Solid lines account for the free photon Green's function g_0. Pairs of dotted lines, connected by $\times$, stand for the two-point correlation function B. The first term Σ_1, proportional to $n_i u_0^2$, accounts for independent scattering events, while the second term Σ_2, proportional to $n_i^2 u_0^4$, describes interference effects between pairs of scatterers.

$$U(\mathbf{R}) = \sum_{l=1}^{N_i} u(\mathbf{R}-\mathbf{R}_l). \tag{38}$$

We assume that the scattering potential is short range compared to the wavelength, and we approximate it by a (conveniently regularized) δ function potential $u(\mathbf{R})=u_0\delta(\mathbf{R})$. In the limit of a high density of weakly scattering pairs, but with a constant value of $n_i u_0^2$, it can be shown [1] that the correlation function defined by

$$B(\mathbf{R}-\mathbf{R}') = n_i \int d\mathbf{R}'' u(\mathbf{R}''-\mathbf{R}) u(\mathbf{R}''-\mathbf{R}') \tag{39}$$

becomes

$$B(\mathbf{R}-\mathbf{R}') = n_i u_0^2 \delta(\mathbf{R}-\mathbf{R}'). \tag{40}$$

In other words, in this limit, the Edwards model reduces to a Gaussian white noise model characterized by the condition (40).

The Green's function g of a scattered photon is related to the free photon Green's function g_0, i.e., in the absence of disorder potential, by the equation [1]

$$g = g_0 + g_0 U g. \tag{41}$$

Averaging (41) over disorder and using the properties of the Gaussian model discussed above yields the Dyson equation

$$\langle g \rangle_d = g_0 + g_0 \Sigma \langle g \rangle_d \tag{42}$$

where $\langle \cdots \rangle_d$ denotes averaging over the random potential. The function Σ, known as the self-energy, represents the sum of all irreducible scattering diagrams. The pertubative expansion of the self-energy in a power series controlled by the parameter $n_i u_0^2$ is represented in Fig. 2.

For small values of $n_i u_0^2$, the main contribution is obtained by keeping only the first term Σ_1 which describes independent scattering events. Therefore, the first contribution to the self-energy is proportional to the density of scatterers and to the average scattering amplitude, and it is given, for $k_0 r \ll 1$, by

$$\Sigma_1 = \frac{6\pi n_i}{k_0} A_{j_g j_e} \hbar \Gamma \overline{G}_e^+ \tag{43}$$

where

$$A_{j_g j_e} = \frac{1}{3}\frac{2j_e+1}{2j_g+1}. \tag{44}$$

The latter quantity is obtained by averaging A in (27) over Zeeman sublevels m that appear in its definition given by (23) and (24).

The additional average, denoted by $\overline{\cdots}$, is taken over distances r up to a maximal value r_m which accounts for all possible mechanisms that may break the pairs.

The value of r_m can be estimated by comparing the kinetic energy K of a superradiant pair to its average potential energy V_e^+. We have $K \simeq \hbar^2/\mu r^2$ and from (17) we obtain that $V_e^+ \simeq -\hbar\Gamma/2k_0 r$. Minimizing the average energy

$$E(r) \simeq \frac{\hbar^2}{\mu r^2} - \frac{\hbar\Gamma}{2k_0 r} \tag{45}$$

with respect to r yields

$$k_0 r_m = 4\frac{\hbar k_0^2}{\mu\Gamma} \tag{46}$$

or

$$k_0 r_m = 4\frac{v_{min}}{v_{max}}, \tag{47}$$

where the speeds v_{min} and v_{max} have been defined in Sec. II. For typical values $\Gamma = 10^7\ \mathrm{s}^{-1}$ and $k_0 = 10^7\ \mathrm{m}^{-1}$ we obtain that $k_0 r_m \simeq 0.05$. Thus, we can use the results obtained in Sec. III C and consider the superradiant term only.

For $j_g = 0$ and $j_e = 1$, $A_{01} = 1$, and using (26) we rewrite (43) as

$$\Sigma_1 = \frac{6\pi n_i}{k_0}\frac{1}{r_m}\int_0^{r_m} \frac{dr}{\delta/\Gamma + 1/(2k_0 r) + i}. \tag{48}$$

We stress again that, in our approach, a pair of atoms in a superradiant state is considered as a single scatterer, and the effective medium parameters are derived from Σ_1 as will be shown in the next sections. In contrast to our treatment, others [16,19] consider multiple scattering of a real photon by *independent* atoms and use the second term Σ_2, which describes interference effects between the scatterers, to calculate corrections to the elastic mean free path and to the refractive index of the medium. A further comparison between these two points of view is given in Sec. VII.

B. Elastic mean free path

The elastic mean free path l_e is obtained from the imaginary part of the self-energy, namely,

$$\frac{k_0}{l_e} = -\,\mathrm{Im}\,\Sigma_1. \tag{49}$$

Let us stress that (49) is equivalent, in the case of a dilute gas, to the known formula

$$l_e = \frac{1}{n_i \sigma_e}, \tag{50}$$

where the total cross section σ_e is obtained for $k_0 r \ll 1$ from (27) by means of the optical theorem

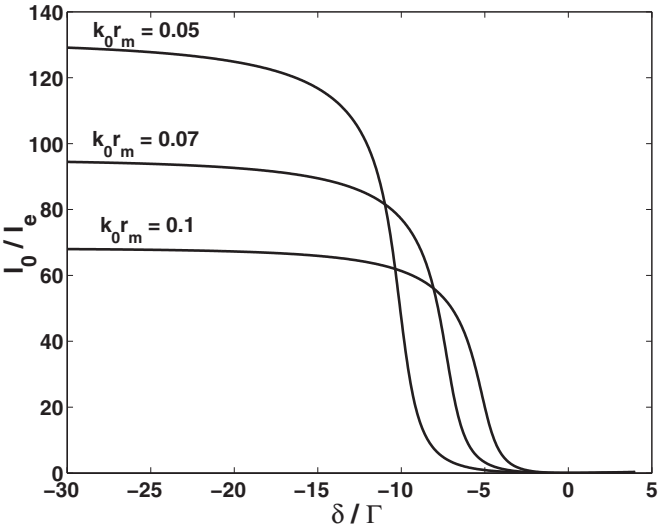

FIG. 3. Ratio between the elastic mean free paths l_0 and l_e as a function of the reduced detuning δ/Γ for $k_0 r_m = 0.05$, 0.07, and 0.1. Away from resonance, for blue detuning, the elastic mean free path l_e becomes smaller than l_0 in a ratio roughly given by $1/(k_0 r_m)^2$. At resonance, the ratio between the elastic mean free paths is given by (57).

$$\sigma_e = -\frac{2\Omega}{\hbar c}\,\mathrm{Im}\langle \overline{T}_e^+(\mathbf{k}=\mathbf{k}', \hat{\varepsilon}=\hat{\varepsilon}')\rangle_m \tag{51}$$

and $\langle\cdots\rangle_m$ represents an averaging over Zeeman sublevels. The equivalence in this case is proven easily if one uses (44) and the usual expression for the inverse lifetime

$$\Gamma = \frac{d^2 k_0^3}{3\pi\epsilon_0\hbar}, \tag{52}$$

where the reduced matrix element is defined in (24). Therefore, from (48) and (49) we obtain that

$$\frac{1}{l_e(\delta)} = \frac{6\pi n_i}{k_0^2} f_1\left(k_0 r_m, \frac{\delta}{\Gamma}\right) \tag{53}$$

where we have defined the function

$$f_1(u,v) = \frac{1}{2u}\int_0^{2u} \frac{dx}{1+(v+1/x)^2}. \tag{54}$$

The integral is easily carried out analytically and the explicit expression is given in Appendix A. It is interesting to compare l_e to the elastic mean free path l_0 that corresponds to near-resonant elastic scattering of a photon by a single atom. The latter quantity is obtained by replacing Γ by $\Gamma/2$ in (53) (since the inverse lifetime of a single atom is half the one related to a superradiant pair) and $1/x$ by 0 in (54) (since the interatomic distance is taken to be infinite for a single atom) and it is given by

$$l_0(\delta) = \frac{k_0^2}{6\pi n_i}\left[1+\left(\frac{2\delta}{\Gamma}\right)^2\right]. \tag{55}$$

In Fig. 3 the ratio between these two quantities is plotted as

a function of the reduced detuning δ/Γ from resonance for several values of $k_0 r_m$.

At resonance, we obtain from (53) that

$$l_e(0) = \frac{k_0^2}{8\pi n_i}\frac{1}{(k_0 r_m)^2} \tag{56}$$

and hence

$$\frac{l_0(0)}{l_e(0)} = \frac{4}{3}(k_0 r_m)^2 \ll 1. \tag{57}$$

Away from resonance, for blue detuning, the elastic mean free path l_e becomes smaller than l_0 in a ratio roughly given by $1/(k_0 r_m)^2$. This is a direct consequence of the existence of the attractive potential V_e.

C. Group velocity

Another important physical quantity that characterizes multiple scattering of a photon is its group velocity v_g given in terms of the refractive index η by the usual relation

$$\frac{c}{v_g} = \eta + \omega\frac{d\eta}{d\omega}. \tag{58}$$

The refractive index for a dilute medium is

$$\eta = (1 + n_i \,\mathrm{Re}\,\alpha)^{1/2}, \tag{59}$$

where the dynamic atomic polarizability α is proportional to the self-energy

$$\alpha = -\frac{1}{n_i}\left(\frac{c}{\omega}\right)^2 \Sigma_1. \tag{60}$$

Thus, we obtain that

$$\eta = \left[1 - \left(\frac{c}{\omega}\right)^2 \mathrm{Re}\,\Sigma_1\right]^{1/2}. \tag{61}$$

Substituting (61) into (58) yields

$$\frac{c}{v_g} = \frac{1}{\eta}\left(1 - \frac{c^2}{2\omega}\frac{d}{d\omega}\,\mathrm{Re}\,\Sigma_1\right). \tag{62}$$

From the self-energy (48), we notice that $\eta \simeq 1$ for all values of the detuning δ/Γ and in a large range of densities n_i, so that

$$\frac{c}{v_g(\delta)} \simeq 1 - \frac{n_i}{n_c} f_2\left(k_0 r_m, \frac{\delta}{\Gamma}\right), \tag{63}$$

where we have defined the characteristic density

$$n_c = \frac{k_0^3}{6\pi}\frac{\Gamma}{\omega_0} \tag{64}$$

and the function

$$f_2(u,v) = \frac{1}{2u}\int_0^{2u} dx \frac{1 - (v + 1/x)^2}{[1 + (v + 1/x)^2]^2}. \tag{65}$$

The integration is easily performed and the explicit expression is given in Appendix A. By replacing Γ by $\Gamma/2$ in (63) and $1/x$ by 0 in (65), we obtain the group velocity v_0 of light interacting with independent two-level atoms,

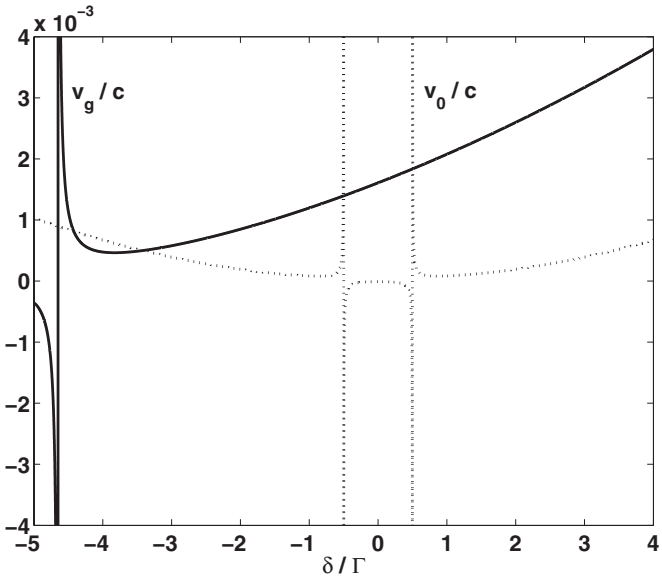

FIG. 4. Group velocities v_g (solid line) and v_0 (dotted line) as a function of the reduced detuning δ/Γ for $n_i/n_c = 10^5$ and $k_0 r_m = 0.1$. The group velocity v_0 diverges at two symmetric values of order unity of the reduced detuning and it takes negative values in between. The group velocity v_g, near resonance, remains finite and positive.

$$\frac{c}{v_0(\delta)} = 1 - \frac{n_i}{n_c}\frac{1 - (2\delta/\Gamma)^2}{[1 + (2\delta/\Gamma)^2]^2}. \tag{66}$$

For the typical values $\Gamma = 10^7\ \mathrm{s}^{-1}$, $k_0 = 10^7\ \mathrm{m}^{-1}$, and $n_i = 10^{10}\ \mathrm{cm}^{-3}$, we obtain that $n_i/n_c \simeq 10^5$.

Figure 4 displays the group velocities v_g and v_0 plotted as a function of the reduced detuning δ/Γ for $n_i/n_c = 10^5$ and $k_0 r_m = 0.1$.

v_g appears to diverge at quite a large and negative value of the detuning $\delta/\Gamma \simeq -1/(2k_0 r_m)$. But near resonance it is well behaved, meaning that it remains finite and positive. At resonance, according to (63), the group velocity is

$$\frac{c}{v_g(0)} = 1 + 4\pi\frac{n_i}{k_0^3}\frac{\omega_0}{\Gamma}(k_0 r_m)^2. \tag{67}$$

This expression of v_g differs substantially from the one obtained for v_0. For densities $n_i > n_c$, the group velocity v_0 diverges at two symmetric values of order unity of the detuning and it takes negative values in between (i.e., also at resonance), as can be seen in Fig. 4. This problem was recognized a long time ago [15] and an energy velocity has been defined which describes energy transport through a diffusive medium [16,17]. However, the diffusion coefficient, which will be discussed in the next section, is derived from the group velocity and not from the energy velocity [1]. Moreover, a closed expression for the energy velocity v_E has been obtained only for the case of resonant Mie scattering [18]. The expression is similar to (67) and is given by

$$\frac{c}{v_E} = 1 + 9\pi \frac{n_i}{k_0^3} \frac{\omega_0}{\Gamma}. \tag{68}$$

It is then interesting to notice that the inclusion of cooperative effects even at the lowest order, i.e., taking into account superradiant pairs, allows one to obtain a group velocity that is well behaved at resonance, unlike the case of resonant scattering by independent atoms.

D. Diffusion coefficient and transport time

Diffusive transport of photons through a gas is characterized by the photon diffusion coefficient

$$D(\delta) = \frac{1}{3} v_g(\delta) l_e(\delta) \tag{69}$$

which combines the elastic mean free path and the group velocity, both derived from the complex-valued self-energy (48). The diffusion coefficient D is of great importance since it enters into expressions of various measured physical quantities, such as the transmission and the reflection coefficients of a disordered medium [1]. In addition to these average quantities, an incident pulse that probes a nearly static configuration of scatterers may provide an instantaneous picture of the medium that displays a random distribution of bright and dark spots. This snapshot, known as a speckle pattern, can be characterized by the angular-correlation function and the time-correlation function of the light intensity (diffusing wave spectroscopy). In the first case, the correlation function of the transmission coefficient between two distinct directions of the transmitted wave is measured. In the second case, the intensity of the transmitted wave is measured at different times, so that the motion of the scatterers must be taken into account. As pointed out before, in both cases the diffusion coefficient plays an important role, as it enters in the relevant expressions. Moreover, the critical behavior of transport close to the Anderson localization transition at strong disorder is also obtained from the scaling form of D. Its expression, deduced from (53) and (63), depends on the range r_m and on the detuning δ/Γ. Since the group velocity and the elastic mean free path are significantly modified for superradiant states, we thus expect the diffusion coefficient to be different from its value obtained for independent atoms.

We define the transport time by

$$\tau_{tr}(\delta) = \frac{l_e(\delta)}{v_g(\delta)}. \tag{70}$$

At resonance and for $n_i \gg n_c$, it can be rewritten with the help of (56) and (67) as

$$\tau_{tr}(0) = \frac{1}{2\Gamma}, \tag{71}$$

in accordance with our assumption of superradiant states. Near resonance, the transport time depends weakly on the detuning. But, away from it, τ_{tr} depends on the detuning and thus on frequency, as can seen from Fig. 5 where the inverse of the transport time τ_{tr}^{-1}/Γ is plotted as a function of the reduced detuning δ/Γ for $n_i = 10^{10}$ cm^{-3}, $\Gamma = 10^7$ s^{-1}, and $k_0 = 10^7$ m^{-1} for several values of $k_0 r_m$.

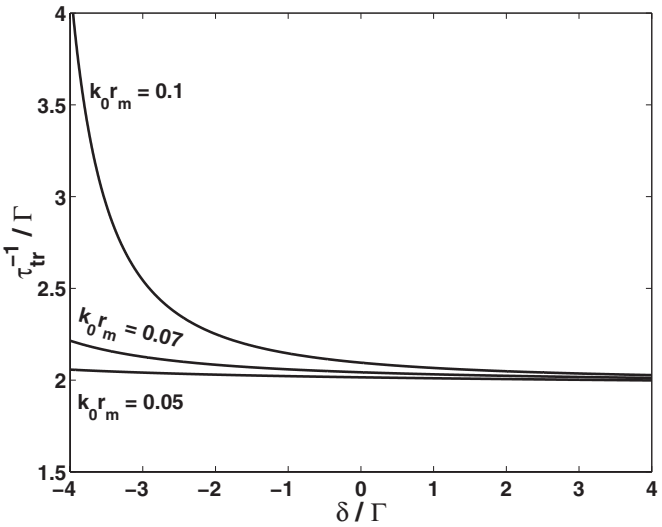

FIG. 5. Inverse of the transport time τ_{tr}^{-1}/Γ as a function of the reduced detuning δ/Γ for $n_i = 10^{10}$ cm^{-3}, $\Gamma = 10^7$ s^{-1}, and $k_0 = 10^7$ m^{-1} for $k_0 r_m = 0.05$, 0.07, and 0.1. Near resonance, the transport time depends weakly on the detuning. But, away from it, τ_{tr} depends on the detuning and thus on frequency.

VI. AVERAGE SELF-ENERGY

So far, we have used the effective approach introduced in Sec. III C, where we have considered the case of a scalar wave being scattered by a pair of two-level atoms. In this simple approach, the propagator of a scalar wave (26) has been calculated and the self-energy (43) has been obtained by averaging (26) over the distance between the two atoms in a pair. This effective approach leads to simple expressions for the elastic mean free path (53) and the group velocity (63) of the wave. In this section we calculate these quantities for a given Δm transition and $k_0 r \ll 1$, while taking into account the vectorial nature of the wave. With this purpose, we average the propagator (25) over the random orientations of the pairs of atoms (with respect to the wave vector of the incident photon) as well as over the distance between the two atoms in a pair. Therefore, the average self-energy is now given by

$$\Sigma_1' = \frac{6\pi n_i}{k_0} \frac{1}{4\pi r_m} \int \hbar \Gamma G^+(\mathbf{r}) d\mathbf{r}, \tag{72}$$

where the averaging is over the interatomic axis $\mathbf{r}$ (over both magnitude and orientations). The evaluation of (72) for a $\Delta m = 0$ transition is rather cumbersome and it is presented in Appendix B. By following the procedure described in the previous section, we obtain the corresponding elastic mean free path l_e' and the group velocity v_g'. In Fig. 6 the ratio between l_0 given by (55) and l_e' is plotted as a function of the reduced detuning δ/Γ for several values of $k_0 r_m$.

As in the effective approach, at resonance l_e' is found to be larger than l_0, but away from resonance it becomes smaller.

In Fig. 7 the group velocity v_g' is plotted as a function of the reduced detuning δ/Γ for $n_i/n_c = 10^5$ and $k_0 r_m = 0.1$.

Around resonance, the group velocity v_g' is finite and positive, as in the scalar case, but much larger as compared to

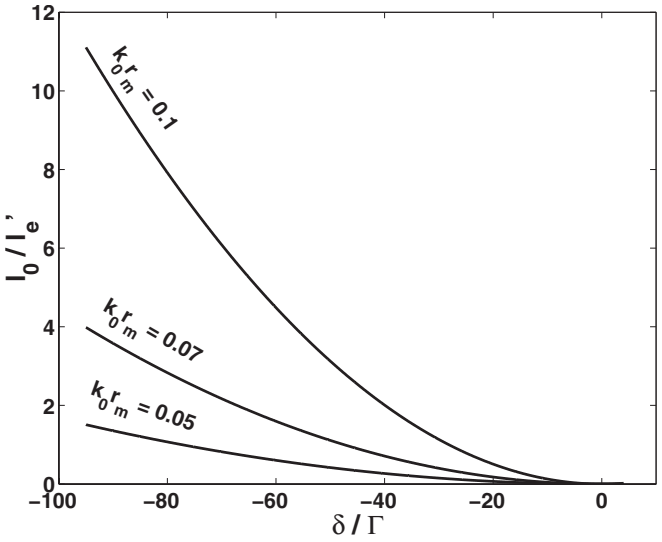

FIG. 6. Ratio between the elastic mean free paths l_0 and l_e' as a function of the reduced detuning δ/Γ for $k_0 r_m = 0.05$, 0.07, and 0.1. At resonance, l_e' is larger than l_0, but away from resonance it becomes smaller.

(63) and it is close to c. Thus, we may conclude that in both approaches the superradiant effect leads to a finite and positive group velocity, unlike the one obtained for light interaction with independent atoms. However, the group velocity of a scalar wave is much smaller compared to the one of a photon.

VII. DISCUSSION

In this section we compare our analysis to other approaches [16,19] where resonant multiple scattering of light has been considered. There, using a multiple-scattering expansion for the calculation of the self-energy up to second order in $n_i u_0^2$, a correction to the elastic mean free path and to the refractive index has been obtained. In the latter approach, no distinction has been made between the external photon that performs multiple scattering on all atoms and virtual photons exchanged between two atoms in a superradiant state, leading to the average interaction potential V_e. This distinction needs to be made for dilute enough atomic gases since in that case the average distance $n_i^{-1/3}$ between atoms is large. Moreover, in this case, the dipole-dipole interaction induced by the external photon depends on the detuning, a situation that corresponds to the case of intense radiation presented in [9] but not to the current experiments made on cold atomic clouds [20].

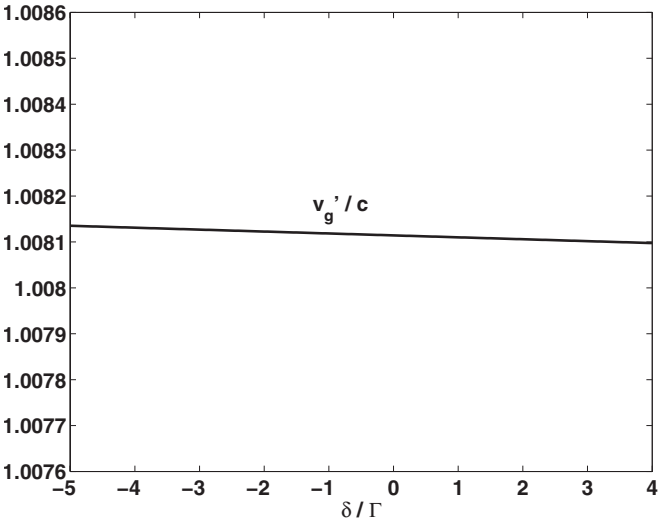

FIG. 7. Group velocity v_g' as a function of the reduced detuning δ/Γ for $n_i/n_c = 10^5$ and $k_0 r_m = 0.1$. Around resonance, the group velocity v_g' is finite and positive and it is close to c.

VIII. CONCLUSIONS

We have considered multiple scattering of a photon by pairs of atoms that are in a superradiant state. On average over disorder configurations, an attractive interaction potential builds up between close enough atoms, which decays as $1/r$. The contribution of superradiant pairs, resulting from this potential, to scattering properties is significantly different from that of independent atoms. This shows up in the behaviors of the group velocity, the elastic mean free path and the diffusion coefficient which are different from their values obtained for independent atoms. We have considered the case of a scalar wave and have shown that it allows to define an effective long-range and attractive potential for pairs of atoms in a superradiant state. Then, we have studied the case of a vector wave and have shown that the results obtained in the scalar case remain qualitatively valid. We have considered a simplified model where only pairs of atoms have been taken into account. A more realistic model should include higher-order terms that account for cooperative effects between more than two atoms [21]. The purpose of the current model is to show that already for a dilute gas in the weak-disorder limit, cooperative effects modify significantly the transport properties of light.

ACKNOWLEDGMENTS

This research is supported in part by the Israel Academy of Sciences and by the Fund for Promotion of Research at the Technion. We would like to thank Jean-Noel Fuchs for constructive remarks.

APPENDIX A

In this appendix, we establish expressions (53) and (63) for the elastic mean free path and the group velocity. At resonance, simple expressions for the elastic mean free path (56) and the group velocity (67) are obtained by a pertubative expansion with respect to the small parameter $k_0 r_m$.

1. Elastic mean free path

The elastic mean free path is given by (53) in terms of the function f_1 defined in (54). The integral in (54) is easily carried out analytically, and it leads to

$$\frac{1}{l_e(\delta)} = \frac{6\pi n_i}{k_0^2}\frac{1}{aC_1}\left(\frac{b}{2a}A_1 + \frac{a-2}{2a}B_1 + C_1\right), \tag{A1}$$

where

$$a = 1 + (\delta/\Gamma)^2, \quad b = \delta/\Gamma, \tag{A2}$$

$$A_1 = \ln\left(\frac{\frac{1}{4}x_m^2}{a + bx_m + \frac{1}{4}x_m^2}\right), \tag{A3}$$

$$B_1 = \frac{\pi}{2} - \tan^{-1}\left(b + \frac{1}{2}x_m\right), \tag{A4}$$

and

$$C_1 = \frac{1}{x_m} = k_0 r_m \ll 1. \tag{A5}$$

At resonance ($\delta=0$) we have $a=1$, $b=0$ and by expanding (A4) with respect to $k_0 r_m$ we obtain

$$B_1 \simeq \frac{2}{x_m}\left(1 - \frac{4}{3x_m^2}\right). \tag{A6}$$

Thus,

$$l_e(0) = \frac{k_0^2}{8\pi n_i}\frac{1}{(k_0 r_m)^2} \tag{A7}$$

as given in (56).

2. Group velocity

The group velocity is given by (63) in terms of the function f_2 defined in (65). The integral in (65) is easily carried out analytically and it yields

$$\frac{c}{v_g(\delta)} = 1 - \frac{n_i}{n_c}\frac{F_1}{a^2 C_1}, \tag{A8}$$

where

$$F_1 = b\left(\frac{1}{a} - \frac{1}{4}\right)A_1 + \frac{a-2}{4}A_1' + \left(\frac{3}{2} - \frac{2}{a}\right)B_1 - bB_1' + \left(1 - \frac{a}{2}\right)C_1, \tag{A9}$$

$$A_1' = -\frac{b + \frac{1}{2}x_m}{a + bx_m + \frac{1}{4}x_m^2}, \tag{A10}$$

and

$$B_1' = -\frac{\frac{1}{2}}{1 + \left(b + \frac{1}{2}x_m\right)^2}. \tag{A11}$$

At resonance ($\delta=0$) we have $a=1$, $b=0$ and by expanding (A10) and (A4) with respect to $k_0 r_m$ we obtain

$$A_1' \simeq \frac{2}{x_m}\left(\frac{4}{x_m^2} - 1\right) \tag{A12}$$

and

$$B_1 \simeq \frac{2}{x_m}\left(1 - \frac{4}{3x_m^2}\right). \tag{A13}$$

Thus,

$$\frac{c}{v_g(0)} = 1 + \frac{2}{3}\frac{n_i}{n_c}(k_0 r_m)^2, \tag{A14}$$

as given in (67).

APPENDIX B

The aim of this appendix is to calculate the average self-energy (72) for a $\Delta m=0$ transition in the case where $k_0 r \ll 1$. First, we average the superradiative propagator (25) over the orientation of the inter-atomic axis and obtain analytical expressions for its real and imaginary parts. Then, by averaging over the interatomic distance up to r_m, we obtain the average self-energy (72).

For a $\Delta m=0$ transition and $k_0 r \ll 1$, the superradiative propagator (25) may be written with the help of (12) and (13) as

$$\hbar\Gamma G^+ = \left[\frac{\delta}{\Gamma} + \frac{3}{4}\left(\frac{3\cos^2\theta - 1}{(k_0 r)^3} + \frac{\frac{1}{2}(1+\cos^2\theta)}{k_0 r}\right) + i\right]^{-1}, \tag{B1}$$

where the interatomic axis is $\mathbf{r}=(r,\theta,\varphi)$. Averaging over the orientations

$$\hbar\Gamma\langle G^+\rangle = \frac{1}{4\pi}\int \hbar\Gamma G^+ d\cos\theta\, d\varphi \tag{B2}$$

yields for the imaginary part

$$\hbar\Gamma\ \mathrm{Im}\langle G^+\rangle = -\frac{P+Q}{\beta^2} \tag{B3}$$

and for the real part

$$\hbar\Gamma\ \mathrm{Re}\langle G^+\rangle = W_- P + W_+ Q, \tag{B4}$$

where we have defined

$$P = \frac{1}{8A_2\beta\cos(\gamma/2)}\ln\left(\frac{1 + 2\beta\cos(\gamma/2) + \beta^2}{1 - 2\beta\cos(\gamma/2) + \beta^2}\right), \tag{B5}$$

$$Q = \frac{1}{4A_2\beta \sin(\gamma/2)}\left(\frac{\pi}{2} + \tan^{-1}\frac{1-\beta^2}{2\beta \sin(\gamma/2)}\right), \quad \text{(B6)}$$

and

$$W\pm = -\sqrt{A_2}(\cos\gamma \mp 1). \quad \text{(B7)}$$

The auxiliary parameters are given by

$$\beta = \left(\frac{C_2}{A_2}\right)^{1/4}, \quad \gamma = \cos^{-1}\left(-\frac{B_2}{2\sqrt{A_2C_2}}\right), \quad \text{(B8)}$$

where

$$A_2 = \frac{9}{16(k_0r)^2}\left(\frac{3}{(k_0r)^2} + \frac{1}{2}\right)^2, \quad \text{(B9)}$$

$$B_2 = \frac{3}{4k_0r}\left(\frac{3}{(k_0r)^2} + \frac{1}{2}\right)\left[\frac{2\delta}{\Gamma} + \frac{3}{2k_0r}\left(\frac{1}{2} - \frac{1}{(k_0r)^2}\right)\right], \quad \text{(B10)}$$

and

$$C_2 = 1 + \frac{1}{4}\left[\frac{2\delta}{\Gamma} + \frac{3}{2k_0r}\left(\frac{1}{2} - \frac{1}{(k_0r)^2}\right)\right]^2. \quad \text{(B11)}$$

Finally, we average (B3) and (B4) over the interatomic distance up to r_m,

$$\hbar\Gamma\ \mathrm{Im}\langle\overline{G^+}\rangle = -\frac{1}{r_m}\int_0^{r_m} dr\frac{P+Q}{\beta^2} \quad \text{(B12)}$$

and

$$\hbar\Gamma\ \mathrm{Re}\langle\overline{G^+}\rangle = \frac{1}{r_m}\int_0^{r_m} dr(W_-P + W_+Q). \quad \text{(B13)}$$

The integrals can be evaluated numerically and give the average self-energy (72) since

$$\frac{1}{4\pi r_m}\int \hbar\Gamma G^+(\mathbf{r})d\mathbf{r} = \hbar\Gamma\langle\overline{G^+}\rangle. \quad \text{(B14)}$$

[1] E. Akkermans and G. Montambaux, *Physique Mésoscopique des Électrons et des Photons* (EDP Sciences, Paris, 2004/ Cambridge University Press, Cambridge, UK, 2007).

[2] B. L. Altshuler and B. Simons, in *Mesoscopic Quantum Physics*, edited by E. Akkermans *et al.*, Proceedings of the Les Houches Summer School of Theoretical Physics, LXI (Elsevier, Amsterdam, 1995); Y. Imry, *Introduction to Mesoscopic Physics*, 2nd ed. (Oxford University Press, Oxford, 2002).

[3] R. H. Dicke, Phys. Rev. **93**, 99 (1954); M. Gross and S. Haroche, Phys. Rep. **93**, 301 (1982).

[4] Superradiance in Bose-Einstein condensates has been investigated experimentally by D. Schneble *et al.*, Science **300**, 475 (2003).

[5] G. Labeyrie, F. de Tomasi, J. C. Bernard, C. A. Müller, C. Miniatura, and R. Kaiser, Phys. Rev. Lett. **83**, 5266 (1999); C. A. Müller and C. Miniatura, J. Phys. A **35**, 10163 (2002).

[6] E. Akkermans, C. Miniatura, and C. A. Müller, e-print arXiv:cond-mat/0206298.

[7] E. Akkermans and R. Maynard, J. Phys. (France) Lett. **46**, L-1045 (1985).

[8] A. Gero and E. Akkermans, Phys. Rev. Lett. **96**, 093601 (2006).

[9] T. Thirunamachandran, Mol. Phys. **40**, 393 (1980).

[10] D. O'Dell, S. Giovanazzi, G. Kurizki, and V. M. Akulin, Phys. Rev. Lett. **84**, 5687 (2000); R. Low *et al.*, e-print arXiv:quant-ph/0503156.

[11] M. J. Stephen, J. Chem. Phys. **40**, 669 (1964); R. H. Lehmberg, Phys. Rev. A **2**, 883 (1970); P. W. Milonni and P. L. Knight, *ibid.* **10**, 1096 (1974).

[12] It can be shown using (7) that the contribution of mixed terms like $\langle\phi^{\pm}|G|\phi^{\mp}\rangle$ vanishes.

[13] Notice, however, that this rewriting of the amplitude T is defined up to a proportionality constant, which accounts for the quantum nature of the problem and the photon polarization.

[14] E. Akkermans and G.Montambaux, in *Cargese Summer School Lecture Notes*, edited by B. A. van Tiggelen and S. E. Skipetrov (Kluwer Academic, Dordrecht, 2003).

[15] L. Brillouin, *Wave Propagation and Group Velocity* (Academic, New York, 1960).

[16] M. P. van Albada, B. A. van Tiggelen, A. Lagendijk, and A. Tip, Phys. Rev. Lett. **66**, 3132 (1991); A. Lagendijk and B. A. van Tiggelen, Phys. Rep. **270**, 143 (1996).

[17] R. Loudon, J. Phys. A **3**, 233 (1970).

[18] B. A. van Tiggelen, in *Mesoscopic Light Scattering in Atomic Physics*, edited by R. Kaiser, C. Westbrook, and F. David, Proceedings of the Les Houches Summer School of Theoretical Physics, LXXII (Springer, Berlin, 1999).

[19] O. Morice, Y. Castin, and J. Dalibard, Phys. Rev. A **51**, 3896 (1995).

[20] G. Labeyrie, E. Vaujour, C. A. Müller, D. Delande, C. Miniatura, D. Wilkowski, and R. Kaiser, Phys. Rev. Lett. **91**, 223904 (2003).

[21] E. Akkermans, A. Gero, and R. Kaiser (unpublished).

Photon localization and Dicke superradiance in atomic gases : crossover to a "small world" network

E. Akkermans[1], A. Gero[1] and R. Kaiser[2]
[1] *Department of Physics, Technion Israel Institute of Technology, 32000 Haifa, Israel*
[2] *Institut Non Linéaire de Nice, UMR 6618 CNRS, France*
(Dated: November 25, 2007)

We study the photon propagation in a gas of N atoms, using an effective Hamiltonian that accounts for photon mediated atomic dipolar interactions. The density $P(\Gamma)$ of photon escape rates is obtained from the spectrum of the $N \times N$ random matrix $\Gamma_{ij} = \sin(x_{ij})/x_{ij}$, where x_{ij} is the dimensionless random distance between any two atoms. A scaling function is defined to study photons escape rates as a function of disorder and system size. Photon localization is described using statistical properties of random networks whose mean field solution displays a "small world" behavior.

PACS numbers: 42.25.Dd,42.50.Fx,72.15.Rn,87.23.Ge

Cold atomic gases provide an interesting framework to study photon localization resulting from coherent multiple scattering. Unlike uncorrelated disordered systems, new additional features such as cooperative effects (*e.g.* super- and subradiance) [1] modify our current description of coherent multiple scattering of photons. The synchronization of the atomic dipoles can be seen as a correlation between the scatterers. Studying cooperative emission is thus a particular example of transport in a system with long range correlations. Photon localization and cooperative effects show up as an overall decrease of the escape rate of photons. For weak disorder, atoms scatter photons independently. For stronger disorder, cooperative effects become important and lead to vanishing escape rates, so that photons are trapped in the gas for very long times. In this letter, we show that this photon localization occurs as a crossover rather than as a phase transition like for Anderson localization [2]. We show that this crossover is described by means of a single scaling function. For large disorder, the atomic system can be viewed as a highly connected random network whose statistical properties are well reproduced by the mean-field solution of a "small-world" network model [3]. For even larger densities, we retrieve the expected Dicke limit which can be mapped onto an ideal fully connected network. We consider a collection of N identical atoms at rest, taken to be degenerate two-level systems respectively denoted, for the atom i, by $|g_i\rangle = |j_g = 0, m_g = 0\rangle$ and $|e_i\rangle = |j_e = 1, m_e = 0, \pm 1\rangle$ for the ground and excited states. j is the total angular momentum and m is its projection on a quantization axis . The energy separation between the two levels, including the radiative shift, is $\hbar\omega_0$ and the natural width of the excited level is $\hbar\Gamma_0$. The atoms are placed at random positions $\mathbf{r}_i$ and are coupled to the electromagnetic field $\mathbf{E}$ through their dipole operator $\mathbf{d}_i$. The Hamiltonian is,

$$H = \sum_{i=1}^{N} \hbar\omega_0 |e_i\rangle\langle e_i| + \sum_{\mathbf{k}\varepsilon} \hbar\omega_k a^\dagger_{\mathbf{k}\varepsilon} a_{\mathbf{k}\varepsilon} - \sum_{i=1}^{N} \mathbf{d}_i \cdot \mathbf{E}(\mathbf{r}_i) \quad (1)$$

where $a^\dagger_{\mathbf{k}\varepsilon}$ is the creation operator of a photon with wave vector $\mathbf{k}$ and polarization ε. We consider the limit where only one photon is present. The trace over the photon degrees of freedom leads to the following effective Hamiltonian for the atomic gas,

$$H_e = (\hbar\omega_0 - i\frac{\hbar\Gamma_0}{2}) \sum_{i=1}^{N} |e_i\rangle\langle e_i| + \frac{\hbar\Gamma_0}{2} \sum_{i\neq j} V_{ij} \Delta_i^+ \Delta_j^- \quad (2)$$

where $\Delta_i^+ = |e_i\rangle\langle g_i|$ is the atomic raising operator and $\Delta_i^- = (\Delta_i^+)^\dagger$. The potential $V_{ij} = \beta_{ij} - i\gamma_{ij}$ is complex valued and,

$$\begin{aligned} \beta_{ij} &= \frac{3}{2}\left[-p\frac{\cos k_0 r_{ij}}{k_0 r_{ij}} + q\left(\frac{\cos k_0 r_{ij}}{(k_0 r_{ij})^3} + \frac{\sin k_0 r_{ij}}{(k_0 r_{ij})^2}\right)\right] \\ \gamma_{ij} &= \frac{3}{2}\left[p\frac{\sin k_0 r_{ij}}{k_0 r_{ij}} - q\left(\frac{\sin k_0 r_{ij}}{(k_0 r_{ij})^3} - \frac{\cos k_0 r_{ij}}{(k_0 r_{ij})^2}\right)\right] \end{aligned} \quad (3)$$

where $k_0 = \omega_0/c$ and $r_{ij} = |\mathbf{r}_i - \mathbf{r}_j|$ is the distance between any two atoms. The quantities p and q depend on the atomic transition. For $\Delta m = m_e - m_g = 0$,

$$p_0 = \sin^2\theta_{ij}, \;\; q_0 = 1 - 3\cos^2\theta_{ij} \quad (4)$$

and for a transition $\Delta m = \pm 1$,

$$p_\pm = \frac{1}{2}(1 + \cos^2\theta_{ij}), \;\; q_\pm = \frac{1}{2}(3\cos^2\theta_{ij} - 1) \;\; . \quad (5)$$

The angle θ_{ij} is obtained from the unit vector $\hat{\mathbf{r}}_{ij} = (1, \theta_{ij}, \varphi_{ij})$ defined along the direction joining two atoms.

Expressions (2) and (3) for the Hamiltonian and the effective interacting potential V_{ij} are well known [4, 5]. For distances between atoms that are small compared to the coherence length of the light emitted by a single atom, we obtain the potential V_{ij}, which corresponds to an instantaneous photon exchange between two atoms [6].

To characterize the photon transport properties, we consider the average density $P(\Gamma)$ of escape rates Γ of a photon propagating in the atomic gas. Escape rates have

already been considered for the study of superradiance [5, 7] and of Anderson localization of classical waves [8]. To obtain $P(\Gamma)$, we consider first the simplest situation of a photon scattered by two atoms, for which it is possible to calculate from (2) the photon propagator [5] whose scalar part, at resonance, is $G = (2/\hbar\Gamma_0)(i - V_{12})^{-1}$, where $\hbar\Gamma_0 V_{12}/2$ is the photon self-energy. Its imaginary part accounts for the correction to the inverse lifetime of the atomic excited state, which is also the photon escape rate. For the case of N atoms, the photon escape rate, expressed in units of Γ_0, is obtained from γ_{ij} given in (3) for $i \neq j$ together with $\gamma_{ii} = 1$. To show this, we calculate the probability to detect a photon outside the gas. This calculation is standard in photo-detection theory [9] and it has been used in the study of superradiance [7]. The $N \times N$ matrix γ_{ij} thus defined, is random and depends on the atomic positions $\mathbf{r}_i$ with the constraint that its trace is equal to N. Related random matrices have been studied in various contexts and they have been termed euclidean random matrices [10]. The average density $P(\Gamma)$ of photon escape rates is then obtained from the eigenvalue spectrum of γ_{ij}, *i.e.*, from the linear system

$$\sum_{j=1}^{N} \gamma_{ij} u_j = \Gamma u_i \ . \tag{6}$$

This equation has been considered in the continuous limit and for very specific geometries of the atomic gas [7]. Here we study a random and uniform distribution of atoms. The average density of escape rates $P(\Gamma)$ is formally defined by $P(\Gamma) = -(1/\pi)\,\mathrm{Im}R(z = \Gamma + i0^+)$, with

$$R(z) = \frac{1}{N}\overline{\mathrm{Tr}\left(\frac{1}{z - [\gamma_{ij}]}\right)} \ . \tag{7}$$

The average $\overline{\cdots}$ is taken, at fixed density, over spatial configurations of the atoms. For Gaussian ensembles of random matrices [11], the average density of states obeys a semi-circle law. Here, as we shall see, the behavior of $P(\Gamma)$ is very different.

The matrix γ_{ij}, defined in (3), depends on the distances r_{ij} between atoms and on the angles θ_{ij}. We expect localization properties and cooperative effects to depend mostly on r_{ij} and not on θ_{ij}. We therefore consider the scalar model obtained from (3) by averaging γ_{ij} over θ_{ij}. Using (4) and (5), we thus obtain for the scalar model, the $N \times N$ matrix,

$$\Gamma_{ij} \equiv \langle \gamma_{ij} \rangle = \frac{\sin x_{ij}}{x_{ij}} \tag{8}$$

where $x_{ij} = k_0 r_{ij}$ are distances expressed in units of the wavelength $\lambda = 2\pi/k_0$. We have checked that $P(\Gamma)$ obtained for the vector case γ_{ij} and for the scalar case Γ_{ij} are qualitatively the same [12]. The scalar model (8) has the advantage of being easier to handle and the remainder of this letter is devoted to its study. To that purpose, we consider N atoms enclosed in a cubic volume $L^3 = (\lambda a)^3$ where distances are measured in units of the wavelength λ. The atoms are distributed with a uniform density $n = N/(\lambda a)^3$. The disorder strength W is defined for resonant scattering, using the total cross section $\sigma \simeq \lambda^2$, by $W \equiv n\sigma\lambda/2\pi = N/2\pi a^3 = \rho/2\pi$ where $\rho = N/a^3$ is the dimensionless density of atoms.

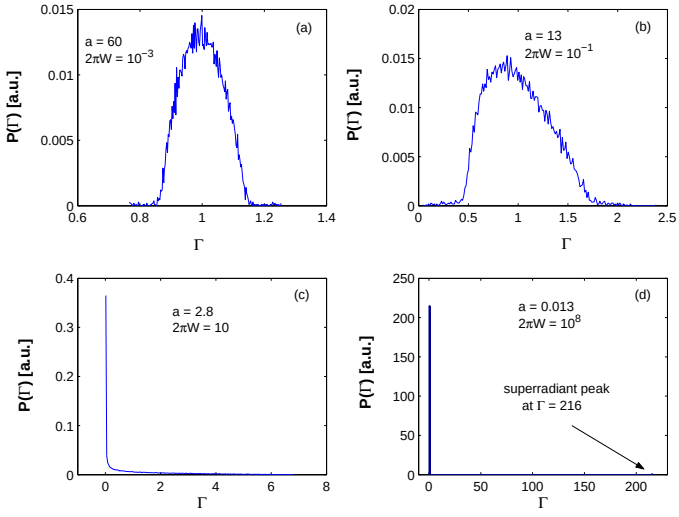

FIG. 1: *Behavior of $P(\Gamma)$ for different values of the disorder strength W, of the size a and for $N = 216$. (a) At low disorder, $P(\Gamma)$ is peaked around $\Gamma = 1$ (b) for larger disorder, $P(\Gamma)$ becomes broader and shifted towards the origin and eventually (c) it accumulates near $\Gamma = 0$ (d) Dicke limit.*

The eigenvalues of the matrix Γ_{ij} are nonnegative since the three-dimensional Fourier transform of $\mathrm{sinc}|x|$ is $\delta(|k| - 1) \geq 0$. This property applies also to the vectorial case γ_{ij} given by (3). We have obtained $P(\Gamma)$ for different values of disorder strength W and size a (see Fig.1). We observe the following behaviors. For a very dilute gas, we recover the single atom limit namely $\Gamma_{ij} \to \delta_{ij}$, so that $P(\Gamma)$ is narrowly peaked around $\Gamma = 1$ (in units of Γ_0) as expected from resonant scattering of a photon by a single atom (Fig.1.a). For stronger disorders, $P(\Gamma)$ becomes broader and it is shifted towards lower values of Γ (Fig.1.b). Eventually for large enough disorders, most of the eigenvalues are close to $\Gamma = 0$ (Fig.1.c). Such a vanishing escape rate corresponds to photons localized in the atomic gas. By increasing further the disorder W, at fixed number N of atoms, we reach another regime (Fig.1.d) where $P(\Gamma)$ has two peaks, one at $\Gamma = 0$ and a second one at $\Gamma = N$. This is the Dicke limit which occurs when the atoms are contained in a volume much smaller than λ^3. The eigenvalue $\Gamma = 0$ is the $(N-1)$-degenerate subradiant mode and $\Gamma = N$ is the non-degenerate superradiant mode. In this limit, the escape rate matrix

$[\Gamma_{ij}]$ given by (8), becomes

$$[\Gamma_{ij}] = \begin{pmatrix} 1 & 1 & \cdots & 1 \\ 1 & 1 & \cdots & 1 \\ \vdots & \vdots & & \vdots \\ 1 & 1 & \cdots & 1 \end{pmatrix} \quad . \tag{9}$$

Using (7), we obtain the density:

$$P(\Gamma) = \frac{N-1}{N}\delta(\Gamma) + \frac{1}{N}\delta(\Gamma - N) \quad . \tag{10}$$

To characterize $P(\Gamma)$, we look for a scaling function. A natural choice when inspecting the shape of $P(\Gamma)$ displayed in Fig.1 is to consider the relative number of states $\Gamma_e(a, W)$ defined by

$$\Gamma_e(a, W) = \int_1^\infty d\Gamma \;\; P(\Gamma) \quad , \tag{11}$$

which have an escape rate larger than 1 (in units of Γ_0). To obtain its dependence upon the system size a and the disorder W, we introduce the conveniently normalized scaling function $g(a, W)$ defined between 0 and 1 by

$$g(a, W) = 1 - 2\Gamma_e(a, W) \quad . \tag{12}$$

g thus defined, measures the relative number of states having a vanishing escape rate. At finite size, we expect $g(a, W)$ to have a scaling form, namely :

$$\frac{d \ln g(a, W)}{d \ln a} = \beta(g) \tag{13}$$

where $\beta(g)$ is a function of g only. The solution of this equation can be written $g(a, W) = a^\mu f(a/\xi(W))$. We have verified this scaling hypothesis over a broad range of size and disorder. The results displayed in Fig.2 for different values of disorder, collapse on a single curve (see Fig.3) when plotted as a function of the scaling parameter aW. Restoring the unit length, this parameter is the optical thickness $2\pi aW = L/l$ where $l = \lambda/2\pi W$ is the photon elastic mean free path [13].

In the Dicke limit (Fig.1.d), $P(\Gamma)$ is given by (10). Using (12), we obtain the scaling behavior $g(a, W) = 1 - (2/N) = 1 - 1/(\pi a^3 W)$ displayed in Fig.4.

These results can be understood in the framework of statistical mechanics of random networks. To show this, we start from the Dicke limit which corresponds to the escape rate matrix (9). This matrix describes a collection of N fully connected atoms with identical strengths equal to 1. This system can be exactly mapped onto an ideal fully connected graph whose spectral density is given by (10) [14]. At lower but still large values, $2\pi aW \simeq 200$ (see Fig.3), the system may be described as a random graph of atoms sitting at vertices and randomly (but not fully) connected to other atoms by exchange of photons. At small values $aW \ll 1$, we recover a gas of independent

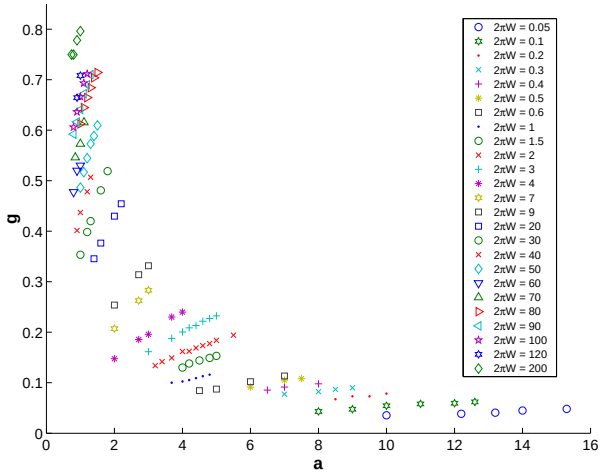

FIG. 2: *Behavior of g as a function of the system size a for different disorder strengths W.*

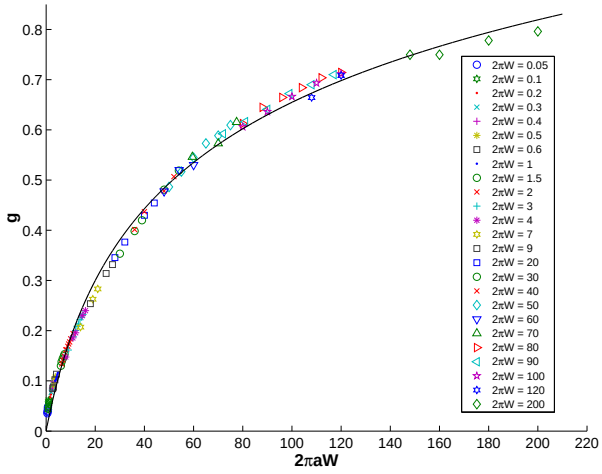

FIG. 3: *All the points represented in Fig.2 collapse on the same curve thus confirming the scaling assumption (13). The solid line represents the mean field solution given by (14).*

atoms, which is the limiting case of a graph of vanishing connectivity (or coordination number). Statistical properties of such disordered networks have been extensively studied [15]. The existence of a crossover between regular and random networks has been obtained numerically [16] and described by means of a mean-field solution [17]. An important feature of this crossover is that for finite but small values of the disorder, the network behaves as a "small world" [18], namely that any two vertices can be connected through only a short chain of intermediate vertices. When applied to our atomic random network, the mean field solution [17] leads to the expression,

$$g(x) = \frac{4Ax}{\sqrt{x^2 + 4x}} \tanh^{-1}\left(\frac{x}{\sqrt{x^2 + 4x}}\right) \tag{14}$$

for the scaling function $g(x)$ [12]. The scaling variable is $x = \pi aW/2$ and $A \simeq 0.1$ is an integration constant. The

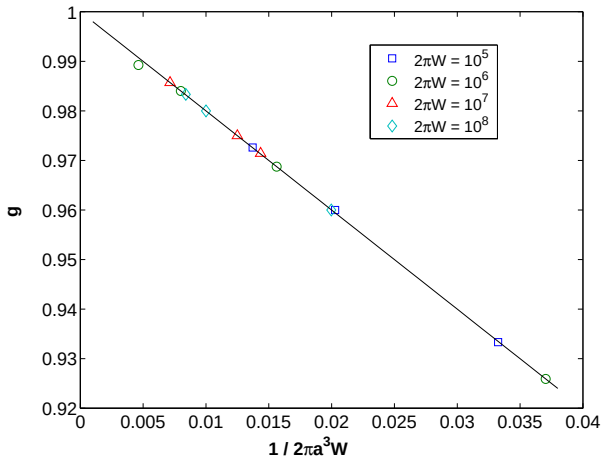

FIG. 4: *Scaling behavior of* $g(a, W) = 1 - 1/(\pi a^3 W)$ *in the Dicke limit.*

solid line in Fig.3 is a fit of the numerical results using the mean field expression (14). The agreement is rather good.

For a small optical thickness, $x \propto aW \ll 1$, the expression (14) gives $g(x) = Ax$. Using (12) leads to $2\Gamma_e \simeq 1 - (A\pi/2)aW$. This is the first correction to the free value $\Gamma_0/2$ obtained for a very dilute gas. In the opposite limit $aW \gg 1$, of a dense gas, we obtain from (14), $g(x) = A \ln x$. This corresponds to the "small world" limit where, as a result of strong cooperative effects, any two atoms can be connected by photon exchange only through small chains of intermediate atoms. This description breaks down for values of x so large that we enter the Dicke regime (10) (see Fig.4). The largest value of x can be estimated by saying that at fixed number N of atoms, $x \propto aW \simeq N$.

To summarize, we have characterized the escape rates of photons propagating in an atomic gas by means of a scaling function $g(x)$, where $x \propto aW$ is proportional to the optical thickness. For weak disorder, it describes delocalized photons with reduced escape rates. In the opposite limit, $g(x)$ saturates to 1, meaning that photons remain localized inside the gas. This last regime includes the Dicke limit. Using a mapping onto a random network problem, we have described the crossover between a weakly connected network of atoms emitting photons almost independently at small disorder to a "small world" network where atoms are related through small chains of intermediate atoms exchanging photons. These results differ substantially from those obtained in the context of Anderson localization of photons where weak and strong disordered phases are separated by a phase transition in dimension $d > 2$. It must be noticed nevertheless, that in our model, we study the spectral properties of the random matrices (8) and not of the Laplacian in the presence of disorder.

The problem we have considered involves a new class of random operators whose behavior is very different from either the disordered Laplacian or Gaussian random matrices [11]. The mapping of the problem of cooperative effects in atomic gases onto a "small world" network may be also interesting to study from a different perspective the statistical mechanics of random networks. Finally, the analysis we present in this letter may suggest a different approach and new protocoles for experiments on photon localization in cold atomic gases.

It is a pleasure to thank M. Mézard and B. Shapiro for their interest. This research is supported in part by the Israel Academy of Sciences, by the Fund for Promotion of Research at the Technion and the ANR program CAROL.

[1] R. H. Dicke, Phys. Rev. **93**, 99 (1954)
[2] P.W. Anderson, Phys. Rev. **109**, 1492 (1958)
[3] M.E.J. Newman, J. Stat. Phys. **101**, 819 (2000)
[4] M. J. Stephen, J. Chem. Phys. **40**, 669 (1964) and R.H. Lehmberg, Phys. Rev. A **2**, 883 (1970)
[5] A. Gero and E. Akkermans, Phys. Rev. Lett. **96**, 093601 (2006) and Phys. Rev. A **75**, 053413 (2007)
[6] P. W. Milonni and P. L. Knight, Phys. Rev. A **10**, 1096 (1974)
[7] V. Ernst and P. Stehle, Phys. Rev. **176**, 1456 (1968), E. Ressayre and A. Tallet, Phys. Rev. Lett. **37**, 424 (1976) and *ibid*, Phys. Rev. A **15**, 2410 (1977)
[8] F.A. Pinheiro *et al.*, Phys. Rev. E **69**, 026605-1 (2004) and M. Patra, *ibid* **67**, 016603 (2003)
[9] C. Cohen-Tannoudji *et al.*, *Atom-photon interactions*, chap. 2, Wiley (1992)
[10] M. Mézard, G. Parisi and A. Zee, Nucl. Phys. B **559**, 689 (1999)
[11] M.L. Mehta, *Random Matrices*, Academic Press, New York, 1991
[12] E. Akkermans, A. Gero and R. Kaiser, unpublished
[13] E. Akkermans and G. Montambaux, *Mesoscopic physics of electrons and photons*, Cambridge Univ. Press (2007)
[14] S.N. Taraskin, Phys. Rev. E **72**, 056126 (2005)
[15] R. Albert and A.L. Barabasi, Rev. Mod. Phys. **74**, 47 (2002)
[16] M. Barthélémy and L.A.N. Amaral, Phys. Rev. Lett. **82**, 3180 (1999)
[17] M.E.J. Newman, C. Moore and D.J. Watts, Phys. Rev. Lett. **84**, 3201 (2000)
[18] S. Milgram, *The small world problem*, Psychology Today, **2**, 60 (1967)

Bibliography

[1] E. Akkermans and G. Montambaux, *Mesoscopic Physics of Electrons and Photons*, Cambridge University Press (2007)

[2] A. Ishimaru, *Wave Propagation and Scattering in Random Media*, Academic Press (1978)

[3] M. Born and E. Wolf, *Principles of Optics*, Cambridge University Press (1999)

[4] C. Cohen-Tannoudji, J. Dupont-Roc and G. Grynberg, *Atom-Photon Interactions*, Wiley (1998)

[5] E. Akkermans, P. E. Wolf and R. Maynard, Phys. Rev. Lett. **56**, 1471 (1986)

[6] E. Akkermans, P. E. Wolf, R. Maynard and G. Maret, J. Phys. France **49**, 77 (1988)

[7] E. Akkermans and G. Montambaux, J. Opt. Soc. Am. B **21**, 101 (2004)

[8] B. A. van Tiggelen, *Mesoscopic Light Scattering in Atomic Physics*, Les Houches summer school, session LXXII, R. Kaiser, C. Westbrook and F. David eds., Springer (1999)

[9] C. A. Müller, T. Jonckheere, C. Miniatura and D. Delande, Phys. Rev. A **64**, 053804 (2001)

[10] C. A. Müller and C. Miniatura, J. Math. Gen. **35**, 10163 (2002)

[11] R. H. Dicke, Phys. Rev. **93**, 99 (1954)

[12] M. Gross and S. Haroche, Phys. Rep. **93**, 301 (1982)

[13] A. Gero and E. Akkermans, Phys. Rev. Lett. **96**, 093601 (2006)

[14] A. Gero and E. Akkermans, Phys. Rev. A **75**, 053413 (2007)

[15] E. Akkermans, A. Gero and R. Kaiser, submitted for publication

[16] C. Cohen-Tannoudji, J. Dupont-Roc and G. Grynberg, *Photons and Atoms*, Wiley (1989)

[17] S. F. Edwards, Philos. Mag. **3**, 1020 (1958)

[18] W. L. Lama, R. Jodoin and L. Mandel, Am. J. Phys. **40**, 32 (1972)

[19] L. Mandel and E. Wolf, *Quantum Coherence and Quantum Optics*, Cambridge University Press (1995)

[20] G. S. Agarwal, A. C. Brown, L. M. Narducci and G. Vetri, Phys. Rev. A **15**, 1613 (1977)

[21] P. W. Milonni and P. L. Knight, Phys. Rev. A **11**, 1090 (1975)

[22] M. J. Stephen, J. Chem. Phys. **40**, 669 (1964)

[23] R. H. Lehmberg, Phys. Rev. A **2**, 883 (1970)

[24] P. W. Milonni and P. L. Knight, Phys. Rev. A **10**, 1096 (1974)

[25] P. W. Milonni and P. L. Knight, Am. J. Phys. **44**, 741 (1976)

[26] P. de Vries, D. V. van Coevorden and A. Langendijk, Rev. Mod. Phys. **70**, 447 (1988)

[27] T. Thirunamachandran, Mol. Phys. **40**, 393 (1980)

[28] D. O'Dell, S. Giovanazzi, G. Kurizki and V. M. Akulin, Phys. Rev. Lett. **84**, 5687 (2000)

[29] B. A. van Tiggelen, A. Lagendijk and A. Tip, J. Phys. C **2**, 7653 (1990)

[30] O. Morice, Y. Castin and J. Dalibard, Phys. Rev. A **51**, 3896 (1995)

[31] L. Brillouin, *Wave Propagation and Group Velocity*, Academic NY (1960)

[32] R. Loudon, J. Phys. A **3**, 233 (1970)

[33] G. Lindblad, Commun. Math. Phys. **48**, 119 (1976)

[34] E. Ressayre and A. Tallet, Phys. Rev. Lett. **37**, 424 (1976)

[35] E. Ressayre and A. Tallet, Phys. Rev. A **15**, 2410 (1977)

[36] V. Ernst and P. Stehle, Phys. Rev. **176**, 1456 (1968)

[37] V. Ernst, Z. Physik **218**, 111 (1969)

[38] M. Mézard, G. Parisi and A. Zee, Nucl. Phys. B **559**, 689 (1999)

[39] E. Abrahams, P. W. Anderson, D. C. Licciardello and T. V. Ramakrishnan, Phys. Rev. Lett. **42**, 673 (1979)

[40] A. Réka and A. Barabási, Rev. Mod. Phys. **74**, 47 (2002)

[41] S. N. Taraskin, Phys. Rev. E **72**, 056126 (2005)

[42] P. Erdös and A. Rényi, Publ. Math. (Debrecen) **6**, 290 (1959)

[43] D. J. Watts and S. H. Strogatz, Nature (London) **393**, 440 (1998)

[44] S. Milgram, Psychol. Today **2**, 60 (1967)

[45] A. Barrat and M. Weigt, Eur. Phys. J. B **13**, 547 (2000)

[46] B. Bollobás, *Random Graphs*, Academic Press (1985)

[47] M. E. J. Newman, C. Moore and D. J. Watts, Phys. Rev. Lett. **84**, 3201 (2000)

[48] M. Barthélémy and L. A. N. Amaral, Phys. Rev. Lett. **82**, 3180 (1999)

[49] M. E. J. Newman and D. J. Watts, Phys. Lett. A **263**, 341 (1999)

פוטנציאל דו-אטומי ארוך טווח הדועך כמו היפוך המרחק הבין-אטומי. במקרה של סופר-קרינתיות פוטנציאל זה הינו מושך עבור זוג אטומים קרובים דיים.
תכונותיהם של זוגות סופר-קרינתיים, הנוצרים מהפוטנציאל הנ"ל, שונות משמעותית מאלו של אטומים מבודדים. תכונות אלה באות לידי ביטוי במרחק האלסטי הממוצע של הפוטון המתפזר, במהירות החבורה שלו ובמקדם הדיפוסיה המתאים, אשר שונים מאלה המתקבלים במקרה של פיזורים רבים של אור מאטומים שאינם באינטראקציה הדדית. לדוגמא, מהירות החבורה של הפוטון המתפזר מזוגות אלה הינה חיובית וסופית סמוך לתהודה (ובכלל זה בתהודה עצמה), בניגוד לזו המתקבלת מפיזור אור מאטומים מבודדים.

בחלקו השני של המחקר, עבור קונפיגורציה בת N אטומים, הממוקמים אקראית בשדה קרינה חיצוני, אנו מגדירים המילטוניאן אפקטיבי המתאר את האינטראקציות הבין-אטומיות המושרות ע"י הקרינה. בעזרתו, אנו מוכיחים כי קצב המילוט של פוטון מגז אטומי זה מתקבל מהספקטרום של מטריצה אקראית ממימד N. עבור גיאומטריה תלת-ממדית, המטריצה הינה $U_{ij}=\sin(x_{ij})/x_{ij}$, בעוד שבמקרה של גז חד-מימדי המטריצה נתונה ע"י $U_{ij}=\cos(x_{ij})$, כאשר x_{ij} הוא המרחק האקראי חסר המימד בין שני אטומים כלשהם. קצב המילוט הנ"ל מחושב נומרית, במקרה של פיזור תהודתי, עבור תחום רחב מאוד של גודל המערכת (נפח הגז) ושל דרגת אי הסדר, החל מאי סדר חלש (גז דליל) וכלה באי סדר חזק (גז צפוף). החישוב מבוצע הן עבור גיאומטריה תלת-ממדית והן עבור גיאומטריה חד-ממדית.
במטרה לנתח את קצב המילוט של הפוטון כתלות בדרגת אי הסדר ובגודל המערכת, אנו מגדירים פונקצית כיול (scaling function) אשר מהווה מדד למספר היחסי של מצבים בעלי קצב מילוט אפסי. באמצעותה, אנו למדים כי במערכת תלת-ממדית גדולה דיה (ביחס לאורך גל הקרינה), כתוצאה מהגדלת העומק האופטי (optical depth) הפוטונים עוברים ממצב לא-ממוקם (delocalization), בו קצב המילוט הוא סופי, למצב ממוקם (localization), בו קצב המילוט שואף לאפס. בנוסף, מתברר כי בגבול התרמודינמי הפוטונים תמיד ממוקמים, ולפיכך הפוטונים עוברים תהליך של חצייה (crossover) ולא של מעבר פאזה. תוצאות אלו שונות באופן מובהק מאלה המתקבלות בהקשר של לוקליזציית אנדרסון (Anderson) של פוטונים, לפיהן במערכת תלת-ממדית קיים מעבר בין הפאזה הלא-ממוקמת ובין זו הממוקמת. בגיאומטריה חד-ממדית קצב המילוט שואף לאפס והפוטונים תמיד ממוקמים (לרבות בגבול התרמודינמי), בהתאמה למצופה עפ"י אנדרסון.
אנו מציעים הסבר לתוצאות שהתקבלו בגיאומטריה התלת-ממדית במסגרת התכונות הסטטיסטיות של רשתות אקראיות. לפיו, הפוטונים עוברים ממצב של אי סדר חלש, בו האטומים מקושרים זה לזה באופן רופף ופולטים פוטון באופן עצמאי כמעט, למצב המכונה *רשת עולם קטן* (small world network) בו האטומים קשורים זה לזה דרך מספר קטן של אטומים שכנים, המחליפים בניהם פוטון.
השוני בין התוצאות שהתקבלו ובין המצופה עפ"י לוקליזציית אנדרסון נעוץ בעובדה שאנו חוקרים את התכונות הספקטראליות של המטריצה האקראית U ולא של הלפלסיאן בנוכחות אי סדר.

תקציר

להתקדמות גלים בתווך לא מסודר חשיבות רבה בשטחים מגוונים בפיסיקה. לדוגמא, תובלה אלקטרונית במתכות, התקדמות אור בתווך גזי, פיזור גלי קול בנוזלים והתקדמות גלים סיסמיים. התכונות הכלליות המאפיינות את ההתקדמות בתווך משותפות לכל המקרים הנ״ל, אולם כל סוג של גל מפגין גם את ההתנהגות הייחודית לו.

כאשר התווך הינו דק – אזי הגל מתפזר רק פעם אחת בטרם הוא עוזב אותו, אולם כאשר התווך עבה דיו – הגל עובר פיזורים רבים טרם עזיבתו. המקרה הראשון מתאר *פיזור יחיד*, בעוד שהאחרון מתאר משטר של *פיזורים רבים*. מחקר זה עוסק בפיזורים רבים של אור ע״י גזים אטומיים.

פיזור אור יחיד מדיאלקטריקון בעל נפח שרירותי נחקר ע״י מי (Mie). כאשר רדיוס המפזר קטן מאוד ביחס לאורך גל הקרינה, פיזור מי מתנוון לפיזור ריילי (Rayleigh), בו חתך הפעולה לפיזור מתכונתי הפוך לאורך הגל בחזקה רביעית. המקרה הנגדי, בו רדיוס המפזר גדול מאוד ביחס לאורך הגל, תואם את חוקי האופטיקה הגיאומטרית, לפיהם חתך הפעולה לפיזור אינו תלוי באורך הגל והוא בסדר גודל של שטח חתך המפזר.

כאשר המפזר הוא אטום ולא עצם קלאסי, המבנה האנרגטי הפנימי שלו מוביל לתופעות חדשות. קיומן של רמות אנרגיה בספקטרום האטומי מתבטא בביטויים עבור חתך הפעולה לפיזור השונים מאלו שהתקבלו בפיזור מי. לדוגמא, בפיזור תהודתי, בו תדירות הקרינה קרובה מאוד לתדירות בוהר האטומית, חתך הפעולה לפיזור מתכונתי לריבוע אורך גל הקרינה.

הסוגיה של פיזורים רבים של אור ע״י גזים אטומיים ניתנת לטיפול במספר גישות:

הראשונה, מתארת את הפיזור של גל סקלרי ע״י מפזרים קלאסיים. גישה בסיסית זו מזניחה את קיטוב האור ואת אופיו הקוונטי, כמו גם את דרגות החופש הפנימיות (רמות האנרגיה האטומיות) של המפזרים. הגישה השנייה לוקחת בחשבון את האופי הוקטורי של האור, אולם המפזרים ושדה הקרינה עדיין מטופלים באופן קלאסי. הגישה השלישית הינה טיפול סמי-קלאסי המתאר פיזורים רבים של גל אלקטרו-מגנטי ע״י אטומים, בעלי מבנה אנרגטי פנימי. הגישה האחרונה דנה בפוטונים (במסגרת הפורמליזם של קוונטיזציה שנייה) ובאטומים ולכן מייצגת טיפול קוונטי מלא.

אולם, כל התיאורים הנ״ל מזניחים את האינטראקציה ההדדית בין המפזרים. לפיכך, מטרתו של מחקר זה היא בלימוד פיזורים רבים של פוטונים בתווך אטומי לא מסודר, תוך התחשבות באפקטים קואופרטיבים, כמו *סופר-קרינתיות* (superradiance) ו-*תת-קרינתיות* (subradiance), הנובעים מהאינטראקציה בין האטומים דרך שדה הקרינה.

סופר-קרינתיות הינה התופעה בה, תחת נסיבות מסוימות, קצב הפליטה הספונטאנית מאוסף של N אטומים מתכונתי ל-N^2 במקום ל-N. התופעה המשלימה הינה תת-קרינתיות, בה תחת נסיבות אחרות, קצב הפליטה הספונטאנית מתאפס למרות שמחצית מ-N האטומים מאכלסים את הרמות האנרגטיות המעוררות.

במחקר זה אנו מראים כי אפקטים אלה משנים באופן ניכר את תכונות האור המתקדם בתווך אטומי אקראי. בחלקו הראשון, אנו מוכיחים כי כתוצאה מהאינטראקציה בין האטומים, נוצר

המחקר נעשה בהנחיית פרופ׳ אריק אקרמן בפקולטה לפיסיקה.

ברצוני להודות מקרב לב לפרופ׳ אריק אקרמן על הנחייתו המסורה, מעורבותו הרבה ועל העניין האמיתי שגילה בנושאי המחקר.

אני מודה לעמיתי אוהד אסף על שיחות רבות שניהלנו בנושאי המחקר ועל הצעותיו הטובות.

תודה לחברי ולעמיתי נתנאל לינדנר על העידוד, על אינספור שעות של אימוני טריאתלון משותפים ועל יסוד המסדר.

אני מודה לטכניון על התמיכה הכספית הנדיבה בהשתלמותי.

להורי, יהודית וטומי

אפקטים קואופרטיבים בפיזורים רבים של פוטונים ע״י גז אטומי

חיבור על מחקר

לשם מילוי חלקי של הדרישות לקבלת התואר
דוקטור לפילוסופיה

אהרון פ. גרו

הוגש לסנט הטכניון – מכון טכנולוגי לישראל

טבת תשס״ח חיפה דצמבר 2007